

https://dspace.org/

Kinetics of pyrolysis and combustion of a South African coal using the distributed activation energy model

Saloojee, Fadeela

2012-01-31
http://hdl.handle.net/10539/11217

Downloaded from a DSpace repository. https://dspace.org/

KINETICS OF PYROLYSIS AND COMBUSTION OF A SOUTH AFRICAN COAL USING THE DISTRIBUTED ACTIVATION ENERGY MODEL

Fadeela Saloojee

A dissertation submitted to the Faculty of Engineering and the Built Environment, University of the Witwatersrand, in fulfillment of the requirements for the degree of Master of Science in Engineering.

Johannesburg, 2011

Declaration

I declare that this dissertation is my own unaided work. It is being submitted to the degree of Master of Science in Engineering to the University of Witwatersrand, Johannesburg. It has not been submitted before for any degree or examination to any other university.

……..

(Signature of Candidate)

…….. day of ……. year ……

Abstract

Most of the energy requirements in South Africa are met by conversion of coal. Kinetics of these coal conversion reactions are necessary for these processes to be run efficiently. In this work, the kinetics of pyrolysis and combustion of a South African coal have been studied. Thermo-gravimetric experiments were carried out on coal and char samples under nitrogen and oxygen atmospheres, at different heating rates. The results were used with appropriate models in order to determine the reaction kinetics.

The Distributed Activation Energy Model (DAEM) is commonly used to describe the coal pyrolysis process. The model states that coal devolatilizes according to a number of first order reactions, each with unique activation energy (E). An algorithm has been developed to invert this model in order to calculate the fraction reacting, E and pre-exponential factor (A) of each reaction using thermo-gravimetric data. The algorithm was tested on pyrolysis data from real and simulated TGA experiments. The parameters obtained were used to model the reaction at different heating rates. It was found that the DAEM is suitable to model the pyrolysis reaction

Further scrutiny of the inversion algorithm has shown that the calculation of the activation energy is a model-free method. The algorithm was therefore applied to real and simulated thermo-gravimetric data for coal combustion. Results show that the DAEM can be used as a model-free method to calculate the E of coal combustion. However, the calculation of the A requires the use of an appropriate structural sub-model. For this particular coal, the shrinking core model was not suitable to describe the combustion reaction. Finding the correct model did not form part of this work.

In addition, the assumption of a constant heating rate used in the algorithm was investigated. Examination of TGA data showed that there was a lag between the program temperature and the actual sample temperature. This temperature lag, however small, impacted the heating rate of the sample. Instantaneous values for the heating rate were used in the algorithm. Again, the algorithm proved able to calculate kinetic parameters.

Finally, data obtained from coal and char combustion reactions was compared. Both the E and temperature at the maximum devolatilization rate indicate that raw coal is more suitable for use in industrial boilers than char.

Acknowledgements

I wish to thank the following persons for their contribution to my work:

- My supervisors, Professor N. Wagner and Dr. S. Kauchali for their assistance, guidance and advice throughout this research
- Professor N. Wagner for provision of funding, lab facilities, purchasing of equipment for this work and vast insight into coal
- Dr. S. Kauchali for help with all aspects of modeling, interpretation of results and support in this work
- Qasim Fakir, for research suggestions, TGA training and assistance with modelling
- Eskom TESPS Bursary for provision of funds
- Members of the Coal and Carbon Research Group, University of the Witwatersrand, for assistance with sample preparation
- University of Johannesburg for crushing of coal
- Professor N. Wagner for petrographic analysis of coal
- My parents for providing me with this opportunity, and my husband, Reza, for encouragement and motivation

Contents

Declaration i
Abstract ii
Acknowledgements iii
List of Figures vi
List of Tables xi
Nomenclature xiii
Chapter 1: Introduction 1
1.1 Introduction 1
1.2 Motivation and Problem Statement 2
1.3 Aim and objectives 2
1.4 Research questions 3
1.5 Hypothesis 3
1.6 Scope of the project 3
1.7 Structure of Dissertation 4
Chapter 2: Literature Review 6
2.1 Introduction 6
2.2 Pyrolysis 6
2.2.1 First-order reaction kinetics 7
2.2.2 The DAEM 8
2.3 Combustion 11
2.3.1 The Shrinking Core Model 12
2.3.2 The Random Pore Model 13
2.3.3 Other Combustion Models 14
2.4 Model-free methods for the calculation of reaction kinetics 16
2.4.1 Rate-isoconversion methods (Type A) 16
2.4.2 p(y)-isoconversion methods (Type B) 17
2.5 Reactivity 20
2.6 Conclusion 22
Chapter 3: Research Methodology 24
3.1 Materials 24
3.2 Sample Preparation 24
3.3 Equipment 25
3.3.1 Perkin-Elmer series STA 600: Standard Furnace 25

3.3.2 TA Instruments series Q600 SDT: High Temperature Furnace 26
3.3.3 Gas Lines 26
3.4 Procedure 26
3.4.1 Perkin-Elmer series STA 600 27
3.4.2 TA Instruments series Q600 SDT 28
3.5 Data Analysis and Modeling 29
Chapter 4: Theoretical Development 31
4.1 Introduction 31
4.2 Simulated first-order reactions 31
4.2.1 Single reaction 31
4.2.2 Seven Reactions 37
4.2.3 Single reaction with variable heating rates 43
4.3 A model-free method for determining the activation energy 51
4.4 Simulated combustion with a shrinking core reaction 53
4.4.1 Calculation of E using the DAEM as a model-free method 53
4.4.2 Determining the pre-exponential factor, A^* 56
4.5 The DAEM modified to model a shrinking core reaction 58
4.6 Model evaluation using data reported in literature 64
4.7 Conclusion 66
Chapter 5: Pyrolysis Results 68
5.1 Low temperature TGA experiments 68
5.1.1 Higher Heating Rates 69
5.1.2 Lower Heating Rates 85
5.2 High temperature TGA experiments 91
5.3 Conclusion 98
Chapter 6: Combustion Results 100
6.1 Low Temperature TGA experiments 100
6.1.1 Char Combustion 100
6.1.2 Raw Coal Combustion 108
6.1.3 Comparison of char combustion and raw coal combustion 112
6.2 High Temperature TGA experiments 112
6.3 Comparison of the calculated values of E to literature values 116
6.4 Conclusion 117
Chapter 7: Conclusions and Recommendations 119

7.1 Conclusions 119
7.1.1 Simulated TGA data 119
7.1.2 Pyrolysis Results 120
7.1.3 Combustion Results 120
7.2 Recommendations 121
7.2.1 Application of the DAEM 121
7.2.2 Mathematical / Statistical improvements to the model 122
7.2.3 Information to be gained from kinetic parameters 122
8. References 123
Appendix A: Experimental Details 129
A1: TGA Specifications 129
A2: Proximate Analysis Procedure 131
Petrographic Analysis Procedure 132
Appendix B: Matlab codes used for simulations and algorithm calculations 134

List of Figures

Figure 2.1: Schematic representation of a particle undergoing combustion (Abdel-Hafez, 1988).....13
Figure 3.1: Schematic diagram of Perkin-Elmer STA 600 TGA (courtesy of Perkin-Elmer).25
Figure 3.2: TA Instruments Q600 TGA balance and furnace (courtesy of TA Instruments)..26
Figure 3.3: Flow Diagram of algorithm steps (Scott *et al*., 2006).....29
Figure 4.1: Simulated TGA curves for pyrolysis with a single, first-order reaction at different heating rates.....32
Figure 4.2: Simulated DTG curves for pyrolysis with a single, first-order reaction at different heating rates.....33
Figure 4.3: Kinetic parameters calculated for simulated single, first-order reaction (a) Initial mass fraction of each component (b) Activation Energy of each reaction (c) Pre-exponential factor of each reaction.....33
Figure 4.4: Simulated TGA curves for pyrolysis with a single, first-order reaction at different heating rates, with DAEM predictions for each of these heating rates……...36
Figure 4.5: Simulated DTG curves for pyrolysis with a single, first order reaction at different heating rates, with DAEM predictions for each of these heating rates.....36
Figure 4.6: Simulated TGA curves for pyrolysis with seven first order reactions at different heating rates.....38
Figure 4.7: Simulated DTG curves for pyrolysis with seven first order reactions at different heating rates.....38
Figure 4.8: Kinetic parameters calculated for seven simulated first-order reactions (a) Initial mass fraction of each component (b) Activation Energy of each reaction (c) Pre-exponential factor of each reaction.....40
Figure 4.9: Simulated TGA curves for seven first-order reactions at different heating rates, with DAEM predictions for each of these heating rates.....42
Figure 4.10: Simulated DTG curves for seven first order reactions at different heating rates, with DAEM predictions for each of these heating rates.....42
Figure 4.11: Heating rates vs. temperature profiles used for simulation of TGA data.....44
Figure 4.12: Simulated TGA curves for pyrolysis with a single, first-order reaction at variable heating rates.....45
Figure 4.13: Simulated DTG curves for pyrolysis with a single, first-order reaction at variable heating rates.....46

Figure 4.14: Simulated TGA curves for pyrolysis with a single, first order reaction at a variable heating rate and constant heating rate of 25 K/min.....47
Figure 4.15: Simulated TGA curves for pyrolysis with a single, first order reaction at a variable heating rate and constant heating rates of 35 K/min and 45 K/min.....48
Figure 4.16: Kinetic parameters calculated for simulated single first-order reaction with variable heating rates (a) Initial mass fraction of each component (b) Activation Energy of each reaction (c) Pre-exponential factor of each reaction.....49
Figure 4.17: Simulated TGA curve pyrolysis with a single, first order reaction at a constant heating rate of 25 K/min, with a DAEM prediction using parameters calculated from variable heating rate curves.....51
Figure 4.18: Simulated TGA curves for a shrinking core reaction at different heating rates simulated using ode45 solver.....53
Figure 4.19: Simulated DTG curves for a shrinking core reaction at different heating rates simulated using ode45 solver.....54
Figure 4.20: Kinetic parameters calculated for a simulated shrinking core reaction using ode45 solver (a) Initial mass fraction of each component (b) Activation Energy of each reaction (c) Pre-exponential factor of each reaction.....55
Figure 4.21: Simulated TGA curves for a shrinking core reaction at different heating rates simulated using ode45 solver, with model predictions for each of these heating rates.....57
Figure 4.22: Simulated DTG curves for a shrinking core reaction at different heating rates simulated using ode45 solver, with model predictions for each of these heating rates.....58
Figure 4.23: Simulated TGA curves for a shrinking core reaction at different heating rates simulated using $\Psi^{s.c.}$.....60
Figure 4.24: Simulated DTG curves for a shrinking core reaction at different heating rates simulated using $\Psi^{s.c}$.....61
Figure 4.25: Kinetic parameters calculated for a simulated shrinking core reaction using $\Psi^{s.c}$ (a) Initial mass fraction of each component (b) Activation Energy of each reaction.....61
Figure 4.26: Simulated TGA curves for a shrinking core reaction at different heating rates simulated using $\Psi^{s.c}$, with model predictions for each of these heating rates.....63
Figure 4.27: Simulated DTG curves for a shrinking core reaction at different heating rates simulated using $\Psi^{s.c}$, with model predictions for each of these heating rates.....64
Figure 4.28: TGA curves for char combustion in air reported by Njapha (2003).....65
Figure 4.29: TGA curves for char combustion in air reported by Njapha (2003) with model predictions using calculated parameters and parameters reported by Njapha (2003).....66

Figure 5.1: TGA curves for the pyrolysis of a South African coal at different heating rates in a Perkin-Elmer STA600 TGA.....68
Figure 5.2: Kinetic parameters calculated for coal pyrolysis (a) Initial mass fraction of each component (b) Activation Energy of each reaction (c) Pre-exponential factor of each reaction.....69
Figure 5.3: TGA curves for coal pyrolysis at heating rates of 35 K/min and 60 K/min, with DAEM predictions for each heating rate.....72
Figure 5.4: DTG curves for coal pyrolysis at heating rates of 35 K/min and 60 K/min, with DAEM predictions for each heating rate.....73
Figure 5.5: TGA curves for coal pyrolysis at heating rates of 20 K/min and 80 K/min with DAEM predictions for each heating rate.....74
Figure 5.6: DTG curves for coal pyrolysis at heating rates of 20 K/min and 80 K/min with DAEM predictions for each heating rate.....75
Figure 5.7: Comparison of programme heating rates and actual heating rates of the samples for coal pyrolysis in a Perkin Elmer STA600 TGA.....76
Figure 5.8: Kinetic parameters calculated for coal pyrolysis using instantaneous heating rates (a) Initial mass fraction of each component (b) Activation Energy of each reaction (c) Pre-exponential factor of each reaction.....77
Figure 5.9: TGA curves for coal pyrolysis at heating rates of 35 K/min and 60 K/min with DAEM predictions using parameters calculated from instantaneous heating rates.....79
Figure 5.10: DTG curves for coal pyrolysis at heating rates of 35 K/min and 60 K/min with DAEM predictions using parameters calculated from instantaneous heating rates.....80
Figure 5.11: TGA curves for coal pyrolysis at heating rates of 20 K/min and 80 K/min with DAEM predictions using parameters calculated from instantaneous heating rates.....81
Figure 5.12: DTG curves for coal pyrolysis at heating rates of 20 K/min and 80 K/min with DAEM predictions using parameters calculated from instantaneous heating rates.....82
Figure 5.13 (a): TGA curves for coal pyrolysis at heating rates of 20 K/min and 80 K/min with DAEM predictions for constant heating rates of 25 K/min and 90 K/min using parameters calculated from instantaneous heating rates.....83
Figure 5.13 (b): TGA curves for coal pyrolysis at heating rates of 20 K/min and 80 K/min with DAEM predictions for actual heating rate profiles using parameters calculated from instantaneous heating rates.....83

Figure 5.14 (a): DTG curves for coal pyrolysis at heating rates of 20 K/min and 80 K/min with DAEM predictions for constant heating rates of 25 K/min and 90 K/min using parameters calculated from instantaneous heating rates.....84
Figure 5.14 (b): DTG curves for coal pyrolysis at heating rates of 20 K/min and 80 K/min with DAEM predictions for actual heating rate profiles using parameters calculated from instantaneous heating rates.....84
Figure 5.15: TGA curves for the pyrolysis of a South African coal at low heating rates.....85
Figure 5.16: DTG curves for the pyrolysis of a South African coal at low heating rates.....86
Figure 5.17: Kinetic Parameters calculated for coal pyrolysis at lower heating rates (a) Initial mass fraction of each component (b) Activation Energy of each reaction (c) Pre-exponential factor of each reaction.....86
Figure 5.18: Comparison of programme heating rates and actual heating rates of the samples for coal pyrolysis at lower heating rates in a Perkin Elmer STA600 TGA.....88
Figure 5.19: TGA curves for coal pyrolysis at heating rates of 5 K/min and 8 K/min with DAEM predictions for each heating rate.....89
Figure 5.20: DTG curves for coal pyrolysis at heating rates of 5 K/min and 8 K/min with DAEM predictions for each heating rate.....89
Figure 5.21: Comparison of model curve to experimental curve for 35 K/min using parameters obtained from lower heating rate data.....90
Figure 5.22: TGA curves for the pyrolysis of South African coal at different heating rates in a TA Instruments Q600 TGA.....91
Figure 5.23: DTG curves for the pyrolysis of South African coal at different heating rates in a TA Instruments Q600 TGA.....92
Figure 5.24: Kinetic Parameters calculated for coal pyrolysis in a high temperature TGA (a)Initial mass fraction of each component (b)Activation Energy of each reaction (c)Pre-exponential factor of each reaction.....94
Figure 5.25: Actual heating rates of the samples for coal pyrolysis in a TA instruments Q600 TGA.....95
Figure 5.26: TGA curves for the pyrolysis of South African coal at different heating rates in a TA Instruments Q600 TGA, with DAEM predictions for each heating rate.....96
Figure 5.27: DTG curves for the pyrolysis of South African coal at different heating rates in a TA Instruments Q600 TGA, with DAEM predictions for each heating rate.....96
Figure 5.28: DAEM prediction of a TGA curve for a heating rate of 10 000 K/min.....97
Figure 5.29: DAEM prediction of a DTG curve for a heating rate of 10 000 K/min.....98

Figure 6.1: TGA curves for the combustion of a South African char at different heating rates in a Perkin-Elmer STA600 TGA.....100
Figure 6.2: DTG curves for the combustion of a South African char at different heating rates in a Perkin-Elmer STA600 TGA.....101
Figure 6.3: Kinetic parameters calculated for char combustion (a) Initial mass fraction of each component (b) Activation Energy of each reaction (c)Pre-exponential factor of each reaction.....102
Figure 6.4: TGA curves for the combustion of a South African char at heating rates of 30 K/min and 60 K/min, with DAEM predictions for each heating rate.....103
Figure 6.5: TGA curves for the combustion of a South African char at heating rates of 35 K/min and 60 K/min, with shrinking core model predictions for each heating rate.....104
Figure 6.6: Comparison of programme heating rates and actual heating rates of the samples for char combustion in a Perkin Elmer STA600 TGA.....106
Figure 6.7: Kinetic parameters calculated for char combustion using instantaneous heating rates (a) Initial mass fraction of each component (b) Activation Energy of each reaction....106
Figure 6.8: TGA curves for the combustion of a South African coal at two different heating rates in a Perkin-Elmer STA600 TGA.....108
Figure 6.9: DTG curves for the combustion of a South African coal at two different heating rates in a Perkin-Elmer STA600 TGA.....109
Figure 6.10: Kinetic parameters calculated for coal combustion (a) Initial mass fraction of each component (b) Activation Energy of each reaction.....109
Figure 6.11: Comparison of programme heating rates and actual heating rates of the samples for coal combustion in a Perkin Elmer STA600 TGA.....111
Figure 6.12: TGA curves for the combustion of a South African char at different heating rates in a TA Instruments Q600 TGA.....113
Figure 6.13: DTG curves for the combustion of a South African char at different heating rates in a TA Instruments Q600 TGA.....114
Figure 6.14: Kinetic parameters calculated for char combustion in a TA Instruments Q600 TGA (a) Initial mass fraction of each component (b) Activation Energy of each reaction...115
Figure 6.15: Actual heating rates of the samples for char combustion in a TA Instruments Q600 TGA.....116

List of Tables

Table 2.1: Temperature regions in coal pyrolysis (Ladner, 1988)..... 7

Table 2.2: Reaction rate models commonly used for solid-gas reactions and their integral forms (Ebrahimi-Kahrizsangi & Abbasi, 2008) 15

Table 3.1: Proximate Analysis of a Witbank coal sample.....24

Table 3.2: Petrographic Analysis of a Witbank coal sample.....24

Table 4.1: Kinetic parameters used for simulation of pyrolysis with a single, first-order reaction.....32

Table 4.2 (a): Comparison of original kinetic parameters and those recovered by the DAEM for a simulated single, first-order reaction using heating rates of 10K and 1000K.....35

Table 4.2 (b): % Error in parameters recovered by the DAEM for a simulated single, first-order reaction using different heating rate combinations…….35

Table 4.3: Kinetic parameters used for simulation of pyrolysis with seven first-order reactions.....37

Table 4.4: Comparison of original kinetic parameters and those recovered by the DAEM for seven simulated first-order reactions.....41

Table 4.5: Comparison of original kinetic parameters and those recovered by the DAEM for a simulated single, first-order reaction with variable heating rates.....50

Table 4.6: Comparison of original kinetic parameters and those recovered by the DAEM for a shrinking core reaction simulated using ode45 solver.....55

Table 4.7: Value of A^* recovered by shrinking core algorithm and original value.....56

Table 4.8: Kinetic parameters used for simulation of coal combustion with a shrinking core reaction using $\Psi^{s.c.}$.....59

Table 4.9: Comparison of original kinetic parameters and those recovered by the DAEM for E shrinking core reaction algorithm for A using $\Psi^{s.c}$.....62

Table 4.10: Values of kinetic parameters calculated for char combustion compared to those reported by Njapha (2003).....65

Table 5.1: Kinetic parameters of coal pyrolysis in a Perkin-Elmer STA600 calculated using the DAEM inversion algorithm.....71

Table 5.2: Kinetic parameters of coal pyrolysis in a Perkin-Elmer STA600 TGA calculated using an instantaneous heating rate in the DAEM inversion algorithm.....78

Table 5.3: Distribution of E's for pyrolysis of different coals.....78

Table 5.4: Kinetic parameters of coal pyrolysis in a Perkin-Elmer STA 600 TGA calculated using lower heating rates in the DAEM inversion algorithm.....87
Table 5.5: Kinetic parameters of coal pyrolysis in a TA Instruments Q600 TGA calculated using the DAEM inversion algorithm.....93
Table 6.1: Kinetic parameters of char combustion in a Perkin-Elmer STA600 TGA calculated using the DAEM inversion algorithm.....103
Table 6.2: Kinetic parameters of char combustion in a Perkin-Elmer STA600 TGA calculated using an instantaneous heating rate in the DAEM inversion algorithm.....107
Table 6.3: Kinetic parameters of coal combustion in a Perkin-Elmer STA600 TGA calculated using the DAEM inversion algorithm.....110
Table 6.4: Kinetic parameters of coal combustion in a Perkin-Elmer STA600 TGA calculated using an instantaneous heating rate the DAEM inversion algorithm.....111
Table 6.5: Comparison of relative reactivity of coal to char.....112
Table 6.6: Kinetic parameters of char combustion in a TA Instruments Q600 TGA calculated using the DAEM inversion algorithm.....115
Table 6.7: Activation energy of combustion for coals, chars and graphite.....116
Table A24: Equipment Specifications of Perkin-Elmer STA 600 TGA.....130
Table A25: Equipment Specifications of TA Instruments Q600 TGA.....131

Nomenclature

A – Pre-exponential factor

A_i – Pre-exponential factor of reaction i

A^* – lumped pre-exponential factor

B – Heating rate

C – Carbon

C_A – Concentration of oxygen in core of combusting coal particle

DAEM – Distributed Activation Energy Model

D_c – Diameter of unreacted core of a combusting coal particle

DTG – Derivative thermo-gravimetric

E – Activation energy of reaction

E_i – Activation energy of reaction i

f_i – Mass fraction of fuel associated with reaction i

$f_{i,0}$ – Initial value of f_i

f(α) – Kinetic function of α

F(α) – Integral form of f(α)

f(X) – Structural function of X

F(X) – Integral form of f(X), as defined by Equation 2.41

g(E) – Fractional density function such that g(E)dE is the fraction of material with activation energy between E and E+dE

g(α) – Integral form of f(α) used in Table 2.2

G(α) – Defined by Equation 2.33

i – Component number in fuel

k – Reaction rate constant, defined by the Arrhenius Equation

k_V – Reaction rate constant based on volume, defined by the Arrhenius Equation

k_0 – Pre-exponential factor of combustion

L_0 – Total pore length per unit volume

$m(E,t)$ – Mass density function such that $m(E, t)dE$ is the mass of material with activation energy between E and E+dE

$m_0(E)$ – Initial value of $m(E, t)$

M(t) – Mass of fuel at time t

M_0 – Initial value of M(t)

M_v – Mass of volatiles

M_{v0} – Initial value of M_v

n – Reaction order with respect to oxygen

O_2 – Oxygen gas

o.d.e. – ordinary differential equation

p(y) – Defined by Equation 2.44

P_{O_2} – Partial pressure of oxygen

r – Reaction rate

r_s – Reaction rate given by the Arrhenius expression

r_A – reaction rate of reactant A

R – Universal gas constant

R_c – Defined by equation 2.49

S_0 – Initial surface area per unit volume of coal particle

t – time

t_{50} – time taken for a sample to reach half its initial mass

T – Temperature

TGA – Thermo-Gravimetric Analyser

u – Dummy variable for integration

V – Mass of volatiles in coal

V_∞ – Value of V at $t=\infty$

w – Mass fraction of inert material

X – fractional conversion of carbon

X_i – fractional conversion of carbon during reaction i

y – transformed variable used in integration, defined by Equation 2.35

y_0 – Initial value of y

Z – Defined by Equation 2.42

α – Fractional conversion of a solid reactant

β – Heating rate

ε_0 – Initial porosity of coal particle

$\Psi(E)$ – Defined by Equation 2.10

Ψ_i – Value of Ψ for reaction i

Ψ_{rp} - Term in random pore expression defined by Equation 2.27

$\Psi^{s.c.}$ – Modified matrix used in DAEM to model a shrinking core reaction

Chapter 1: Introduction

1.1 Introduction

In South Africa, coal is the primary source of electricity, providing more than 90% of power (South Africa.info, 2008). Direct combustion of coal takes place in coal-fired power plants in order to produce electricity. This type of coal fired process has a large environmental impact. Impurities in the coal, such as sulphur and nitrogen, are released into the atmosphere, causing problems such as acid rain and smog. Mineral matter which does not burn can also be released into the air as particulate matter. However, the biggest concern is the emission of carbon dioxide. For this reason, South Africa is considered a major contributor to global warming.

Carbon dioxide emissions can be reduced by increasing the efficiency of coal conversion processes. Equipment needs to be designed so that coal conversion reactions can occur at optimum conditions. It is therefore important to understand how coal behaves in these processes. This can be achieved by developing and testing kinetic models for coal conversion reactions.

The most widely used technique in the study of solid-gas reaction kinetics is thermo-gravimetric analysis (Dhar, 1986; Ebrahimi-Kahrizsangi & Abbasi, 2008). This is an analytical procedure used to determine the mass change profile of a sample as it is heated in a controlled environment. A thermo-gravimetric analyser (TGA) consists of a highly sensitive mass balance, a sample pan, a thermocouple and an electric furnace.

The Distributed Activation Energy Model (DAEM) has been used to model pyrolysis of coal (Donskoi & McElwain, 2000; Please *et al*., 2003). It is based in the assumption that coal pyrolysis is made up of a number of first-order decomposition reactions. Application of this model to thermo-gravimetric data allows the calculation of kinetic parameters for coal pyrolysis.

In this work, the combustion of coal and char particles in a thermo-gravimetric analyser (TGA) has been studied. The intention was to calculate the kinetic parameters of coal combustion and model the reaction based on these kinetics. It was postulated that the DAEM could be used to provide information on reaction kinetics. Thermo-gravimetric analysis was

carried out on char samples under combustion conditions. The results were used with the DAEM to calculate kinetic parameters.

In preparing the char, the raw coal was devolatilized in an inert atmosphere. The devolatilization conditions of coal have an effect on the porosity and internal surface area of the resulting char, therefore affecting its combustion reactivity (Arenillas *et al.*, 2001). Pre-pyrolysis of the coal under specific conditions could improve the reactivity of the char and allow combustion to take place at a lower temperature, which would decrease the overall energy requirements of the process.

1.2 Motivation and Problem Statement

Due to the role that coal plays in South African energy production, it would be worthwhile to direct attention to increasing the efficiency of coal conversion processes. Accurate models for pyrolysis and combustion are needed for assessing and improving the design of coal gasification and combustion equipment.

An ongoing project at the University of the Witwatersrand focuses on the modelling of coal pyrolysis. A method of inverting and solving the DAEM (Scott *et al.*, 2006) was developed and applied to a typical South African coal. Initial results show that this method successfully describes the pyrolysis of this South African coal. A recommendation from this work was to investigate whether the DAEM inversion algorithm could be used to calculate the kinetic parameters for combustion of a South African coal.

Current models for pyrolysis and combustion are computationally intensive and time consuming (Everson *et* al., 2005; Mitchell *et al.*, 2007). They often incorporate a function which depends on the structure of the coal as it reacts (Abdel-Hafez, 1988; Sadhukhan *et al.*, 2009; Sadhukhan *et al*, 2010). The structure of South African coals can vary greatly from seam to seam as well as within seams. A method of evaluating certain kinetic parameters which is independent of the coal structure would therefore simplify the modelling process. Such a method is termed “model-free”.

1.3 Aim and objectives

The aim of this work is to develop the DAEM (Scott *et* al., 2006) so that it may be used to determine the activation energy (E) for coal and char combustion. The model will then be applied to real and simulated thermo-gravimetric experiments in order to test its validity.

The objectives are:

- To model the kinetics of pyrolysis of a South African coal using the DAEM and results from thermo-gravimetric experiments.
- To calculate the E's of combustion of a South African char using the DAEM and thermo-gravimetric results.
- To test whether the DAEM predicts the E correctly.
- To calculate the pre-exponential factor (A) for combustion of the char using the shrinking core model.
- To investigate the difference in E between coal and char combustion.

1.4 Research questions

1. Is the DAEM a reliable model which can be used to model pyrolysis reactions?
2. Are modifications to the DAEM necessary to improve pyrolysis modelling?
3. Can the DAEM be used as a model free method to find the E for combustion?
4. Can the DAEM be used to find the A for combustion?
5. Can the shrinking core model be used to accurately determine the pre-exponential factor for combustion?
6. Does pre-charring of coal have an effect on its combustion characteristics?

1.5 Hypothesis

The DAEM can be used as a model free method to determine the E for combustion of coal char.

1.6 Scope of the project

The project will be broken down into steps as follows:

1. Develop an algorithm in Matlab^{TM} to calculate the kinetic parameters, which are initial mass fraction of a volatile component ($f_{i,0}$), E and A, according to the DAEM for any reaction from mass *vs*. temperature data.

2. Simulate TGA data for different types of pyrolysis reactions using given values of $f_{i,0}$, E and A.
3. Apply the DAEM algorithm to the data to test whether the calculated parameters correspond to the original parameters in a simulated environment.
4. Use the calculated parameters to model the reaction and compare modelled curves to experimental curves.
5. Simulate TGA data for a shrinking core combustion reaction.
6. Apply the DAEM algorithm to the data in order to test whether the calculated E corresponds to the original E for a simulated case.
7. Develop an algorithm in Matlab^{TM} to calculate the value of A using the shrinking core model and the calculated value of E.
8. Use the calculated parameters to model the reaction and compare modelled curves to experimental curves.
9. Perform TGA experiments on the pyrolysis of coal.
10. Apply the DAEM algorithm to the real pyrolysis data to calculate kinetics, model the reaction and compare curves.
11. Perform TGA experiments on the combustion of char.
12. Use the DAEM algorithm with the combustion data to calculate the E and the shrinking core algorithm to calculate the A for combustion.
13. Model a shrinking core reaction using the calculated kinetic parameters and compare the modelled curves to the experimental curves. It is not within the scope of this work to use other models, such as the random pore model, to model the coal or char combustion reactions.
14. Perform TGA experiments on the combustion of raw coal and obtain the E of combustion.
15. Compare the E of raw coal combustion to the E of char combustion.

1.7 Structure of Dissertation

The dissertation is made up of seven chapters covering the different aspects of this work. Chapter 1 is an introduction, followed by a literature review in Chapter 2 which covers the models used for pyrolysis and combustion. In Chapter 3, the research methodology is discussed and this includes the experimental work in the TGA's as well as the modelling component. Chapter 4 presents the simulated TGA results and associated model development

and testing. In Chapter 5 and Chapter 6, the results of real pyrolysis and combustion experiments are presented respectively. This is followed by a summary of conclusions drawn from the results and recommendations from this work in Chapter 7.

Chapter 2: Literature Review

2.1 Introduction

Coal is defined as a sedimentary rock consisting mainly of organic material (Haenel, 1992; UN-ECE, 1998), which is used as a fossil fuel. It is composed of fossilized plant material, known as macerals, as well as inorganic minerals (Haenel, 1992). The structure of coal is complex and a detailed description will not be provided here. It is sufficient to state that coal is a macromoecular network, consisting of polyaromatic and aromatic units linked by covalent and non-covalent bonds (Van Niekerk & Mathews, 2010), with high, unknown molecular mass (Bjorkman, 2001).

During conversion processes of coal, such as pyrolysis and combustion, coal decomposes to give off organic vapours as it is heated (Scott *et al*., 2006). Many models are presented in literature to describe these processes (Anthony *et al*, 1975; Kobayashi *et al*., 1977; Scott *et al*., 2006; Everson *et al*., 2006; Sadhukhan *et al*., 2010). An important tool used for the understanding of these conversion reactions is thermo-gravimetric analysis, since these reactions involve mass change (Kok & Pamir, 1995). The mass change *vs*. temperature profiles of the coal as it is subjected to different heating regimes can be used to determine kinetic parameters of coal conversion reactions. These parameters are important as they provide an idea of the optimum conditions for reactions (Keuleers *et al*., 2002) and are thus necessary in the design of any type of coal decomposition equipment (Ebrahimi-Kahrizsangi and Abbasi, 2008).

In this chapter, the basic processes involved in coal conversion are explained, commencing with pyrolysis and followed by combustion. Models which have been and are currently used for pyrolysis and combustion are discussed. Special attention is given to the DAEM, as explained by Scott *et al*. (2006). The effects of pre-charring of coal on coal reactivity are also discussed.

2.2 Pyrolysis

Coal pyrolysis is the thermal decomposition of coal in a non-reactive atmosphere to produce volatile gases, char and possibly tar. Char is the solid content derived from coal, which is richer in carbon than the parent coal and is subsequently combusted. Tar is described by Migliavacca *et al*., (2005) as “the room-temperature condensable species formed during pyrolysis”. The chemical processes occurring during coal pyrolysis are the decomposition of

individual functional groups to form light gases, and the decomposition of macromolecular networks to produce smaller fragments, which can form tar (Arenillas *et al.*, 2001).

The pyrolysis process has been described by Ladner (1988) by dividing it into distinct temperatures as shown in Table 2.1:

Table 2.1: Temperature regions in coal pyrolysis (Ladner, 1988)

Region	Temperature Range (° c)	Reactions	Products	Use
	< 350	Mainly Evaporation	Water and Volatile Organics	Fundamental studies
Low Temp.	400 - 750	Primary degradation	Gas, tar and liquor	Smokeless fuels and chemicals
Medium temp.	750 – 900	Secondary Reactions	Gas, tar, liquor plus additional hydrogen	Smokeless fuels and chemicals, metallurgical coke and chemicals
High temp.	900 – 1100			
Plasma	> 1650		Acetylene, carbon black	Uneconomic

It is clear that pyrolysis is made up of a set of reactions and that a description of its kinetics is very complex, and would have to depend on simplifying assumptions.

2.2.1 First-order reaction kinetics

The earliest and simplest models for coal pyrolysis, as described by Kobayashi *et al* (1977) assume a single, first-order reaction, following the Arrhenius expression, as described below:

$$Coal \xrightarrow{k} V + char \qquad \text{(Arenillas } et\ al.\text{, 2001)} \quad (2.1)$$

where V is the mass of volatiles in the coal. The reaction rate is then given by:

$$\frac{dV}{dt} = k \cdot (V_\infty - V) \qquad \text{(Kobayashi } et\ al.\text{, 1977)} \quad (2.2)$$

where V_∞ is the value of V at t=∞, k is the rate constant, given by the Arrhenius equation below:

$$k = A \cdot \exp\left(\frac{-E}{RT}\right) \quad (2.3)$$

where A is the pre-exponential factor in s^{-1}, E is the activation energy in J/mol, R is the molar gas constant in J/mol.K and T is the temperature in K.

Mass loss vs. temperature measurements have been used to calculate the values of A and E for this model, by assuming a constant value for V_∞ (Anthony *et al*., 1975; Arenillas *et al*., 2001; Kobayashi *et al*., 1977). However, this model is basic and only applicable for a limited range of experimental conditions. A model which takes into account the different reactions and the diversity of reaction conditions during coal devolatilization was therefore sought.

2.2.2 The DAEM

The DAEM is a model which considers the numerous reactions involved in devolatilization. It is based on the assumption that coal is a mixture of components and each component decomposes according to a first order reaction (Pitt, 1962). Each of the parallel reactions is uniquely characterised by its activation energy (Scott *et al*., 2006). It is further assumed that there is a continuous distribution of activation energies. The derivation of this model is explained here.

The mass of volatile material with activation energies between *E* and *E+dE* at a particular time *t* is given as *m(E,t)dE* (Scott *et al*., 2006). The total mass of volatiles at time *t*, $M_v(t)$, can be expressed as:

$$M_v(t) = \int_0^\infty m(E,t)dE \tag{2.4}$$

and the initial mass of volatiles is:

$$M_{v0} = \int_0^\infty m_0(E)dE \tag{2.5}$$

If it is assumed that the decomposition reaction is first order, then:

$$\frac{dm(E,t)}{dt} = -A(E)\exp\left(\frac{-E}{RT}\right)m(E,t) \tag{2.6}$$

where A(E) is the pre-exponential factor.

Solving the above differential equation yields:

$$m(E,t) = m_0(E)\exp\left[-A(E)\int_0^t \exp\left(\frac{-E}{RT}\right)dt\right] \tag{2.7}$$

where m_0(E) is the initial mass of volatile material in the interval E to E+dE.

Integrating the above equation over the range of all E's yields:

$$\frac{M_v(t)}{M_{v0}} = \int_0^\infty g(E) \exp\left[-A(E)\int_0^t \exp\left(\frac{-E}{RT}\right)dt\right]dE \qquad \text{(Scott } et\ al.\text{, 2006)} \quad (2.8)$$

Where the initial distribution of activation energies, g(E), is given by:

$$g(E) = \frac{m_0(E)}{\int_0^\infty m_0(E)dE} \qquad (2.9)$$

and the double exponential term can be written as Ψ(E):

$$\Psi(E) = \exp\left[-A(E)\int_0^t \exp\left(\frac{-E}{RT}\right)dt\right] \qquad (2.10)$$

The problems associated with solving Equation 2.8 are discussed by Donskoi and McElwain (2000), the main issue being evaluation of the double integral over all activation energies. For a non-isothermal system, the integral needs to be evaluated for each temperature, which causes the calculation to be intensive and time-consuming. It is also not possible to estimate the error of integration prior to the calculation in order to minimise this error. These authors present a numerical method of evaluating the integral, by modifying the Gauss-Hermite quadrature method. It is claimed that the errors of integration are significantly smaller when compared to other numerical integration techniques. However, this method is based on a known value of A and a known initial distribution of activation energies. It is used to model the evolution of volatiles during coal pyrolysis.

Calculation of the values of E and A is more complex, since g(E) is not known. Scott *et al* (2006) presents an algorithm for determining the kinetic parameters A(E) and E, using TGA data, which does not depend on assuming an initial distribution of activation energies. If it is assumed that a component of the coal with initial mass fraction $f_{i,0}$ reacts with activation energy E_i and pre-exponential factor A_i, Equation 2.7 can be expressed as:

$$f_i = f_{i,0} \exp\left[-A_i\int_0^t \exp\left(\frac{-E_i}{RT}\right)dt\right] \qquad (2.11)$$

where f_i is the fraction of the *i*th component remaining as the fuel is heated. For a fuel decomposing according to several first order reactions, Eq. 2.8 can thus be expressed as:

$$\frac{M(t)}{M_0} = w + \sum_{All\ reactions,i} f_{i,0} \exp\left[-A_i\int_0^t \exp\left(\frac{-E_i}{RT}\right)dt\right] \qquad \text{(Scott } et\ al.\text{, 2006)} \quad (2.12)$$

where M(t) is the mass of the sample at time t, M_0 is the initial mass of the fuel and *w* is the fraction of inert material. The double-exponential term can be expressed as Ψ_i. Scott *et al.* (2006) then states that Equation 2.12 can be written in matrix form as follows:

$$\frac{1}{M_0}\begin{bmatrix}M(t_0)\\M(t_1)\\M(t_2)\end{bmatrix}=\begin{bmatrix}\Psi_1(t_0) & \Psi_2(t_0)\cdots\Psi_n(t_0) & 1\\ \Psi_1(t_1) & \Psi_2(t_1)\cdots\Psi_n(t_1) & 1\\ \Psi_1(t_2) & \Psi_2(t_2)\cdots\Psi_n(t_2) & 1\end{bmatrix}\times\begin{bmatrix}f_{1,0}\\f_{2,0}\\f_{3,0}\end{bmatrix} \quad (2.13)$$

This matrix equation is a modified form of the DAEM. If the fuel is heated at a constant rate, i.e. dT/dt=B, then:

$$\Psi_i(t)=\Psi_i(T)=\exp\left[-\frac{A_i}{B}\int_{T_0}^{T}\exp\left(\frac{-E_i}{RT}\right)dT\right] \quad (2.14)$$

and:

$$f_i(T)=f_{i,0}\Psi_i(T) \quad (2.15)$$

Two TGA experiments, conducted at two different heating rates, B_1 and B_2, can be used to calculate the values of E_i and A_i. For a given conversion in the two experiments, if it is assumed that the *i*th reaction is the only reaction taking place at this conversion, then:

$$f_i(B_1,T_1)=f_i(B_2,T_2) \quad (2.16\ a)$$

Therefore:

$$\Psi_i(B_1,T_1)=\Psi_i(B_2,T_2) \quad (2.16\ b)$$

Substituting for Ψ_i gives:

$$\frac{1}{B_1}\left[T_0\exp\left(\frac{-E_i}{RT_0}\right)-\frac{-E_i}{R}\int_{E/RT_0}^{\infty}\frac{\exp(-u)}{u}du-T_1\exp\left(\frac{-E_i}{RT_1}\right)+\frac{E_i}{R}\int_{E/RT_1}^{\infty}\frac{\exp(-u)}{u}du\right]=\frac{1}{B_2}\left[T_0\exp\left(\frac{-E_i}{RT_0}\right)-\frac{-E_i}{R}\int_{E/RT_0}^{\infty}\frac{\exp(-u)}{u}du-T_1\exp\left(\frac{-E_i}{RT_1}\right)+\frac{E_i}{R}\int_{E/RT_1}^{\infty}\frac{\exp(-u)}{u}du\right] \quad (2.17)$$

The above equation can then be solved for E_i. Once E_i has been found, the value of A_i can be calculated and the matrix equation in Equation 2.13 can be solved. In order to calculate A, it is assumed that each reaction reaches a particular conversion. In this case, this conversion is assumed to be:

$$X_i=1-e^{-1} \quad (2.18)$$

so:

$$\Psi_i=e^{-1} \quad (2.19)$$

and

$$ln(\Psi_i)=-1 \quad (2.20)$$

This value of Ψ corresponds to a conversion at which the rate of reaction is at a maximum, i.e. when:

$$\frac{d}{dt}\left(\frac{df_i}{dt}\right)=0 \quad (2.21)$$

However, the assumption that each reaction reaches a conversion of 63.21% does lead to a slight error in the calculation of A.

The value of A can then be calculated from Equation 2.14, using the approximation to the integral term from Equation 2.17:

$$ln(\Psi_i) = -1 = \frac{A_i}{B_1}\left[T_0 \exp\left(\frac{-E_i}{RT_0}\right) - \frac{E_i}{R}\int_{E/RT_0}^{\infty} \frac{\exp(-u)}{u}du - T_2 \exp\left(\frac{-E_i}{RT_2}\right) + \frac{E_i}{R}\int_{E/RT_2}^{\infty} \frac{\exp(-u)}{u}du\right] \quad (2.22)$$

Scott *et al* (2006) tested the algorithm on simulated TGA curves for three different types of reactions. These were a single, first order reaction, seven first order reactions and reactions with a Gaussian distribution of activation energies. Data for two different heating rates was used in order to calculate the values of f_0, E and A. In all three cases, the algorithm was able to calculate these values, which corresponded to the values used for the simulation. These values were then used to model the pyrolysis reactions at the two heating rates used for the calculation and a third heating rate. The model was a good prediction of the actual curves.

The algorithm was then applied to real TGA curves for the pyrolysis of dried sewage sludge. The kinetic parameters obtained from the algorithm allowed an excellent model fit to the data. Scott *et al* (2006) concluded that the algorithm can be used for complex solid fuels which are assumed to react with one or more first-order reactions.

2.3 Combustion

When coal is heated in an oxidising atmosphere, it loses moisture and volatiles. Homogeneous combustion of the volatile matter occurs, heterogeneous combustion of the char occurs and mineral matter is oxidised to ash (Filho & Milioli, 2008). Devolitilization is usually complete before the bulk of the char is combusted, but the two processes are not completely separated (Morgan *et al*., 1986). The reaction of coal with oxygen proceeds as follows:

$$C + O_2 \rightarrow CO/CO_2 \quad (2.23)$$

Smith *et al* (1981) conducted experiments on coal combustion using a TGA and established four different zones in which combustion occurs, characterised by four distinct activation energies. In zone I, combustion takes place in the lowest temperature range and light volatiles are released and combusted. In this zone, the rate of mass loss is controlled by the rate of

chemical reaction. In zone II, volatiles with higher molecular mass diffuse through the pores in the coal and are combusted. The reaction rate is controlled by the rate of diffusion through the pores. Zone III represents a transition between a process controlled by chemical reaction and a process controlled by pore diffusion. In zone IV, combustion occurs at higher temperatures, so it is assumed that the rate of chemical reaction is higher than the rate of diffusion. Combustion in this zone is therefore controlled by pore diffusion.

When considering the combustion of pulverised coal particles, the reaction rate of volatile matter combustion is negligible when compared to the rate of char combustion (Baranco *et al*., 2009). This is because the reaction temperature is high and coal particles are so small that diffusion through the pores happens fast enough to neglect its effect on reaction rate. For the design of pulverised fuel combustion equipment, it is therefore important that char reaction kinetics are available.

2.3.1 The Shrinking Core Model

The combustion of coal char particles is often described by the shrinking core model. The effects of chemical reaction and diffusion are considered. In this model, a burning char particle is divided into a number of concentric volume elements (Mitchell *et al*., 2007). As the particle shrinks, the reaction rate is decreased (Everson *et al*., 2006[a]). The model takes into account the initial structural properties of the coal, namely surface area and porosity, and predicts the particle's burning rate, temperature, diameter, apparent density, and specific surface area during the combustion process (Everson *et al*., 2006[a]; Mitchell *et al*., 2007). This model is commonly used to describe the combustion of high ash coals (Filho & Milioli, 2008; Sadhukhan *et al*., 2010) and Everson *et al*. (2005) found it was applicable to South African coals in particular. The reaction rate, r_s, of coal is given by the equation below:

$$r_s = \frac{dX}{dt} = k_0 \exp\left(\frac{-E}{RT}\right) {P_{O_2}}^n f(X) \qquad \text{(Everson } et\ al., 2006^{a}\text{)(2.24)}$$

where k_0 is the pre-exponential factor, P_{O_2} is the partial pressure of oxygen, n is the reaction order with respect to oxygen and f(X) is the function describing the shrinking core model.

The model is divided into the shrinking reacted core model and the shrinking unreacted core model. In the shrinking unreacted core model, a burning coal particle has an unreacted core of char with diameter D_c which changes with time. This core shrinks during the combustion process. It is completely surrounded by converted material and inert solid, except at the start

of the process (Abdel-Hafez, 1988). Equation 2.25 is used to describe the process (Everson *et al*, 2006[a]):

$$f(X) = \frac{S_0(1-X)^{2/3}}{(1-\varepsilon_0)} \qquad \text{(Everson } et\ al., 2006^{a}\text{)(2.25)}$$

Where X is the conversion of coal, S_0 is the initial surface area of the particle per unit volume and ε_0 is the initial porosity of the particle.

This phenomenon is described in Figure 2.1:

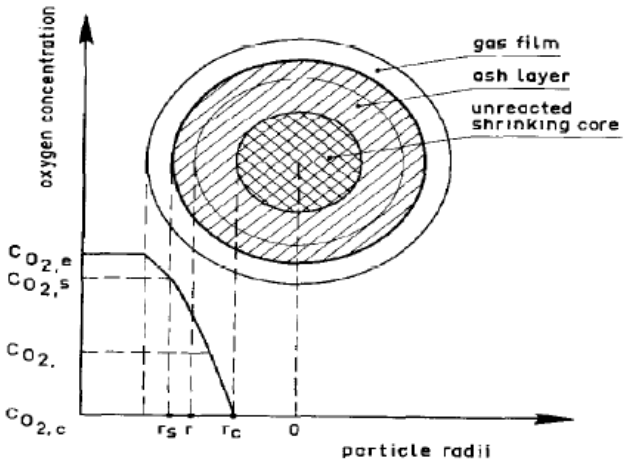


Figure 2.1: Schematic representation of a particle undergoing combustion (Abdel-Hafez, 1988)

A major shortcoming of this model is that it does not take into account the effects of pore diffusion in the char and is therefore mostly applicable to highly non-porous char (Sadhukhan *et al*., 2010).

In the shrinking reacted core model, the reaction rate is based on the particle volume. It is considered faster at the surface of the particle than inside the particle, so the carbon at the surface will react first, forming an ash layer. As the reaction proceeds, the thickness of the ash layer increases and the radius of the porous core decreases (Ishida & Wen, 1968).

2.3.2 The Random Pore Model

As volatiles are driven off from the coal, the structure of coal becomes more porous. Rapid devolatilization leads to a highly porous char while fewer pores are evolved during slow devolatilization, due to a lower volatile yield (Sadhukhan *et al*, 2009). These pores are used for gas transport and their surfaces as reaction sites. The random pore model is used to predict the pore structure and surface area during combustion.

The pore size in coal particles is not uniform. A particle is assumed to consist of microporous grains, surrounded by macropores (Wang & Bhatia, 2001). According to Wang & Bhatia (2001), reactions occur mainly in the micropores, while the macropores serve to transport gaseous reactants and products. As the reaction proceeds, the size of the micropores increases. The random pore model takes into account the structural changes in coal as it reacts.

The equation used to describe a reaction occurring according to the random pore model is given below:

$$\frac{dX}{dt} = \frac{r_s(1-X)S_0\sqrt{1-\Psi_{\mathrm{rp}}\ln(1-\mathrm{X})}}{(1-\varepsilon_0)} \qquad (Everson\ et\ al, 2008)(2.26)$$

where X is the conversion, r_s is the reaction rate given by the Arrhenius equation, S_0 is the initial surface area of the particle, ε_0 is the initial porosity of the particle and Ψ_{rp} is a characteristic of the initial char structure, given by:

$$\Psi_{\mathrm{rp}} = \frac{4\pi L_0(1-\varepsilon_0)}{{S_0}^2} \qquad (2.27)$$

where L_0 is the length of the pore per unit volume in mm^{-2}.

2.3.3 Other Combustion Models

The DAEM has less commonly been used to describe the ignition of coal. Chen (1996) used this model with the assumption of a Gaussian distribution of activation energies. The author refers to it as the Distributed Activation Energy Model of Ignition (DAEMI) and justifies its use by assuming that the particles within a coal sample have a distribution of reactivity. The difference between this model and the DAEM as discussed by Scott *et al* (2006) is that the DAEMI assumes an ignition reaction for each component in the coal as opposed to a devolatilization reaction.

Thermo-gravimetric analysis was used by Filho & Milioli (2008) in order to calculate an E and A for coal combustion. The authors assumed global first order Arrhenius kinetics. A global kinetic function was used in order to deal with the problem of individually quantifying effects such as mass transport, particle structure, reacting atmosphere and process temperature. In addition, the global kinetic takes into account the homogeneous combustion

of volatiles as well the heterogeneous combustion of solids. This method was found to be suitable for high ash Brazilian bituminous coals.

If the combustion model is known, TGA data can be used in conjunction with the reaction model to calculate the kinetic parameters. The algorithms used for these calculations often involve an integration of the rate expression. Combustion models (f(X)) and their integral forms g(X), as functions of conversion (X) have been summarised by Ebrahimi-Kahrizsangi & Abbasi (2008) and are presented in Table 2.2.

Table 2.2: Reaction rate models commonly used for solid-gas reactions and their integral forms (Ebrahimi-Kahrizsangi & Abbasi, 2008)

	Reaction Model	**Kinetic Model - f(X)**	**Integral form - g(X)**
Nucleation Models			
1	Power Law	$4X^{3/4}$	$X1/4$
2	Power Law	$X^{2/3}$	$X^{1/3}$
3	Power Law	$2X^{1/2}$	$X^{1/2}$
4	Avrami-Erofeev	$4(1- X)[-\ln(1- X)]^{3/4}$	$[-\ln(1- X)]^{1/4}$
5	Avrami-Erofeev	$3(1- X)[-\ln(1- X)]^{2/3}$	$[-\ln(1- X)]^{1/3}$
6	Avrami-Erofeev	$2(1- X)[-\ln(1- X)]^{1/2}$	$[-\ln(1- X)]^{1/2}$
Diffusion Models			
7	One-Dimensional Diffusion	$(1/2)\ X^{-1}$	X^2
8	Diffusion Control (Janders)	$2(1- X)^{2/3}[1-(1-X)^{1/3}-1$	$[1-(1- X)^{1/3}]^2$
9	Diffusion Control (Crank)	$(3/2)[\ (1- X)^{-2/3}-1]^{-1}$	$1-(2/3)\ X-(1- X)^{2/3}$
Reaction order and geometrical contraction models			
10	Mampel (first order)	1- X	-ln(1- X)
11	Second order	$(1- X)^2$	$(1- X)^{-1}-1$
12	Contracting cylinder	$2(1- X)^{1/2}$	$1-(1- X)^{1/2}$
13	Contracting sphere	$3(1- X)^{2/3}$	$1-(1- X)^{1/3}$

2.4 Model-free methods for the calculation of reaction kinetics

Since the structure of coal varies greatly, it is clear that a kinetic model based on the structure of coal would be limited in its applicability. A model-free method for the calculation of kinetic parameters would be useful for design purposes. These methods are usually based on TGA results at a constant heating rate and rely on a stage at which all reactions are considered equal. This stage is usually defined as the stage at which a fixed fraction of the initial mass of the solid has reacted (Starinck 2003). The methods are therefore referred to as isoconversion methods.

Most of these isoconversion methods are based on the assumption that the reaction rate can be expressed as the product of the Arrhenius Equation and a kinetic function as follows:

$$\frac{dX}{dt} = Af(X)\exp\left(\frac{-\mathrm{E}}{\mathrm{RT}}\right) \qquad \text{(Li \& } Tang, 1999\text{)} (2.28)$$

where A is the pre-exponential factor, X is the fractional conversion of the solid and f(X) is the kinetic function depending on the reaction mechanism. The form of the kinetic function f(X) is generally not known. If the heating rate is represented by B, the above expression can be written as follows, which is usually the starting point of these methods:

$$\int_0^X \frac{dX}{f(X)} = \frac{A}{B}\int_{T_0}^{T} \exp\left(-\frac{E}{RT}\right) dT \qquad (2.29)$$

Starinck (2003) categorised isoconversion methods as either rate-isoconversion methods, or p(y)-isoconversion methods. The rate-isoconversion methods, also known as Type A methods, make use of the reaction rate at a fixed mass fraction for various heating rates, while p(y)-isoconversion (Type B) methods rely on an approximation to the temperature integral in Equation 2.29.

2.4.1 Rate-isoconversion methods (Type A)

Rate isoconversion methods can be obtained from Equation 2.28, where taking the natural logarithms of both sides yields:

$$\ln\left(\frac{dX}{dt}\right) = \left(-\frac{E}{RT}\right) + \mathrm{A}\ln f(X) \qquad (2.30)$$

If the heating rate of the sample is considered, Equation 2.30 can be rewritten as:

$$\ln\left(\frac{dX}{dT}B\right) = \left(-\frac{E}{RT}\right) - \mathrm{A}\ln f(X) \tag{2.31}$$

Thermo-gravimetric analysis can be used to heat the sample at a linear heating rate and obtain values for the rate of mass loss at all temperatures. If the left hand side of Equation 2.31 is plotted against 1/T, the slope of the graph will provide the value of E.

One example of a rate-isoconversion method was developed by Li & Tang (1999) for the calculation of kinetics of heterogeneous reactions of solids. The authors claim that their method does not use an approximation to the temperature integral. The reaction rate is given by Equation 2.30. Integrating both sides gives:

$$\int_0^\infty ln\left(\frac{dX}{dt}\right)dX = -\frac{E}{R}\int_0^X \frac{1}{T}dX + G(X) \tag{2.32}$$

where:

$$G(X) = XlnA + \int_0^X lnf(X)dX \tag{2.33}$$

For a given conversion, assuming only one reaction is taking place at that conversion, the value of G(X) is the same at all heating rates. Therefore, plotting the integral on the left hand side against the integral on the right hand side will give a curve with slope E/R. By fitting this curve to a straight line, the value of E can be obtained. The integration is carried out numerically on the TGA data. A further advantage of this method is that instead of using a fixed heating rate, the program calculates the instantaneous heating rate from temperature *vs*. time data. This is important since Li & Tang (1999) report a difference between the actual sample temperature and the equipment program temperature of around 1 K.

2.4.2 p(y)-isoconversion methods (Type B)

Type B isoconversion methods are based on variable transformation of Equation 2.29 to the following form:

$$F(X) = \frac{A}{BR}E\int_y^{y_0} y^{-2}\exp(-y)\,dy \tag{2.34}$$

where F(X) is the integral on the left hand side of the equation and *y* is the integration variable after transformation:

$$y = \frac{E}{RT} \tag{2.35}$$

Equation 2.34 can be rewritten as:

$$lnF(X) = ln\left(\frac{A}{BR}E\right) + ln\int_{y}^{y_0} y^2 \exp(-y)\, dy \tag{2.36}$$

where the integral term on the right hand side of Equation 2.36 is termed the temperature integral. These methods then depend on an approximation to the temperature integral. The steps following this in the calculation of E are best described in the example by Everson *et al*., (2006)[a&b].

Everson *et al*., (2006)[a&b] used a p(y)-isoconversion method for determining the activation energy of char combustion from the results of TGA experiments at constant heating rates. This method was applied particularly to the combustion of coal. The reaction rate depends on the partial pressure of oxygen only and follows the power law rate equation suggested by Suuberg *et al*. (1988) and confirmed by Hurt and Haynes (2005):

$$r = k_0 \cdot \exp\left(\frac{-E}{RT}\right) P_{O_2}^n \tag{2.37}$$

where k_0 is the pre-exponential factor (also represented by A), P_{O_2} is the partial pressure of oxygen and *n* is the reaction order with respect to oxygen. The overall reaction rate needs to incorporate the structure of the coal particles and this is achieved by using a structure factor, f(X), where X is the fractional conversion of carbon. The overall reaction rate is therefore given by:

$$\frac{dX}{dt} = r\left(T, P_{O_2}\right) \cdot f(X) \qquad (\text{Everson } et\ al., 2006^{a}) \tag{2.38}$$

Since the heating rate is constant (*dT/dt=B*), multiplying both sides of Equation 2.38 by *dt/dT* and combining Equations 2.37 to 2.38 gives:

$$\frac{dX}{dT} = \frac{1}{B} k_0 \exp\left(\frac{-E}{RT}\right) P_{O_2}^n f(X) \tag{2.39}$$

Integrating Equation 2.39 results in:

$$\int_0^X \frac{1}{f(X)} dX = \frac{1}{B} k_0 P_{O_2}^n \int_{T_0}^{T} \exp\left(\frac{-E}{RT}\right) dT \tag{2.40}$$

The above equation is simplified by Flynn & Wall (1966) and used by Everson *et al*. (2006)[a&b] as:

$$F(X) = \frac{ZE}{RB} p(y) \tag{2.41}$$

where *F(X)* represents the left hand side of the equation and *Z* is:

$$Z = k_0 P_{O_2}^n \tag{2.42}$$

The temperature integral in Equation 2.40 is represented by *E/R.p(y)* after variable transformation, where y is:

$$y = \frac{E}{RT} \tag{2.43}$$

and p(y) is therefore:

$$p(y) = \frac{e^{-y}}{y} + \int_{y_0}^{y} \frac{e^{-y}}{y} dy \tag{2.44}$$

There are many approximations to p(y). The following, derived by Doyle (1962) is used by Everson *et al.* (2006)[a]:

$$\log p(y) = -2.315 - 0.457 \frac{E}{RT} \tag{2.45}$$

Substituting Equation 2.45 into Equation 2.41 gives:

$$\log[F(X)] = \log Z - \log B - 2.315 - 0.457 \frac{E}{RT} \tag{2.46}$$

TGA experiments were conducted at several heating rates by Everson *et al* (2006[a]). A particular conversion was chosen for the approximation of the kinetic parameters. At constant conversion, F(X) and Z are constant. Differentiating Equation 2.46 with respect to 1/T gives:

$$E = \frac{-R}{0.457} \frac{d \log B}{d\left(\frac{1}{T}\right)} \tag{2.47}$$

Everson *et al*. (2006)[a] plotted log(B) vs. 1/T and used the slope of this graph to calculate the value of E. A plot of log(Z) vs. log(P_{O_2}) was used to obtain the values of n and k_0. However, in order to calculate these parameters, a reaction model must be assumed.

A modification to the method of Flynn & Wall (1966) was then developed by Everson *et al* (2006[b]). In this new method, Equation 2.41 is expressed as:

$$\log\big(p(y)\big) = \log(B) - \log\left(\frac{ZE}{R}\right) + \log(F(X)) \qquad \text{(Everson } et\ al., 2006^{b}\text{)} \tag{2.48}$$

It is assumed that a plot of log(*B*) *vs*. log(p(y)) for an activation energy E and constant partial pressure of oxygen has a slope of one. The authors plotted log(B) against log (p(y)) for at different conversions and used a regression method to calculate E. A second regression was used with Equation 2.41 and the calculated value E to calculate the value of Z. A reaction model is again needed to evaluate F(X) in Equation 2.41.

It is important to note that the model-free methods presented in this section can only be used to calculate E. A reaction model is necessary to calculate other kinetic parameters. Evaluation of these parameters is simpler once the value of E is known.

2.5 Reactivity

The intrinsic reactivity of chars to oxygen is an important indicator of the burn-out properties of coal under combustion conditions (Russell *et al*., 1998). Knowledge of the reactivity of fuels is required in order to optimize the design of boiler furnaces (Cumming, 1989). Methods of measuring char reactivity to oxygen using thermo-gravimetric analysis are described in literature. These are divided into isothermal and non-isothermal methods.

Isothermal methods usually involve heating the sample to the desired temperature in an inert environment, then switching the gas to oxygen or air and holding the temperature constant. The oxygen or air concentration is increased as the char reacts. Reactivity is often defined as the time taken for the sample to reach 50% of its mass measured when the gas was switched, also called the t_{50} value.

Russell *et al*. (1998) presents a number of criticisms for the isothermal methods. The time taken for the gas switch is finite, which causes t_{50} values to be larger for more reactive samples. In addition, the first 50% of the sample's weight may not be representative of the entire sample, and allowing the sample to reach complete conversion could lead to extremely long test times.

Isothermal methods which do not make use of the t_{50} value have also been used (Li *et al*., 2010; Cai *et al*., 1996). In both studies, the char was heated to 500° C in N_2, after which the gas was switched to air. In addition, Li *et al*. (2010) measured reactivity in oxy-fuel. The reactivity was calculated using the following equation:

$$R_c = -\frac{1}{w}\frac{dw}{dt} \tag{2.49}$$

where w is the mass of the sample at time t. Cai *et al*. (1996) uses the value of R_c at the maximum rate of weight loss as the value of reactivity, while Li *et al*. (2010) prefer to use instantaneous values.

In order to overcome the issues associated with isothermal methods, Russel *et al*. (1998) proposed a method of measuring reactivity, using a thermo-gravimetric, non-isothermal method. This method claims the advantages of complete conversion in a short time and

applicability to a wide range of chars. A disadvantage is that processing of the data is not as simple as the isothermal method. It also uses an oxygen concentration which is similar to that found in certain stages of pulverized fuel combustion. In this method, the char is heated from 400°C to 900°C in oxygen at a concentration of 6.3% O_2 by volume. The data is first collected and then processed using the appropriate software, to obtain reactivity values.

Another non-isothermal method of measuring char reactivity involves the use of the derivative thermo-gravimetric (DTG) curve. This is a plot of *dw/dT* or the discreet derivative calculated at each point of the TGA curve. The temperature at the maximum of the DTG curve is used as a measure of relative reactivity. The higher the peak temperature, the less reactive the char. This method has been used by Ciuryla *et al.* (1979) and Cumming (1989). However, this method is only useful as a comparison since the peak temperature only indicates relative reactivity and is not a measure of the actual reactivity.

An important factor affecting the reactivity of char to oxygen is the thermal treatment of the coal during devolatilization (Arenillas *et al*., 2001). Chemical differences amongst coals affect their combustion mainly through their behaviour during devolatilization and the extent of devolatilization affects char reactivity (Migliavacca *et al*., 2005).

Cumming (1989) used the DTG burning profile to test the effect of pyrolysis conditions on char reactivity. The chars were prepared at temperatures ranging from 600° C to 1200° C. The two conclusions drawn from this study were that at constant temperature, the reactivities of the chars follow the same order as the reactivities of their parent coals, and that increasing the charring temperatures results in chars of decreasing reactivity.

The first conclusion is in agreement with that of Cai *et al*. (1996), who studied five coals of different rank. A wire-mesh reactor was used for the pyrolysis and combustion of the chars was carried out in a TGA under isothermal conditions. Coal samples were devolatilized at heating rates from 1K/s to 5000K/s, to temperatures between 700° C and 1500° C in hydrogen gas or helium gas at pressures ranging between atmospheric and 150 bar. The reactivity was measured as a function of devolatilization temperature, heating rate and pressure. Char reactivity was found to decrease with increasing devolatilization temperature, exhibiting a linear relationship, with the parameters dependant on coal rank. The reactivity also increased with increasing heating rate up to a 1000K/s, and then levelled off between 1000K/s and 5000K/s. This effect was also dependant on coal rank, as well as the

thermoplasticity of the coal. Under hydropyrolysis conditions, char reactivity decreased with small increases in pressure.

Thermo-gravimetric experiments were conducted by Ciuryla *et al*. (1979) on four North American coals and their chars, in order to obtain information on their reactivities. The coals were first pyrolized and the resulting chars heated in air. Samples of the raw coal were also heated in air. The maximum rate of devolatilization was used as an indicator of reactivity. The study showed that coal rank is the most important factor influencing the reactivity of coal and chars. It was also noted that each char was more reactive than its parent coal.

The pyrolysis and combustion characteristics of coal were studied by Li *et al*. (2010). The aim of this work was to determine the effects of drying and binderless briquetting of coal on its reactivity. The char was formed in a drop tube furnace under pyrolysis and gasification conditions. Reactivity of the char under air and oxy-fuel conditions was investigated. The rate of mass change with time was used as a measure of specific reactivity. The study found that drying and briquetting caused changes in the structure of the coal, which in turn decreased the reactivity.

2.6 Conclusion

From this chapter, it can be seen that many models are available in literature to describe coal conversion processes. It has been found that the DAEM provides an accurate description of the pyrolysis process (Scott *et al*., 2006). According to this model, coal decomposes according to a number of first order reactions, each with a distinct E. Mathematical inversion of this model, applied to TGA data, allows the calculation of the number of reactions as well as the E and A for each reaction.

It has been noted that when calculating the E, the inversion algorithm does not rely on any particular form of the curve. It is therefore considered a "model-free" method of calculation. However, the second step of the algorithm, in which the A factor is calculated, does rely on a model. In order to apply the algorithm to combustion data, an appropriate combustion model needs to be used. One of the more commonly used models for coal combustion is the shrinking core model.

In this research, the algorithm was applied to TGA data for coal combustion, to test whether it could calculate the E of combustion. It was then investigated whether the DAEM could be

used in conjunction with a structural model for combustion to calculate the A. The particular model used was the shrinking core model, as described by Everson *et al*. (2006[b]).

Chapter 3: Research Methodology

3.1 Materials

Experiments were conducted on a South African coal from the Witbank coalfield. Results of the proximate analysis and petrography of the sample are available in Table 3.1 and Table 3.2 respectively. The procedures for the proximate and petrographic analyses are given in Appendix A2. The coal sample is a high ash, inertinite-rich, medium rank C coal. For the pyrolysis and combustion reactions, ultra-high purity nitrogen and oxygen gases were used respectively.

Table 3.1: Proximate Analysis of a Witbank coal sample

Component	**Composition (Mass %)**
Moisture	3.0
Volatile Matter	16.9
Fixed Carbon	46.1
Ash	34.1

Table 3.2: Petrographic Analysis of a Witbank coal sample

Maceral Group	**Composition (Volume %)**
Vitrinite	10.2
Liptinite	3.8
Inertinite	35.8
Total reactive macerals	17
Total mineral matter	50.2
Reflectance of Vitrinite (RoVmr %)	0.6
Rank	Medium Rank C

3.2 Sample Preparation

The coal sample first underwent stage crushing to reach a size of -3mm, rendering the sample suitable for secondary crushing. Following the stage crushing, a coned and quartered portion of the sample was crushed in a Retsch ZM 200 centrifugal mill. Secondary crushing reduced the particle size to -150 microns. A portion of -1mm particles was kept aside for coal

petrography. Details of the sample preparation for petrographic analysis are given in Appendix A2.

3.3 Equipment

A TGA measures the mass change of a sample in relation to temperature as it is subjected to a specified heating programme in a controlled atmosphere. The equipment consists of a sample pan loaded on to a highly sensitive mass balance, a furnace and a thermocouple. Two TGAs were available for this work, one equipped with a standard furnace and the other with a high temperature furnace.

3.3.1 Perkin-Elmer series STA 600: Standard Furnace

The Perkin-Elmer TGA contains a standard furnace, which can be heated to a temperature of 1000° C. However, the highest temperature that samples were heated to was 900° C in order to avoid burnout of the furnace. The heating rates used ranged from 5 K/min to 80 K/min. A cooling unit was connected to the TGA in order to cool the equipment between runs. Aluminium Oxide crucibles were used for loading the samples. A schematic diagram of the equipment is presented in Figure 3.1, courtesy of Perkin-Elmer. The TGA was linked to a computer loaded with Pyris software, which was used to control the equipment and display the results of the experiments. Further specifications of the equipment are given in Table A1, Appendix A1.

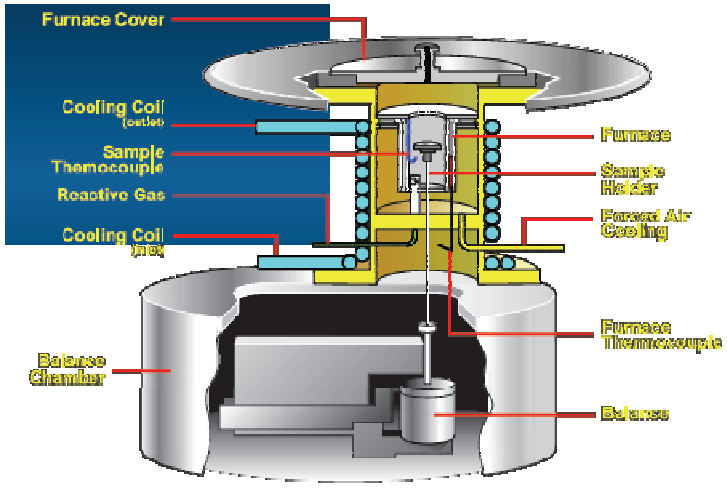


Figure 3.1: Schematic diagram of Perkin-Elmer STA 600 TGA (courtesy of Perkin-Elmer)

3.3.2 TA Instruments series Q600 SDT: High Temperature Furnace

The TA Q600 SDT is a high temperature TGA purchased for the purposes of this project. This TGA is equipped with a high temperature furnace, which can reach a temperature of 1500° C. Again, samples were only heated to 1400° C. The mass balance contains two beams, one for the sample pan and one for the reference pan. Aluminium Oxide sample pans were also used. The TGA does not have a cooling unit, but uses compressed air to cool the furnace between runs. The TGA was placed on a granite slab with anti-vibration rubber legs. The equipment is shown in Figure 3.2, courtesy of TA Instruments. The equipment's built-in computer was interfaced with a desktop computer loaded with Thermal Advantage software, which was used to set up and control the runs. The analysis software was also loaded onto the desktop computer. Equipment Specifications can be found in Table A2, Appendix A1.

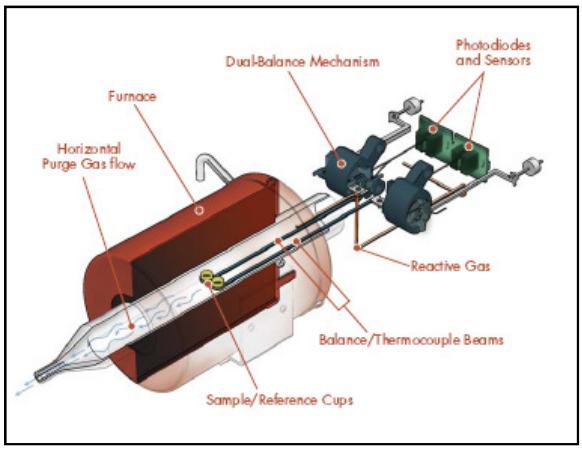


Figure 3.2: TA Instruments Q600 TGA balance and furnace (courtesy of TA Instruments)

3.3.3 Gas Lines

Gas cylinders containing oxygen and nitrogen of ultra high purity were connected via gas lines to the equipment. Valves were used to control the outlet pressure of the gases. The flowrate of the gases into the equipment was controlled by the software. The software is also able to switch between the gases.

3.4 Procedure

In this work, kinetic analysis done on the pyrolysis of coal and the combustion of coal and char. Chars were prepared in the TGA's used for combustion under fixed pyrolysis conditions. Details of the experimental procedures for each piece of equipment are provided.

3.4.1 Perkin-Elmer series STA 600

Prior to conducting a run on the TGA, the gas lines were opened, the TGA, cooling unit and computer were switched on and the Pyris software was opened.

The empty crucible was heated to a temperature of 373 K (100°C) in nitrogen. The purpose of heating the crucible was to remove any moisture which may have been present in the TGA, so as not to give an inaccurate indication of the sample moisture. The nitrogen purge was intended to remove any fine particles which may have settled in the crucible. After purging the crucible at 373 K for two minutes, it was cooled down to 303 K. The crucible mass was set to zero. The crucible was then removed from the TGA and the sample was placed inside it. It was then dropped gently into the TGA, taking precaution not to place too much pressure on the balance stem. The ideal sample mass for the TGA is 10-15 mg. Once the sample mass reading had stabilised, the weight percent was set to 100 %. The details of the experimental runs were set up with the software as follows:

(a) Pyrolysis

1. Select nitrogen gas at a flowrate of 40 ml/min.
2. Heat the sample at specified heating rate from 303 K to 1173 K.
3. Hold at 1173 K for 2 minutes.
4. Stop the run.

(b) Char Preparation

The procedure for char preparation was the same as that for pyrolysis, except that a fixed heating rate of 15 K/min was used.

(c) Combustion

1. Set the weight percent to 100 %.
2. Select oxygen at a flowrate of 40 ml/min
3. Heat the sample at specified heating rate from 303 K to 1173 K.
4. Hold at 1173 K for 2 minutes.
5. Stop the run.

The heating rates used varied between 5 K/min and 80 K/min. For certain runs, the samples were only subjected to pyrolysis. Readings of mass and temperature were taken every 0.5 seconds.

3.4.2 TA Instruments series Q600 SDT

Since this TGA was purchased for the project, installation, commissioning and calibration of the TGA formed part of this work. This included weight, temperature and heat flow calibration. Prior to conducting runs, the gas line valves were opened and the software was opened. The furnace was opened using the command on the TGA touch screen and the sample and reference pans were loaded onto the balance beams. The tare command was then used to set the pan weights to zero. The sample pan was removed and the sample placed into the pan, after which the pan was replaced and the furnace closed. The experimental runs were carried out as follows:

(a) Pyrolysis

1. Select nitrogen gas at a flowrate of 100 ml/min.
2. Equilibrate the temperature for 10 minutes.
3. Heat the sample at specified heating rate to 1573 K.
4. Hold at 1573 K for 10 minutes.
5. Switch on air cool
6. Equilibrate at 303 K
7. Stop the run.

(b) Char Preparation

The procedure for char preparation was the same as that for pyrolysis, except that a fixed heating rate of 15 K/min was used.

(c) Combustion

1. Select Oxygen gas at a flowrate of 60 ml/min.
2. Equilibrate the temperature for 10 minutes.
3. Heat the sample at specified heating rate to 1173 K.
4. Hold at 1173 K for 10 minutes.
5. Switch on air cool
6. Equilibrate at 303 K.
7. Stop the run.

Due to limitations of the furnace, the highest heating rate that could be used for pyrolysis was 20 K/min. Higher heating rates could possibly cause damage to the furnace above 1273 K. For combustion in this TGA, the heating rates used were 1 K/min and 5 K/min. This is

because the furnace was unable to control the exothermicity of reactions at higher heating rates, resulting in a temperature decrease shown on the TGA curves.

3.5 Data Analysis and Modeling

Data obtained from the TGA experiments was copied to a personal computer for further processing and modelling, using Matlab software. The calculations of the kinetic parameters are based on the algorithm used by Scott *et al*. (2006). The major difference between the methods is that, in this work, the number of TGA points is reduced by interpolation before the calculation. This is done in order to simplify the calculation and reduce computing time on an ordinary computer. The TGA data for the two intermediate heating rates was used for the calculation of the kinetic parameters of pyrolysis and combustion. A flow diagram of the method used for the modeling is given in Figure 3.3. The Matlab codes for each of these steps can be found in Appendix B.

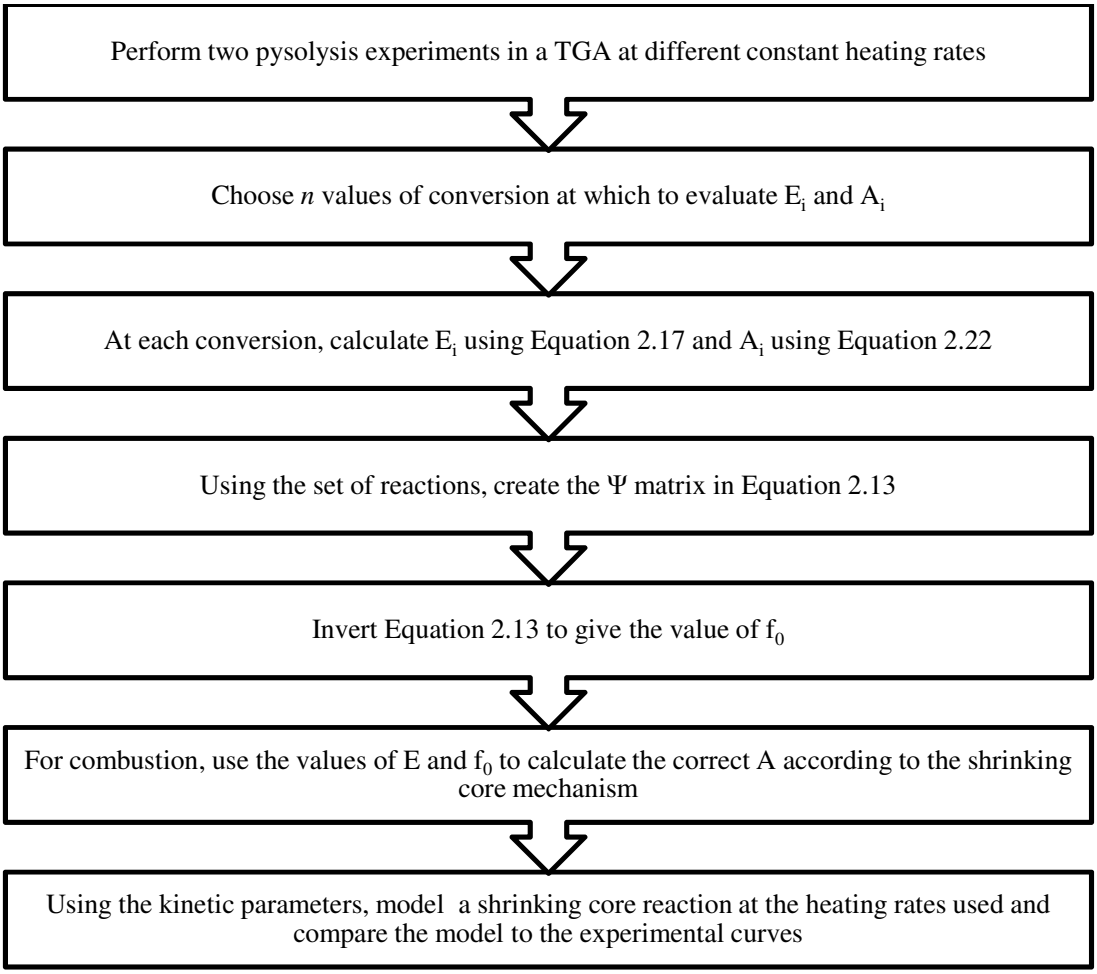


Figure 3.3: Flow Diagram of algorithm steps (Scott *et al*., 2006)

The kinetic parameters obtained from the algorithm were then used to model conversion process at the two heating rates not used in the calculation. For pyrolysis, first order reactions were used for the modelling; and for combustion, the shrinking core model was used. The model fits were compared to experimental data in order to test whether the shrinking core model is suitable for the description of combustion of a South African coal. It should be noted that the actual combustion model was a secondary interest in this work. The major focus was the use of the DAEM as a model-free method to calculate E.

Chapter 4: Theoretical Development

4.1 Introduction

Prior to the commencement of experiments, thermo-gravimetric data was simulated with known kinetic parameters using programmes developed in Matlab™. The purpose of this was to test whether the DAEM algorithm could correctly calculate the kinetic parameters of coal conversion reactions. The simulation provided a controlled environment and consistent profiles could be created for heating rates unachievable in laboratories.

For the simulation of TGA curves, values for the $f_{i,0}$, E_i and A_i of each reaction need to be specified. The heating rates of each reaction also need to be specified. Details of the Matlab™ code used for the simulations are provided in Appendix B.

Once the TGA curves for a reaction have been created, the DAEM algorithm can be applied to any two curves with different heating rates. The algorithm first reduces the TGA data sets in order to simplify computation. A number of conversions or reactions need to be selected at which to calculate the kinetic parameters. The algorithm chooses these conversions at equally spaced intervals and finds the temperatures associated with each conversion by interpolation. At each conversion, Equation 2.17 is used to calculate the activation energy of the reaction and Equation 2.22 is then used to calculate the pre-exponential factor. This equation is based on the assumption that each first-order reaction reaches a conversion of 63.21% (Scott *et al.*, 2006). These two kinetic parameters for each reaction can then be used to create the matrix Ψ. Equation 2.13 is then inverted to yield the value of f_0, the initial mass fraction associated with each component. The code used for the calculations is discussed further in Appendix B.

4.2 Simulated first-order reactions

4.2.1 Single reaction

In the first simulation, a TGA curve was created for a single, first-order reaction of a fuel assumed to contain no ash. The values of the kinetic parameters used for the simulation are given in Table 4.1.

Table 4.1: Kinetic parameters used for simulation of pyrolysis with a single, first-order reaction

Kinetic Parameter	Value used for Simulation
f_0	[1 0]
E (KJ/mol)	135.2
A(min^{-1})	1.1×10^{10}

Curves were generated for pyrolysis at heating rates of 0.001K/min, 10 K/min, 1000 K/min and 10 000 K/min. These curves are shown in Figure 4.1.

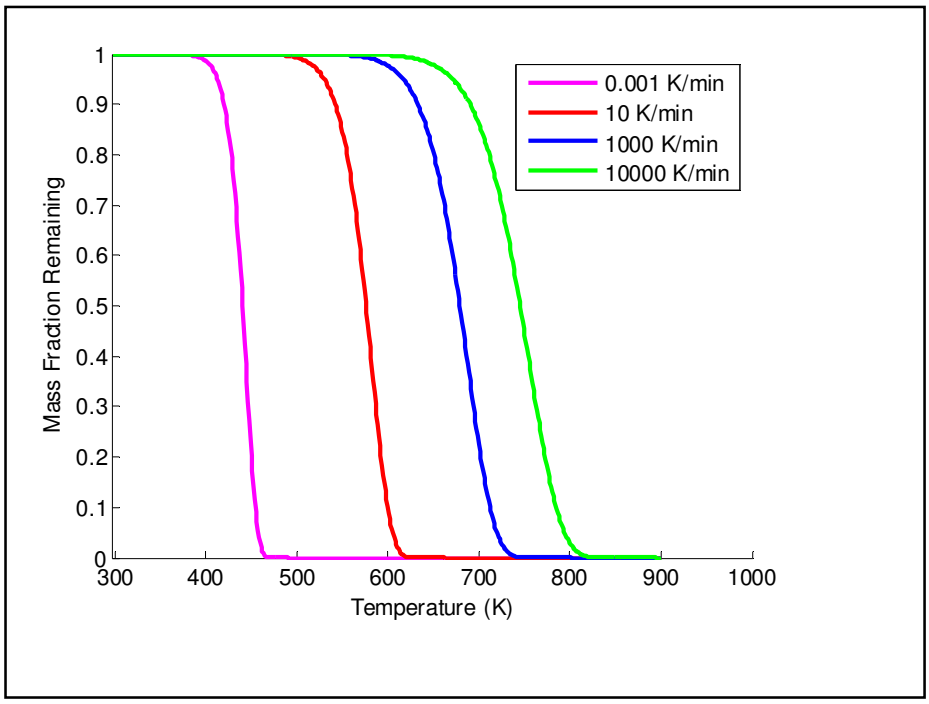


Figure 4.1: Simulated TGA curves for pyrolysis with a single, first-order reaction at different heating rates

For these curves, the discreet derivatives at each point were calculated in order to provide the DTG curves, shown in Figure 4.2. The area under a peak of DTG curve corresponds to the value of f_0.

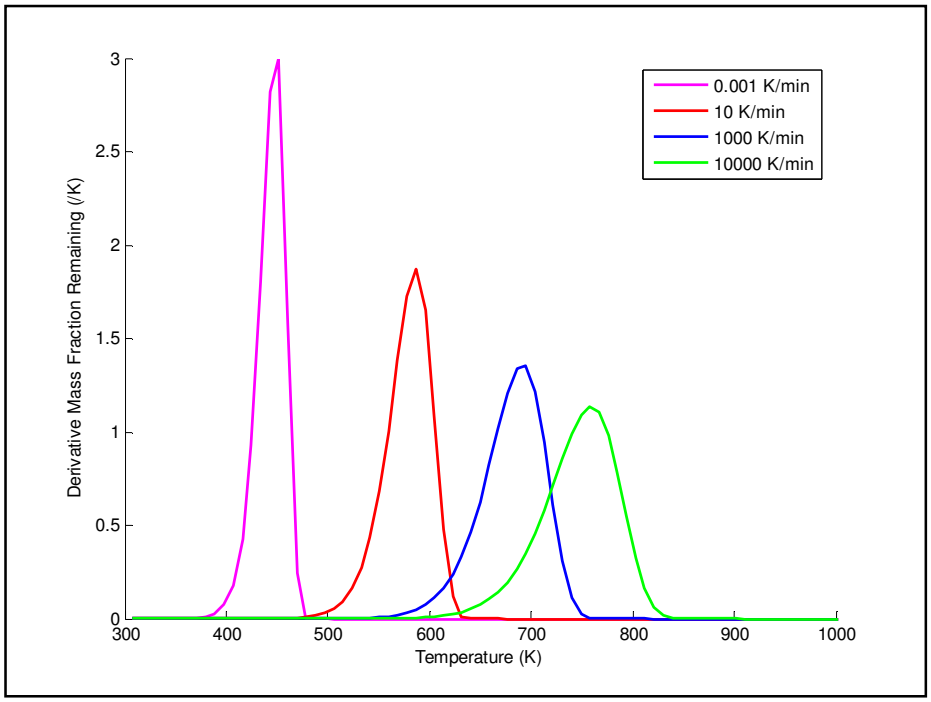
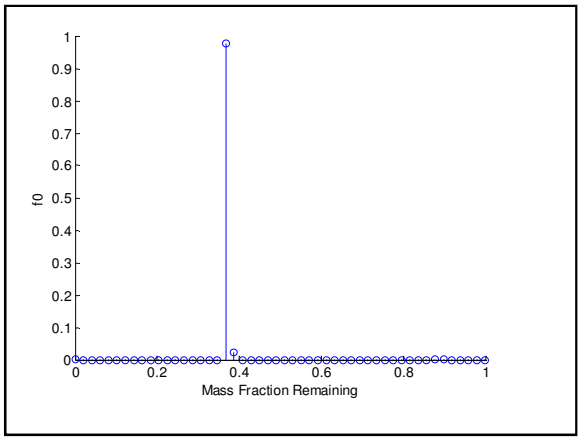


Figure 4.2: Simulated DTG curves for pyrolysis with a single, first-order reaction at different heating rates

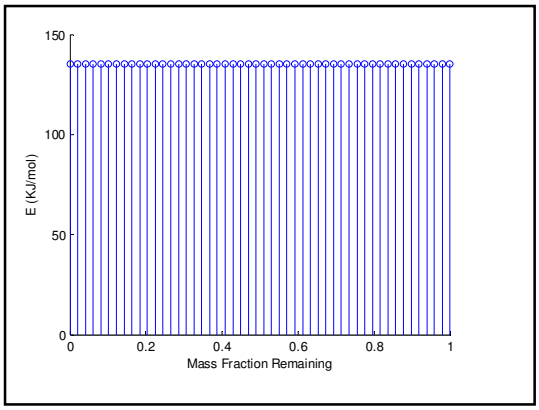
As the heating rate increases, the curve shifts to the right, as seen in Figure 4.1 and Figure 4.2. This indicates that each event takes place at a higher temperature as the heating rate increases. The area under the DTG curve corresponds to the value of $f_{i,0}$, which is 1 in this case.

The generated data for the heating rates of 10 K/min and 1000 K/min was then fed into the algorithm to test whether the original values of E and A could be reproduced. The values of f_0, E and A obtained at each of the 50 conversions are plotted in Figure 4.3.

(a)



(b)



(c)

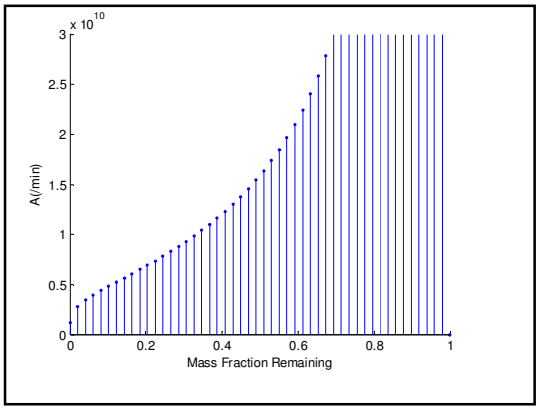


Figure 4.3: Kinetic parameters calculated for simulated single, first-order reaction (a) Initial mass fraction of each component (b) Activation Energy of each reaction (c) Pre-exponential factor of each reaction

For this particular example, 50 candidate reactions were chosen, so 50 values of E and A were calculated. The number of reactions actually occurring is determined by the number of non-zero f_0's calculated by the DAEM algorithm. Figure 4.3 (a) shows that the value of f_0 is 0 at all points except two, where the mass fraction remaining is 0.368. Summing these two values gives a value of 1, corresponding to a single reaction. Only the values of E and A at this conversion are assumed to be the correct values. Even if the calculated value of E or A for a particular reaction is incorrect, the mass allocated to that reaction is set to zero. This is done automatically in the algorithm and does not depend on any graphical methods. Figure 4.3 (b) and (c) show that at a conversion of 0.368, the values of E and A recovered by the algorithm are the correct values. These values are provided in Table 4.2 (a):

Table 4.2 (a): Comparison of original kinetic parameters and those recovered by the DAEM for a simulated single, first-order reaction using heating rates of 10K and 1000K

Parameter	Recovered Value	Original Value	% Error
f_0	0.9999	1	0.01
E (KJ/mol)	135.1974	135.2	0.0019
A(min^{-1})	1.13×10^{10}	1.1001×10^{10}	2.80

Table 4.2 (a) indicates an excellent correlation between the original parameters and those recovered by the DAEM algorithm. The error in E is 0.0019% and the error in A is 2.8%. Both of these are considered acceptable values. Different sets of heating rates were then used in the DAEM algorithm to investigate the effect on calculated parameters. The parameters obtained from these heating rates are shown in Table 4.2 (b).

Table 4.2 (b): % Error in parameters recovered by the DAEM for a simulated single, first-order reaction using different heating rate combinations

Heating Rates (K/min)	% Error in f_0	% Error in E	% Error in A
0.001 & 10	0.05	0.01	2.22
0.001 & 1000	0.05	0.00	2.37
0.001 & 10000	0.04	0.00	2.40
10 & 10000	0.03	0.00	1.99
1000 & 10000	0.04	0.01	1.74

The values in Table 4.2 (b) show that all combinations of heating rates yield similar results and good accuracy in the calculation of kinetic parameters. From this point forward, only the two middle heating rates will be used in DAEM calculations. The purpose of this is to test whether the DAEM is capable of extrapolation to higher and lower heating rates.

The recovered parameters were then used to simulate TGA and DTG curves at the four heating rates used above. These were then compared to the original TGA curves. This provides an additional test of how well the DAEM is able to model coal pyrolysis reactions at the heating rates used in the algorithm and at higher and lower heating rates. The comparison of the original curves and model fits are shown in Figure 4.4 and Figure 4.5.

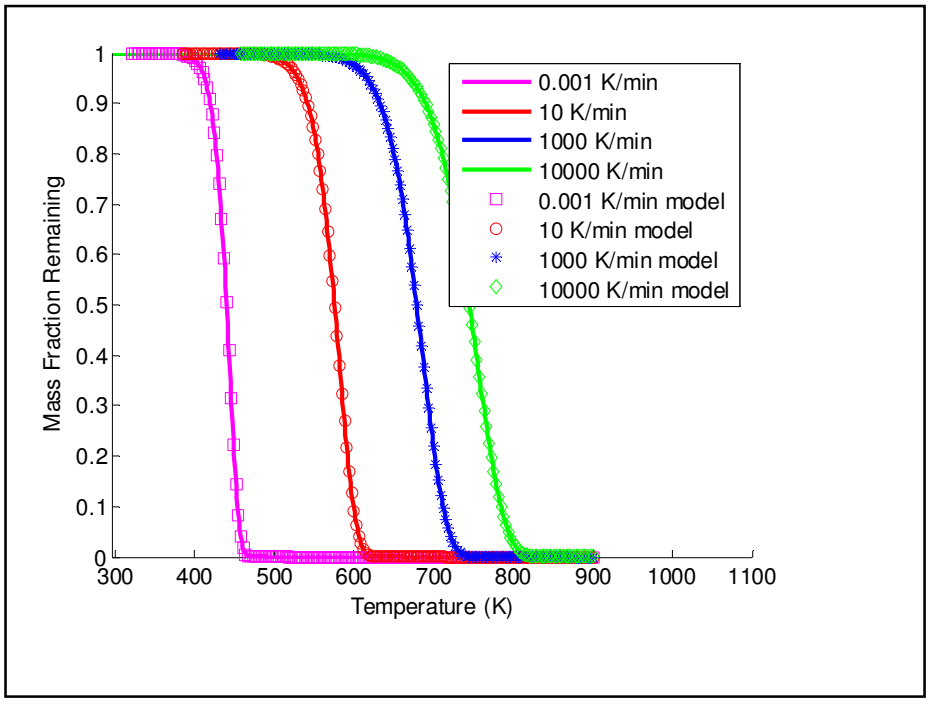


Figure 4.4: Simulated TGA curves for pyrolysis with a single, first-order reaction at different heating rates, with DAEM predictions for each of these heating rates

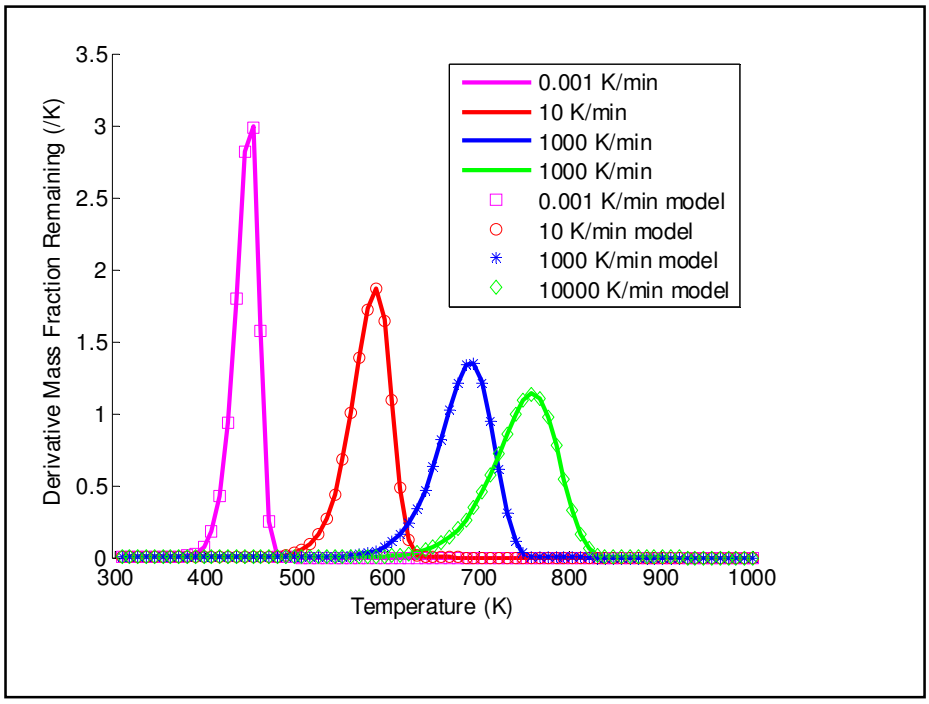


Figure 4.5: Simulated DTG curves for pyrolysis with a single, first order reaction at different heating rates, with DAEM predictions for each of these heating rates

Figure 4.4 and Figure 4.5 show that the modeled curves are an excellent fit to the original TGA and DTG curves. This indicates that the kinetic data obtained from TGA curves at two different heating rates can be used to model a first order reaction at higher and lower heating rates.

4.2.2 Seven Reactions

For the second simulation test, TGA curves were created for the pyrolysis of a fuel with no ash decomposing according to seven first order reactions. The values of E and A are the same values used by Scott *et al*. (2006) and are provided in Table 4.3. The initial mass fractions of each component are equally distributed.

Table 4.3: Kinetic parameters used for simulation of pyrolysis with seven first-order reactions

Kinetic Parameter	**Value used for Simulation**
f_0	[1/7 1/7 1/7 1/7 1/7 1/7 1/7 0]
E (KJ/mol)	[150 175 190 200 225 250 275]
A(min^{-1})	[10^{15} 10^{15} 10^{15} 10^{15} 10^{15} 10^{15} 10^{15}]

TGA and DTG curves were again generated for pyrolysis at heating rates of 0.001K/min, 10 K/min, 1000 K/min and 10 000 K/min. These curves are shown in Figure 4.6 and Figure 4.7.

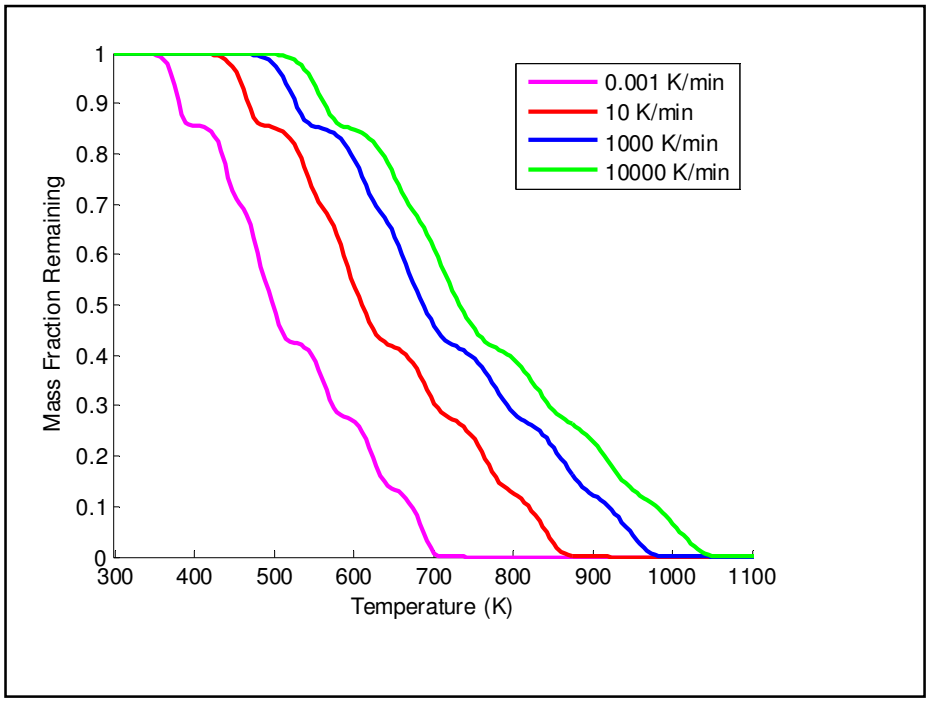


Figure 4.6: Simulated TGA curves for pyrolysis with seven first order reactions at different heating rates

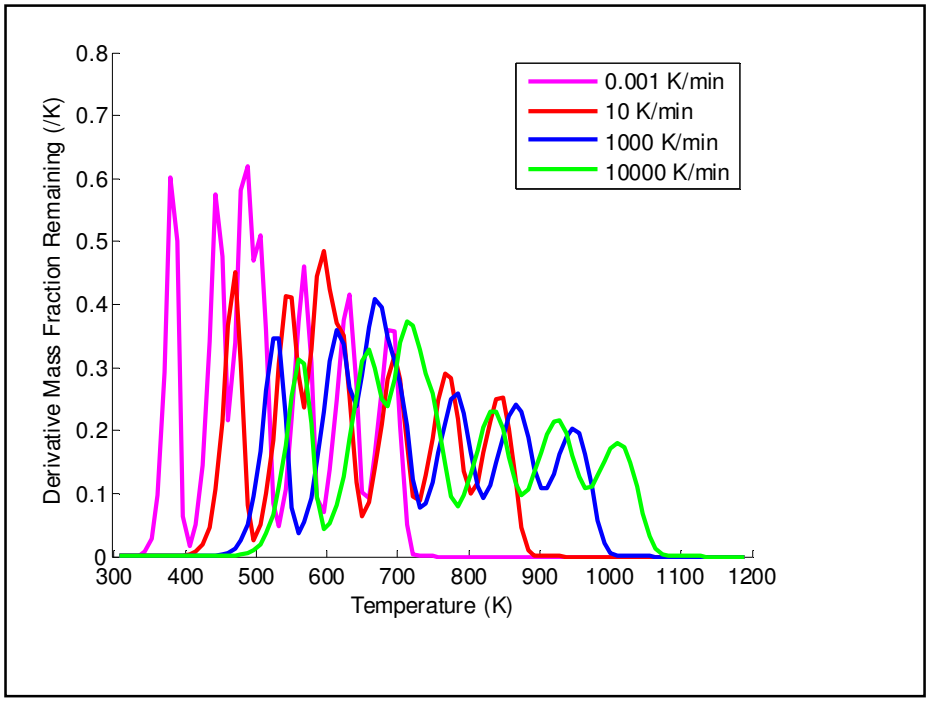
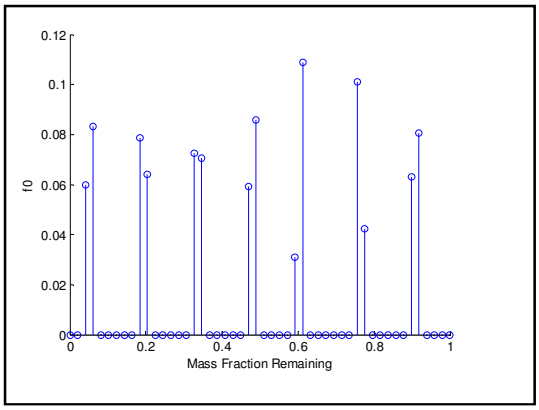


Figure 4.7: Simulated DTG curves for pyrolysis with seven first order reactions at different heating rates

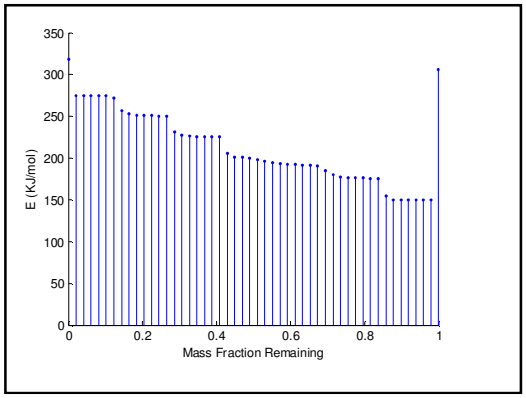
It is again noted that the curves shift to the right as the heating rate increases and that there is no intersection of the curves. The derivative curve has 7 distinct peaks, corresponding to the 7 reactions as stated in the simulation. Figure 4.7 also shows that these 7 peaks become less distinct at higher heating rates. Lower heating rates thus provide a more high resolution picture of the steps involved in the reaction process. This is important as peaks may appear merged at higher heating rates and can be interpreted as a single event. An advantage of the DAEM is that it accurately calculates the number of peaks by discretization of the TGA profile. The number of peaks is given by the number of non-zero values for f_0.

The TGA points for the two heating rates of 10 K/min and 1000 K/min were used in the algorithm to calculate the kinetic parameters. As in the previous example, 50 candidate reactions were chosen at which to evaluate E and A. The values of f_0, E and A obtained at each chosen conversion are plotted in Figure 4.8.

(a)



(b)



(c)

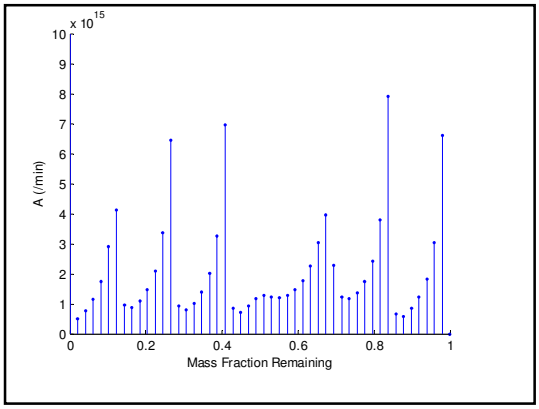


Figure 4.8: Kinetic parameters calculated for seven simulated first-order reactions (a) Initial mass fraction of each component (b) Activation Energy of each reaction (c) Pre-exponential factor of each reaction

The value of f_0 was automatically set to 0 for any reaction that was not actually taking place from the 50 candidate reactions. It can be seen from Figure 4.8(a) that there are effectively 7 conversions at which f_0 is not equal to 0. At each conversion, the two values of f_0 are added since it is assumed that they form part of one reaction. The values of E and A need to be

considered at these points only, since these are the only points at which a reaction happens. The values of f_0, E and A for the 7 conversions are shown in Table 4.4.

Table 4.4: Comparison of original kinetic parameters and those recovered by the DAEM for seven simulated first-order reactions

Reaction	f_0	Sum of f_0	Original f_0	E (KJ/mol)	Average E	Original E	A (min^{-1})	Average A	Original A
1	0.081	0.144	0.143	150.13	150.16	150	1.23E+15	1.04E+15	1E+15
	0.063			150.19			8.45E+14		
2	0.042	0.143	0.143	176.36	176.60	175	1.74E+15	1.552E+15	1E+15
	0.101			176.85			1.36E+15		
3	0.109	0.140	0.143	192.35	192.62	190	1.77E+15	1.62E+15	1E+15
	0.031			192.88			1.47E+15		
4	0.086	0.145	0.143	199.91	200.28	200	1.18E+15	1.06E+15	1E+15
	0.059			200.65			9.34E+14		
5	0.071	0.144	0.143	225.74	225.93	225	1.40E+15	1.21E+15	1E+15
	0.073			226.13			1.02E+15		
6	0.064	0.143	0.143	251.00	251.25	250	1.46E+15	1.28E+15	1E+15
	0.079			251.50			1.09E+15		
7	0.083	0.143	0.143	274.74	274.74	275	1.15E+15	9.68E+14	1E+15
	0.060			274.74			7.81E+14		

It is clear from these results that the algorithm is able to regenerate the original kinetic parameters used for the simulation. The error in the recovered values of E is range from -0.09% to +1.38%. The recovered parameters were then used to model the reaction at the different heating rates and the model was compared to the simulated data. The comparison is presented in Figure 4.9 and Figure 4.10

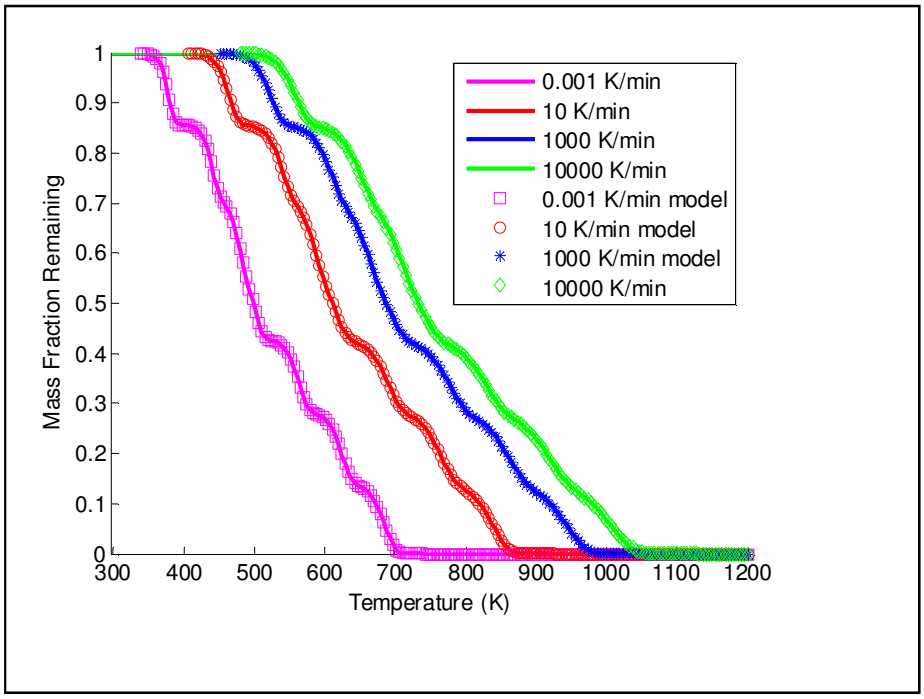


Figure 4.9: Simulated TGA curves for seven first-order reactions at different heating rates, with DAEM predictions for each of these heating rates

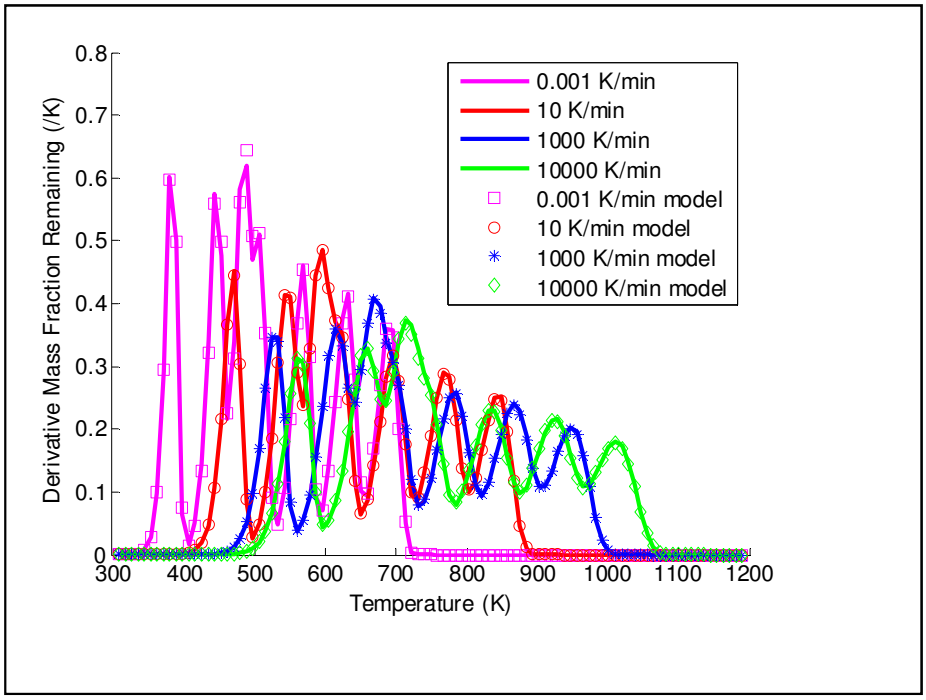


Figure 4.10: Simulated DTG curves for seven first order reactions at different heating rates, with DAEM predictions for each of these heating rates

It can be seen from Figure 4.9 and Figure 4.10 that the model fits the data well for the two heating rates used in the calculation of the kinetic parameters. The model is also able to use these parameters to predict the curves at lower and higher heating rates.

As is evident from the first two simulation examples, the DAEM can be used to model single-step and multiple-step processes, while the method used by Everson *et al*. (2010) is only applicable to processes which can be characterised as single thermal events. This provides the DAEM with a major advantage in the modelling of solid-gas reaction kinetics. The modelling of multiple-step processes is possible because the mass loss vs. temperature profile is split up into sections, or discretized. Each section is effectively a temperature interval, and therefore corresponds to an f_0 value or the area under a peak of the DTG curve. The discretization of the function is achieved in the algorithm by choosing a number of reactions. Since it is assumed that only one reaction dominates at a particular temperature, this is equivalent to choosing a number of conversions.

The problem with discretization of the function comes up when two reactions happen closely in a particular temperature interval. The activation energy predicted will then likely be an average of the activation energies for each reaction and it may be wrongly interpreted as a single event. However, this problem can be overcome by decreasing the size of the increments, or choosing a higher number of conversions. This can then be easily handled by the DAEM.

Another advantage of using the DAEM is that it can predict curves at high heating rates, similar to those experienced in industry, as well as at low heating rates. This is clear from the curves presented in Figure 4.4 and Figure 4.9. In addition, Scott *et al*. (2006) found that the model can be used for a continuous distribution of activation energies and for a discrete set of reactions. This is because the model assumes a finite number of reactions, but this number is large enough to approximate a continuous distribution of activation energies (Scott *et al*., 2006).

4.2.3 Single reaction with variable heating rates

The next step was to investigate the effect of the constant heating rate assumption on the DAEM algorithm calculations. In real TGA experiments seen in Chapter 5 and Chapter 6, it has been noted that there is some discrepancy between the actual sample temperature and that specified by the TGA program. The sample is therefore not exposed to the actual heating rate specified by the programme. Although the difference in temperatures may be small, the

difference in instantaneous heating rates at that particular temperature may be large. This affects the calculations because the assumption of a constant heating rate would not be valid. Simulation of TGA curves with variable heating rates was carried out to test this effect.

A single, first-order reaction was simulated, in which the heating rates followed the arbitrary profiles shown in Figure 4.11. The values of E and A used for this simulation were 135.2 KJ/mol and 1.1×10^{10} min^{-1} respectively.

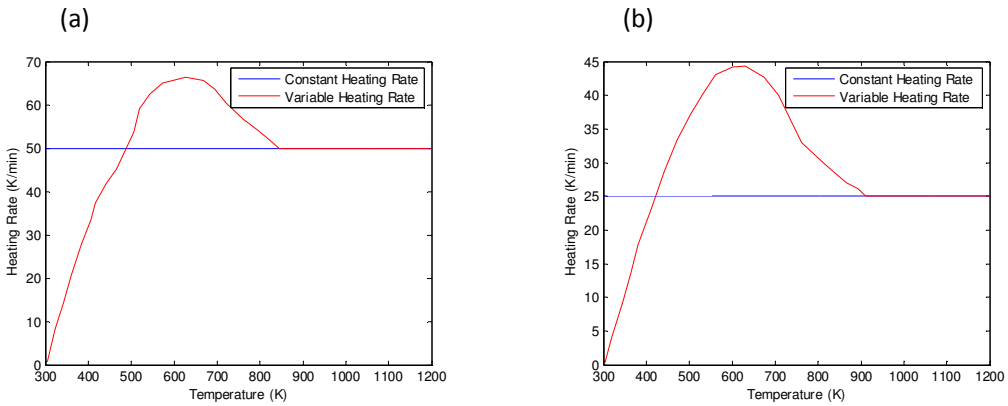


Figure 4.11: Heating rates vs. temperature profiles used for simulation of TGA data

The chosen heating rate profiles had asymptotes at 25 K/min and 50 K/min respectively, so the TGA curves will be referred to as such. The simulated TGA curves for the variable heating rate profiles are plotted in Figure 4.12 below:

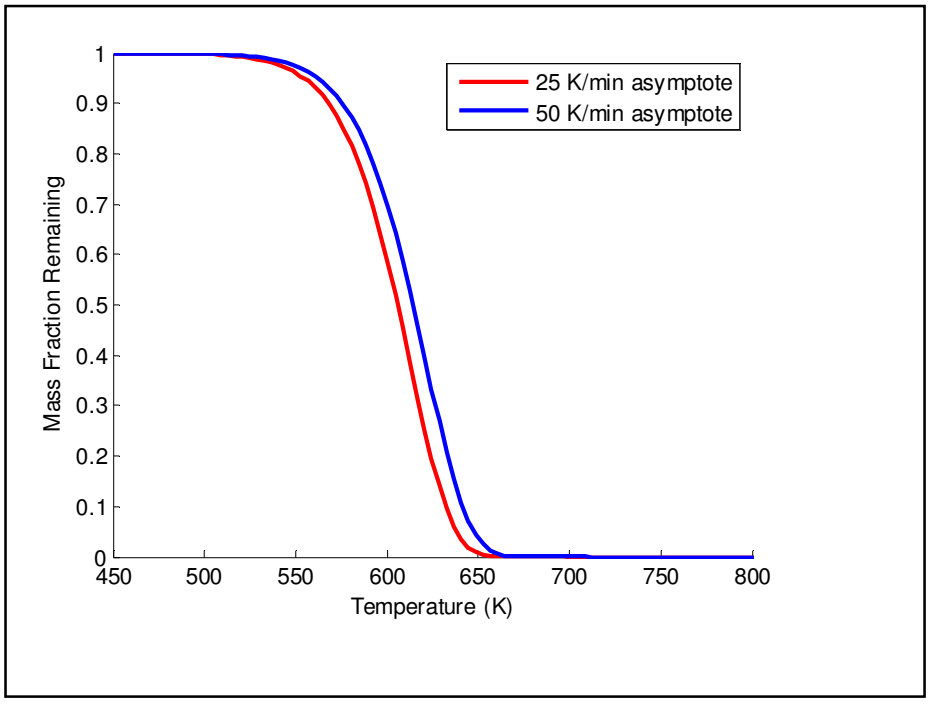


Figure 4.12: Simulated TGA curves for pyrolysis with a single, first-order reaction at variable heating rates

The DTG curves for the two TGA curves are plotted in Figure 4.13:

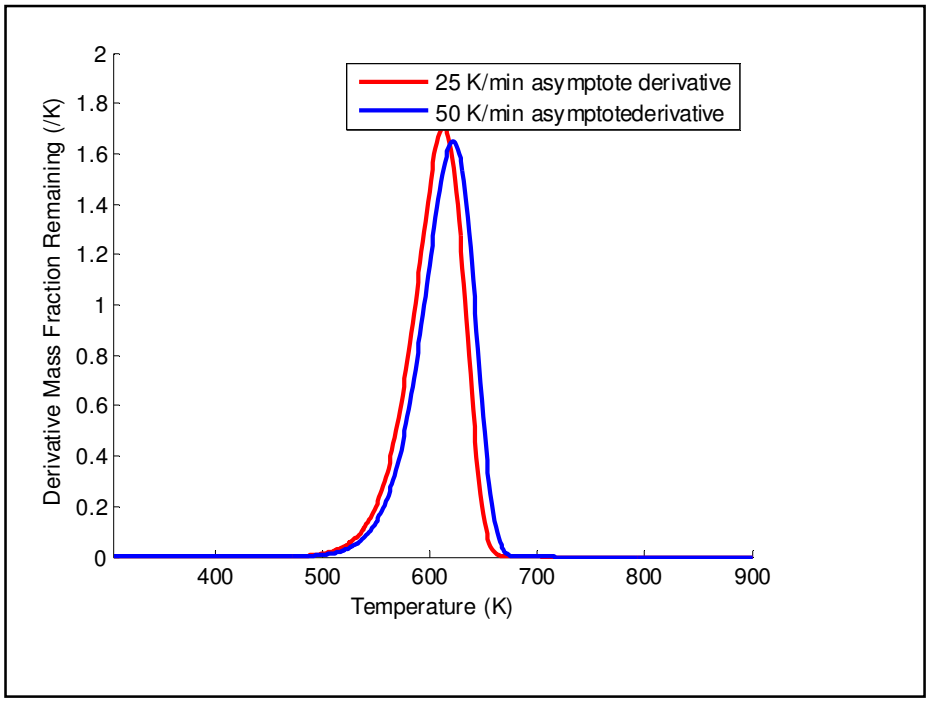


Figure 4.13: Simulated DTG curves for pyrolysis with a single, first-order reaction at variable heating rates

The derivative curves exhibit a single peak, which indicates that only one reaction is occurring.

The simulated curve for the lower heating rate was then compared to a curve for a first order reaction at a constant heating rate of 25 K/min. This is shown in Figure 4.14.

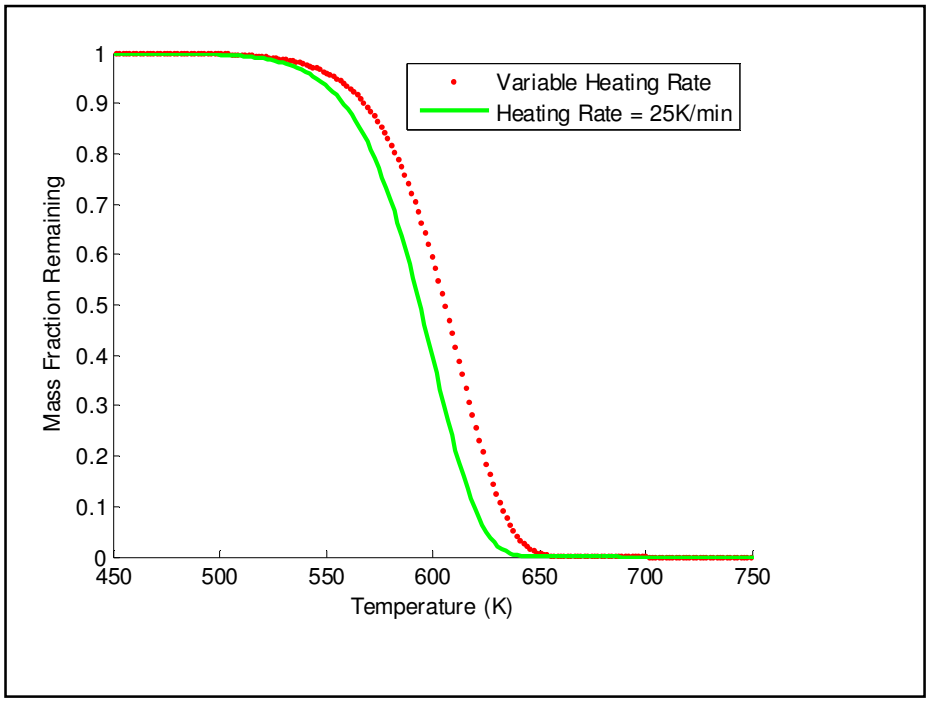


Figure 4.14: Simulated TGA curves for pyrolysis with a single, first order reaction at a variable heating rate and constant heating rate of 25 K/min

Figure 4.14 shows that there is a significant difference between the constant and variable heating rate curves. This indicates that if a constant heating rate is assumed, the model will not necessarily fit the experimental results well. Inaccurate results are obtained even though the sample and programme heating rates do become equal after a particular amount of time. In the case of this particular simulation, the heating rates merge at a temperature of 900 K. However, the reaction is already complete at that temperature, so the constant heating rate assumption would not be valid.

Figure 4.11 (a) shows that the actual heating rates between temperatures of 500 K and 900 K are higher than 25K/min. Curves were then plotted for higher constant heating rates to test whether these could better approximate the variable heating rate curve. Values of 35 K/min and 45 K/min were chosen to simulate curves for comparison to the variable rate curve. The comparisons are shown in Figure 4.15.

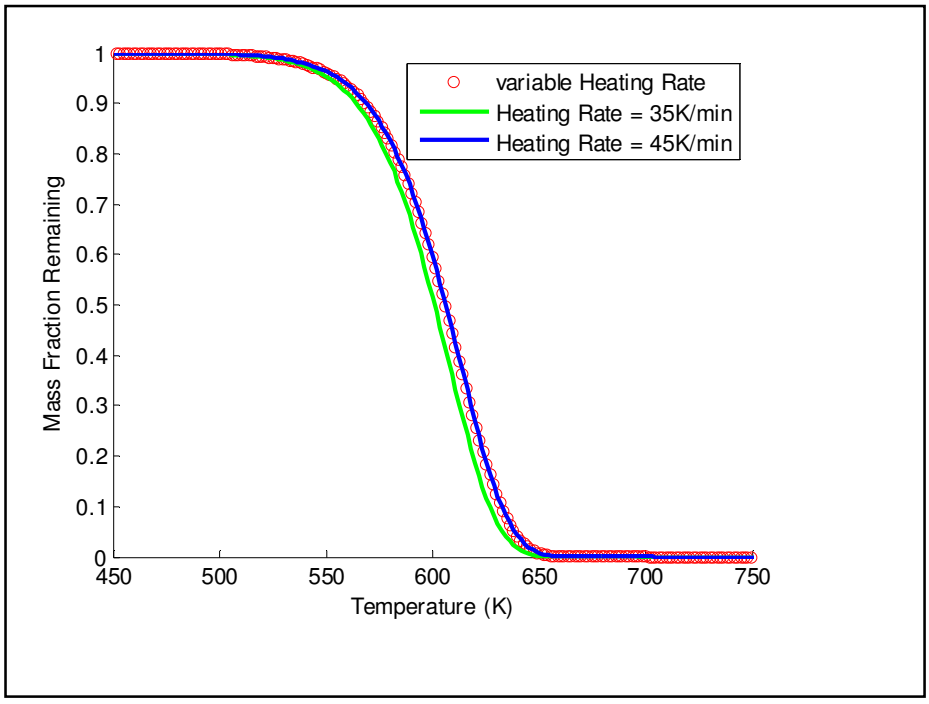


Figure 4.15: Simulated TGA curves for pyrolysis with a single, first order reaction at a variable heating rate and constant heating rates of 35 K/min and 45 K/min

Figure 4.15 shows that the 45 K/min curve is the closest fit to the curve simulated with the variable heating rate. If Figure 4.12 is examined, it can be seen that most of the weight loss occurred between temperatures of 500 K and 700K. At these temperatures, the heating rates ranged between 35 K/min to 45 K/min, shown in Figure 4.11 (a). The actual heating rate of the sample was closer to 45 K/min than to 25 K/min. This is the reason for the close fit of the curves. It is therefore important to always check the sample temperature data when conducting TGA experiments, instead of assuming a constant heating rate.

The data from the two simulated TGA curves was then fed into the DAEM algorithm to test whether it could regenerate the kinetic parameters using instantaneous values for heating rate and predict the TGA curve. In this case, the algorithm was modified to read temperature *vs*. time data and calculate instantaneous values of heating rate. These instantaneous values were used in Equation 2.17 in the calculation of E, and then in Equation 2.22 to calculate A. For this calculation, 100 conversions were chosen. The values of f_0, E and A at each chosen conversion are plotted in Figure 4.16:

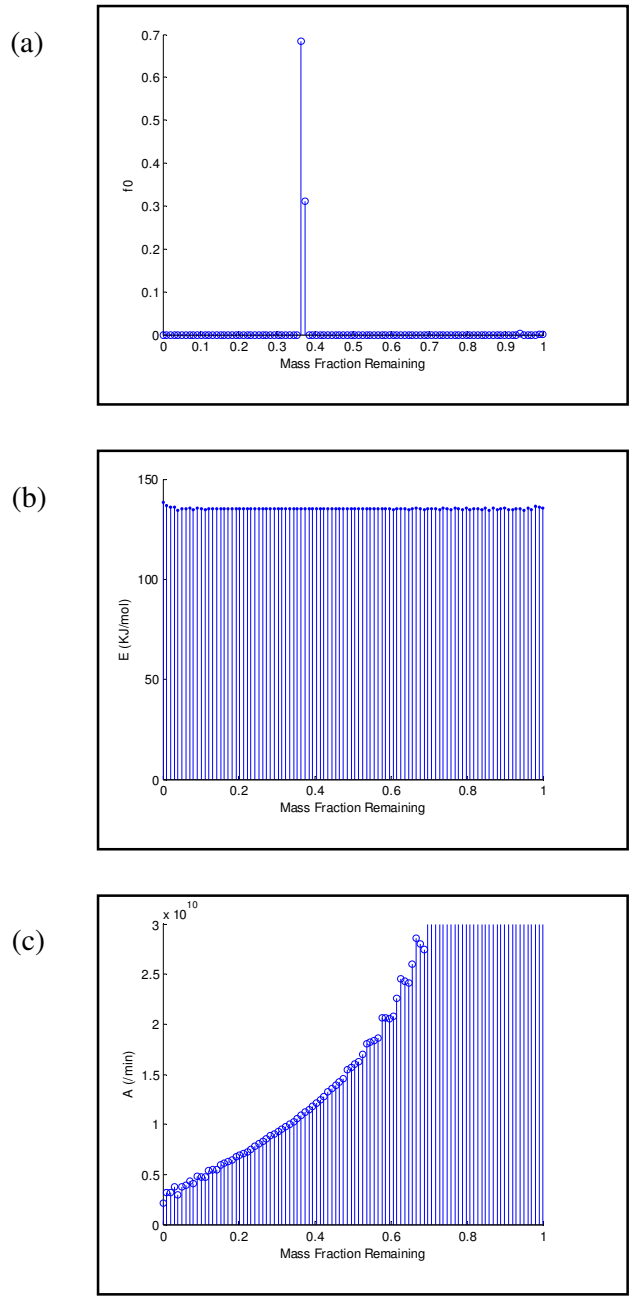


Figure 4.16: Kinetic parameters calculated for simulated single first-order reaction with variable heating rates (a) Initial mass fraction of each component (b) Activation Energy of each reaction (c) Pre-exponential factor of each reaction

Figure 4.16 shows that the values of f_0 are all zero, except for the two points at a conversion of 0.368. This indicates a single event and corresponds to the single peak of the DTG curve in Figure 4.13. These two points are assumed to form part of one reaction, so the f_0 values were

summed and the values of E and A at these two points were averaged. The parameters obtained from this calculation are provided in Table 4.5.

Table 4.5: Comparison of original kinetic parameters and those recovered by the DAEM for a simulated single, first-order reaction with variable heating rates

Parameter	**Recovered Value**	**Original Value**
f_0	1.00	1
E (KJ/mol)	135.21	135.2
A(min^{-1})	1.1×10^{10}	1.1001×10^{10}

If the actual values of the heating rate are used, as opposed to assuming a constant heating rate, the algorithm is able to regenerate the original kinetic parameters. The values of E and A calculated at this conversion correspond to the original values used in the simulation, as indicated by Figure 4.16 (b) and (c), and Table 4.5.

Following this, it was tested whether the kinetic data obtained from this simulation could be used to predict TGA curves for constant heating rates. The original values of E and A were used to create a curves for a heating rate of 25 K/min. The values recovered from the algorithm were also used to generate a curve at this heating rate. These curves are compared in Figure 4.17:

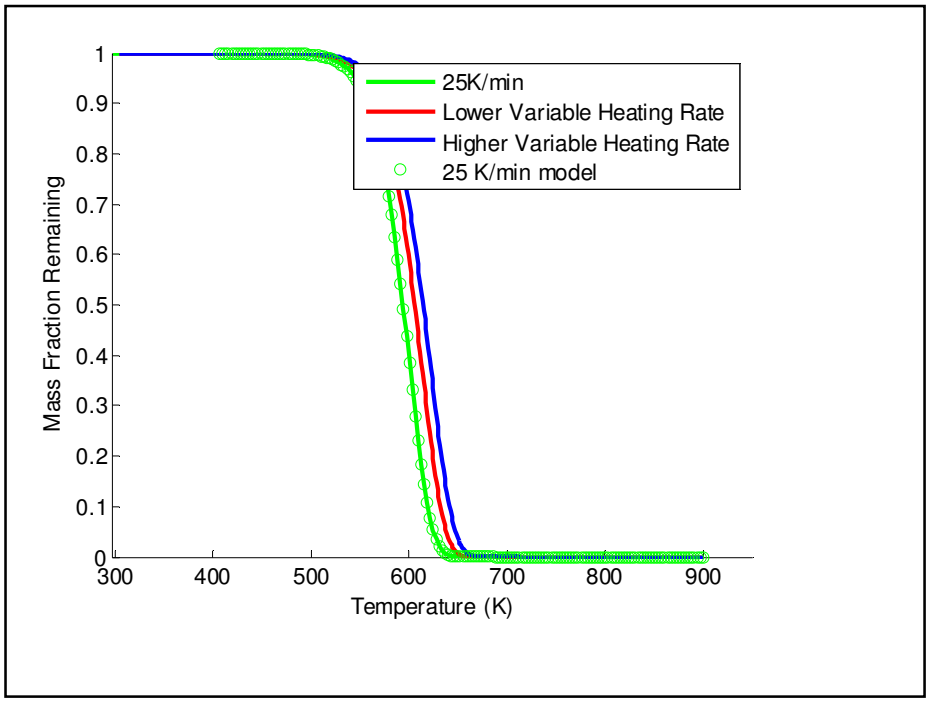


Figure 4.17: Simulated TGA curve pyrolysis with a single, first order reaction at a constant heating rate of 25 K/min, with a DAEM prediction using parameters calculated from variable heating rate curves

Figure 4.17 shows that the kinetic data obtained from the DAEM can be used to predict TGA curves with constant heating rates. Figures 4.16 and Figure 4.17 show that a non-constant heating rate in real TGA experiments would not pose a problem in the DAEM calculations. The algorithm would be able to calculate kinetic parameters from TGA data as long as instantaneous values for the heating rates are fed into it. It is again emphasised that the sample temperature data should be monitored when conducting TGA experiments, instead of assuming a constant heating rate.

The above simulations and calculations establish that the DAEM can be used to calculate kinetic parameters for the decomposition of coal according to single or multiple first order reactions. These kinetic parameters can then be used to accurately model coal pyrolysis at different heating rates.

4.3 A model-free method for determining the activation energy

The following step was to test this algorithm on a reaction which is not first-order. Upon examination of the method of calculating E according to Equation 2.17, it was found that this is in fact a model-free method. The proof of this is provided in this section.

If the rate equation for a particular component of the coal is written without a specific model (i.e. without the assumption of a first order reaction) it can be expressed as:

$$\frac{df_i}{dt} = -A \exp\left(\frac{-E_i}{RT}\right) g(f_i) \tag{4.1}$$

where $g(f_i)$ is a function describing the reaction model of component i and A is a lumped pre-exponential factor which may incorporate gas pressure and initial structural coal properties. Rearranging Equation 4.1 and taking the integrals on both sides gives:

$$\int_{f_{i.0}}^{f_i} \frac{f_i}{g(f_i)} = -A \int_0^t \exp\left(\frac{-E_i}{RT}\right) dt \tag{4.2}$$

where $f_{i,0}$ is the initial mass fraction of component i and f_i is the fraction remaining at time t. If a constant heating rate, B, is used, Equation 4.2 can be expressed in terms of temperature instead of time as suggested by Scott *et al* (2006):

$$\int_{f_{i.0}}^{f_i} \frac{df_i}{g(f_i)} = -\frac{A}{B} \int_{T_0}^{T} \exp\left(\frac{-E_i}{RT}\right) dT \tag{4.3}$$

where T_0 is the initial temperature and T is the temperature at time t. The right hand side of Equation 4.3 can be expressed as $\ln\Psi$, where Ψ is defined by Equation 2.10 (Scott *et al.*, 2006).

The integral form of g(f) is expressed as G(f). Integrating both sides of Equation 4.3 gives:

$$G(f_i) - G(f_{i,0}) = \ln \Psi(\mathrm{B}, \mathrm{T}) \tag{4.4}$$

Where $G(f_i) - G(f_{i,0})$ represents the integral on the right hand side of Equation 4.3 between limits f_i and $f_{i,0}$.

At a specific conversion, the value of f_i at temperature T_1 and heating rate B_1 is equal to the value of f_i at T_2 and B_2 (Scott *et al.*, 2006). For any two heating rates, the right hand sides of Equation 4.4 can therefore be equated.

$$\ln \Psi(\mathrm{B}_1, \mathrm{T}_1) = \ln \Psi(\mathrm{B}_2, \mathrm{T}_2) \tag{4.5}$$

This reduces to Equation 2.16 b, from which the value of E can be calculated, proving that the method is indeed a model-free method.

4.4 Simulated combustion with a shrinking core reaction

4.4.1 Calculation of E using the DAEM as a model-free method

In order to test the model-free method explained in Section 4.3, a combustion reaction was simulated as a single shrinking core reaction described by Everson *et al* (2006[a]). The rate equation is as follows:

$$\frac{dX}{dT} = \frac{A^*}{B} \times \exp\left(\frac{-E}{RT}\right)(1-X)^{2/3} \tag{4.6}$$

The pre-exponential factor, A^*, is a lumped value which takes into account the surface area and porosity of the particle, and the partial pressure of oxygen. The values of E and A^* used for this simulation were 135.2 KJ/mol and 1.1×10^{10} min^{-1} respectively, while the heating rates chosen were constant at 1 K/min, 10 K/min, 100 K/min and 1000 K/min. The simplest way to simulate the TGA curves was to apply one of Matlab™'s built-in ordinary differential equation (o.d.e) solvers, ode45, to the reaction equation. The resulting curves are presented in Figure 4.18:

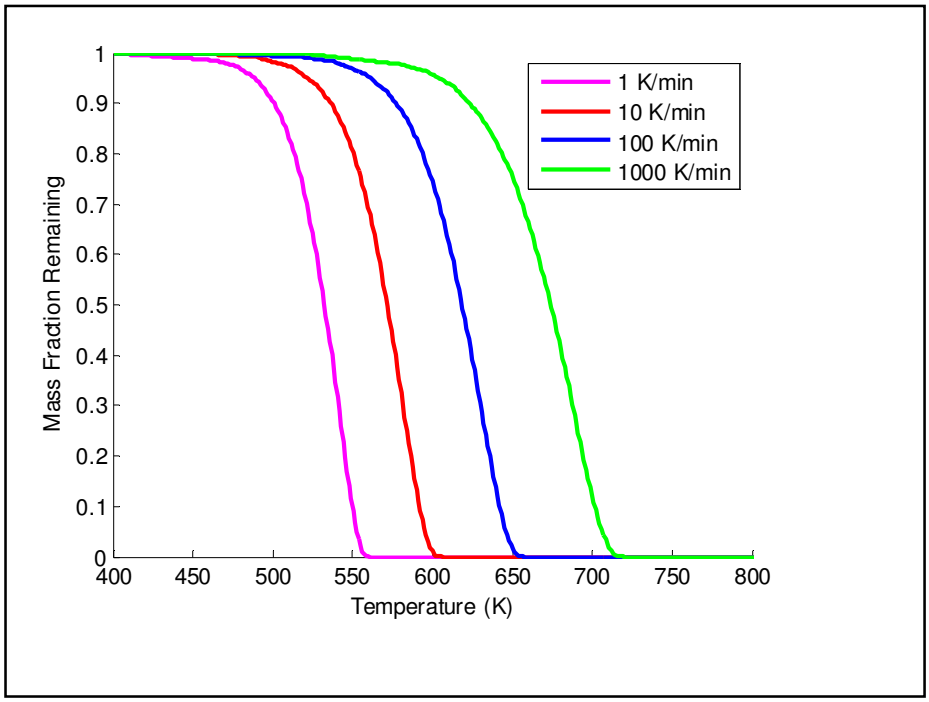


Figure 4.18: Simulated TGA curves for a shrinking core reaction at different heating rates simulated using ode45 solver

The DTG curves for the curves in Figure 4.18 are plotted in Figure 4.19:

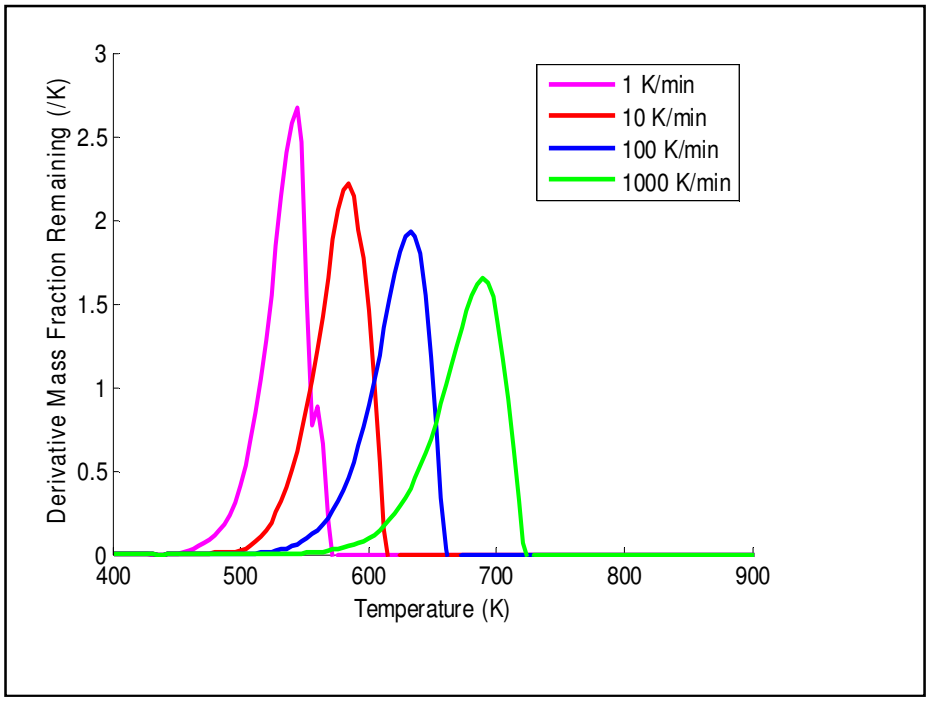
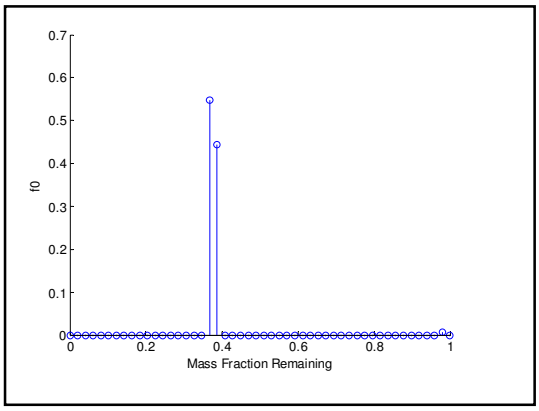


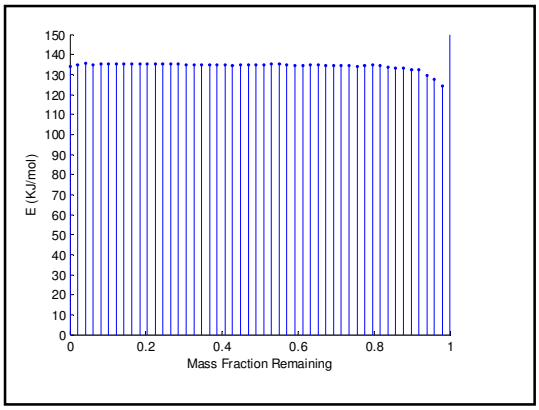
Figure 4.19: Simulated DTG curves for a shrinking core reaction at different heating rates simulated using ode45 solver

The DTG curve has only one peak, indicating that only one event is taking place. The DAEM algorithm was again used to calculate kinetic parameters from the TGA data at the two intermediate heating rates. These parameters are plotted against conversion in Figure 4.20.

(a)



(b)



(c)

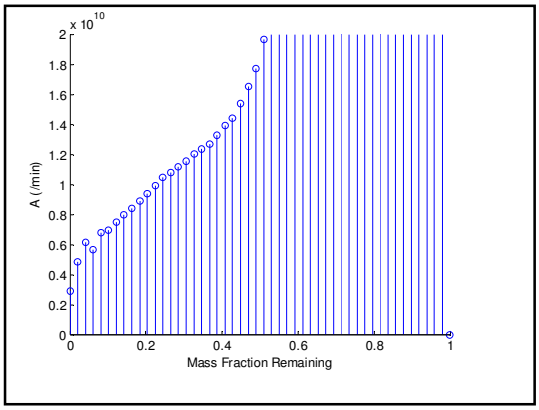


Figure 4.20: Kinetic parameters calculated for a simulated shrinking core reaction using ode45 solver (a) Initial mass fraction of each component (b) Activation Energy of each reaction (c) Pre-exponential factor of each reaction

Figure 4.20 (a) shows that the values of f_0 have all been set to zero, except at one point, indicating that a single reaction has occurred. At this point, the E calculated by the algorithm is close to the value specified for the simulation. The sum of the f_0 values, as well as the averages of the E and A values, at this conversion are given in Table 4.6.

Table 4.6: Comparison of original kinetic parameters and those recovered by the DAEM for a shrinking core reaction simulated using ode45 solver

Parameter	Recovered Value	Original Value	Error
f_0	1.00	1	0.33 %
E (KJ/mol)	135.17	135.2	0.02 %
A^* (min^{-1})	1.32×10^{10}	1.1001×10^{10}	19.81 %

The results in Figure 4.20 and Table 4.6 show that the DAEM can be used to calculate the E of a combustion reaction with a shrinking core mechanism. In this calculation, the reaction model is not specified. The DAEM can therefore be used as a model free method to calculate the activation energy of coal combustion. This finding is in agreement with the hypothesis made in the research.

4.4.2 Determining the pre-exponential factor, A^*

The value of A^* calculated by the algorithm is incorrect as indicated by the error of 19.81 %. This is because the calculation of A^* requires knowledge of the reaction model. This finding provides an answer to Research Question 4. A second code was therefore written to calculate the value of A^* based on the shrinking core mechanism. This was done by rearranging Equation 4.1 as follows:

$$\int_0^X \frac{dX}{(1-X)^{2/3}} = \frac{A^*}{B}\int_{T_0}^{T} \exp\left(\frac{-E}{RT}\right) dT \tag{4.7}$$

The upper limit of the temperature integral is that temperature corresponding to the conversion at which f_0 is non-zero. It is again assumed that the conversion of each component is 63.21% (Scott *et al*., 2006). Since there is only a single reaction, and the value of E for this reaction is known from the model-free calculation, performing an integration calculation is simple. Further details of the code used are provided in Appendix B. The value of A^* calculated by the new algorithm is given in Table 4.7:

Table 4.7: Value of A^* recovered by shrinking core algorithm and original value

Original Value	Recovered Value	Error
1.1001×10^{10}	1.1201×10^{10}	1.82 %

The new algorithm is able to accurately calculate the correct value of A^* based on the shrinking core model, using the calculated value of E. This answers Research Question 5 in part, but the algorithm must be applied to real TGA data for combustion. The calculated parameters were then used to model a single, shrinking core reaction at the different heating rates used for the simulation. The modelled curves are compared to the simulated curves in Figure 4.21:

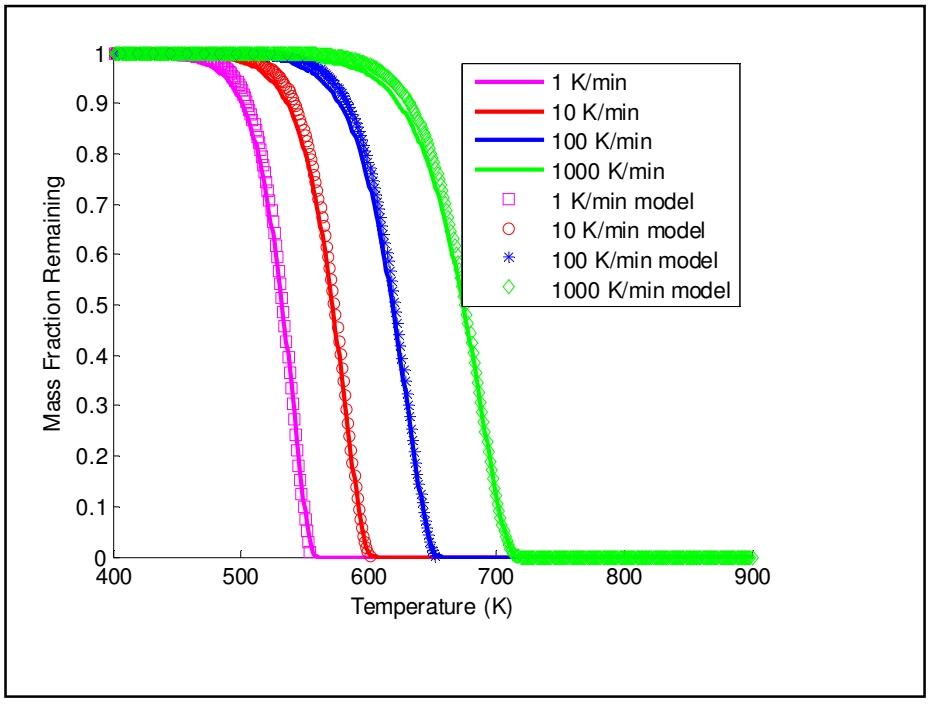


Figure 4.21: Simulated TGA curves for a shrinking core reaction at different heating rates simulated using ode45 solver, with model predictions for each of these heating rates

Figure 4.21 shows that the regenerated parameters can be used to model the reaction accurately. This provides a further validation of the methods used for the calculation of the activation energy and pre-exponential factor. The model comparisons to the derivative curves are shown in Figure 4.22:

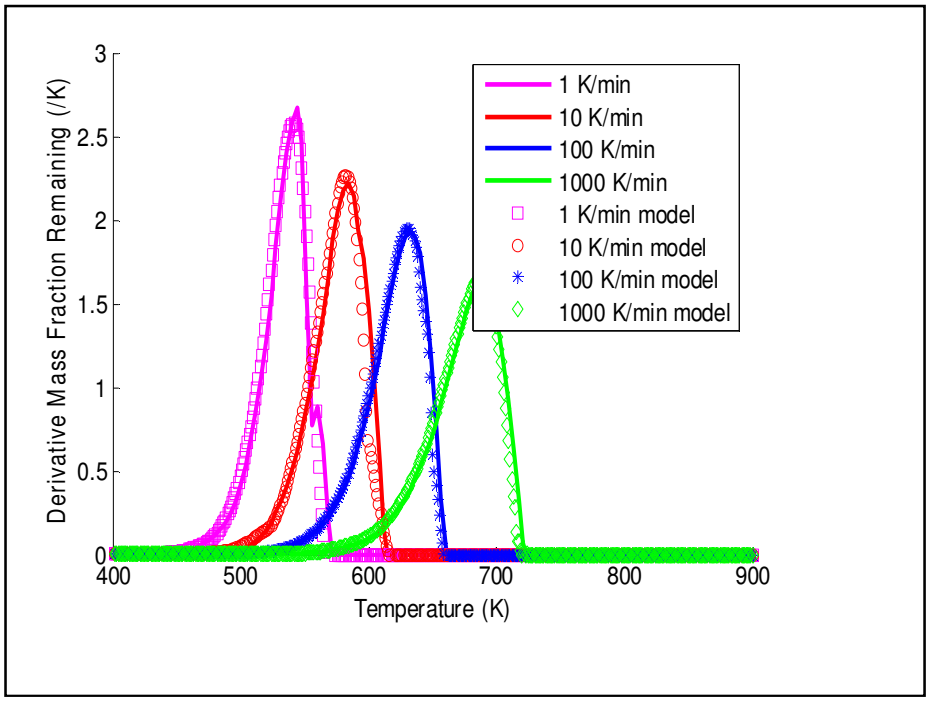


Figure 4.22: Simulated DTG curves for a shrinking core reaction at different heating rates simulated using ode45 solver, with model predictions for each of these heating rates

The model fit to the derivative curves show a good agreement between simulated data and model results. It is possible that the use of a different o.d.e solver in Matlab™ could cause errors in the model fits. This is because the solvers use numerical methods of integration. These numerical methods rely on approximations and therefore have some degree of error.

4.5 The DAEM modified to model a shrinking core reaction

Following the above calculations, it was attempted to rewrite the DAEM in a form which incorporates the shrinking core reaction. This would mean that an o.d.e. solver would not be needed to simulate the curves and curves can be simulated for multiple reactions with or without ash. If Equation 4.1 is rewritten for a shrinking core reaction:

$$\frac{df_i}{dt} = A^* \exp\left(\frac{-E}{RT}\right)\left(f_i^{\frac{2}{3}}\right) \tag{4.8}$$

Rearranging the above Equation and assuming a constant heating rate, B, gives:

$$\int_{f_{i,0}}^{f_i} \frac{df_i}{f_i^{2/3}} = \frac{A^*}{B}\int_{T_0}^{T} \exp\left(\frac{-E}{RT}\right) dT \tag{4.9}$$

Integrating the left hand side:

$$3{f_i}^{1/3} - 3{f_{i,0}}^{1/3} = \frac{A^*}{B}\int_{T_0}^{T} \exp\left(\frac{-E}{RT}\right) dT \tag{4.10}$$

So:

$$3{f_{i,0}}^{1/3}\left(\frac{{f_i}^{1/3}}{{f_{i,0}}^{1/3}} - 1\right) = \ln \Psi \tag{4.11}$$

where Ψ is defined according to Equation 2.10.

Solving for f_i yields:

$$f_i = f_{i,0}\left(1 + \frac{\ln \Psi}{3{f_{i,0}}^{1/3}}\right)^3 \tag{4.12}$$

And the cubed term can be expressed as $\Psi^{s.c.}$

So:

$$\frac{M(T)}{M_0} = w + \sum f_i(T) = w + \sum f_{i,0}\Psi^{s.c.} \tag{4.13}$$

A curve of $\frac{M(T)}{M_0}$ *vs.* T can be created for known reaction parameters. Since it is assumed that combustion reactions are generally single reactions, the value of f_0 is 1 for an ash-free coal or (1-w) for a real coal. Using Equation 4.13, an algorithm was created to model the shrinking core reaction using this altered form of the Ψ-matrix in the DAEM. The parameters used to simulate the TGA curves are shown in Table 4.8:

Table 4.8: Kinetic parameters used for simulation of coal combustion with a shrinking core reaction using $\Psi^{s.c.}$

Kinetic Parameter	**Value used for Simulation**
f_0	[1 0]
E (KJ/mol)	135
A^* (min^{-1})	10^{15}

These simulated TGA curves are shown in Figure 4.23:

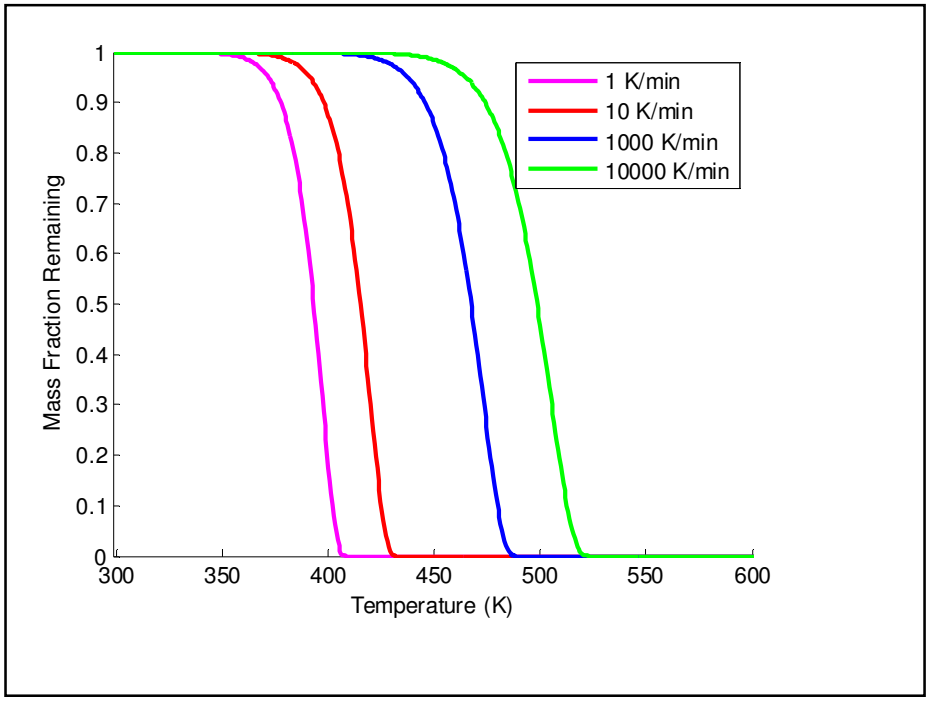


Figure 4.23: Simulated TGA curves for a shrinking core reaction at different heating rates simulated using $\Psi^{s.c.}$

The DTG curves for these heating rates are presented in Figure 4.24.

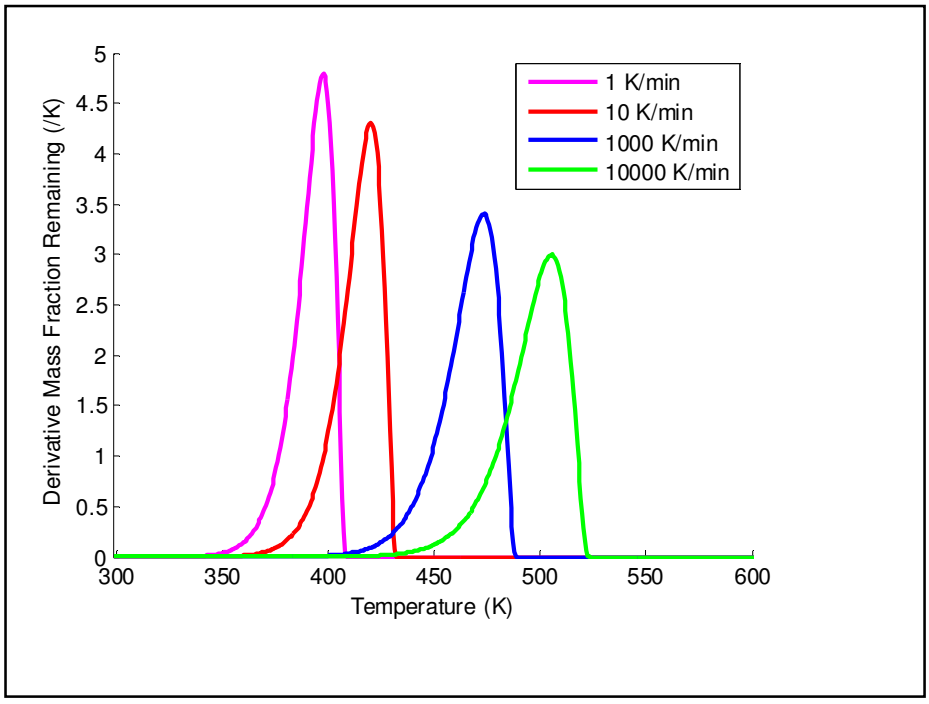
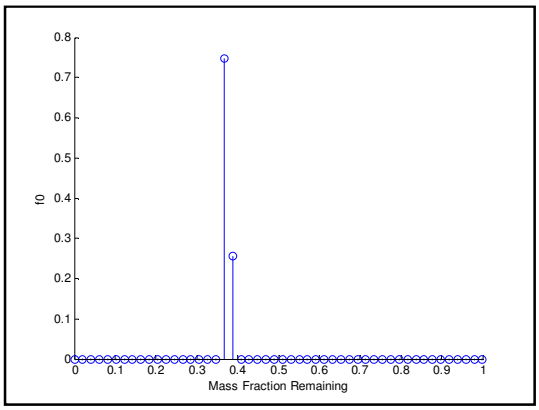


Figure 4.24: Simulated DTG curves for a shrinking core reaction at different heating rates simulated using $\Psi^{s.c}$

The DAEM algorithm was again used with the two middle heating rates to predict the activation energy of combustion. The values obtained at each conversion are shown in Figure 4.25.

(a)



(b)

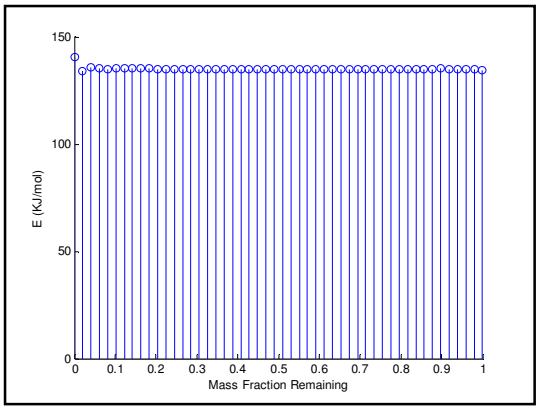


Figure 4.25: Kinetic parameters calculated for a simulated shrinking core reaction using $\Psi^{s.c}$ (a) Initial mass fraction of each component (b) Activation Energy of each reaction

Figure 4.25 (a) shows a single reaction with the value of E in Figure 4.25 (b) corresponding to the value used for the simulation. The value of A^* obtained at each conversion has not been plotted here since it is known that this value is incorrect. The value of E for the reaction was then used with the shrinking core algorithm to calculate A^*. The values of the kinetic parameters obtained are provided in Table 4.9.

Table 4.9: Comparison of original kinetic parameters and those recovered by the DAEM for E shrinking core reaction algorithm for A using $\Psi^{s.c}$

Parameter	Recovered Value	Original Value	Error
f_0	1.0039	1	0.39 %
E (KJ/mol)	134.96	135	0.0324 %
A^* (min^{-1})	1.012×10^{15}	10^{15}	1.19 %

These kinetic parameters were used to model the reaction using the new Ψ matrix. The comparison between model curves and simulated curves is presented in Figure 4.26 and Figure 4.27.

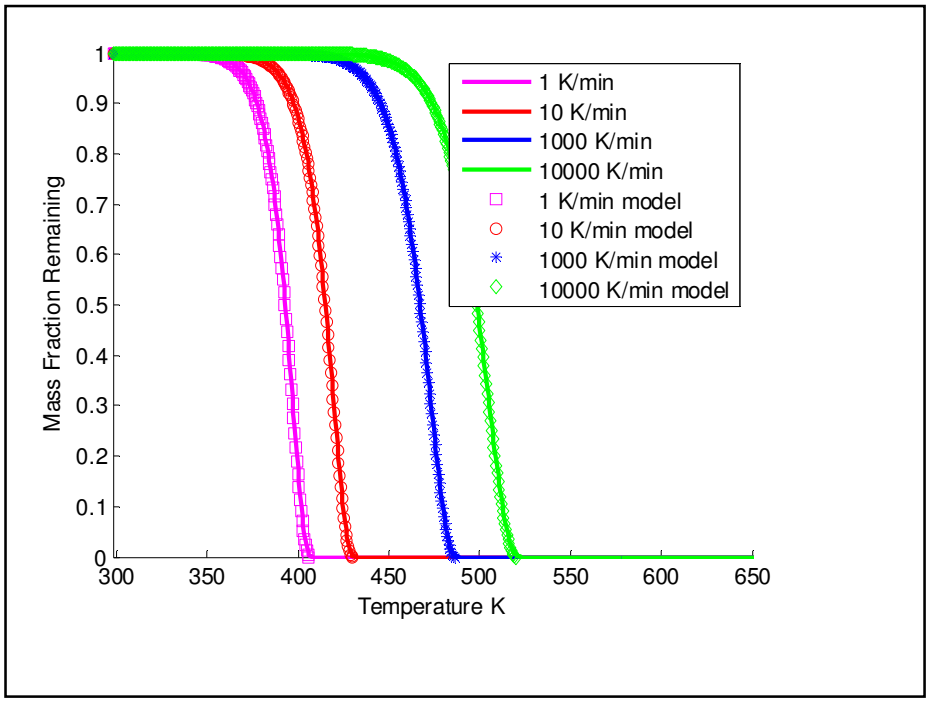


Figure 4.26: Simulated TGA curves for a shrinking core reaction at different heating rates simulated using $\Psi^{s.c}$, with model predictions for each of these heating rates

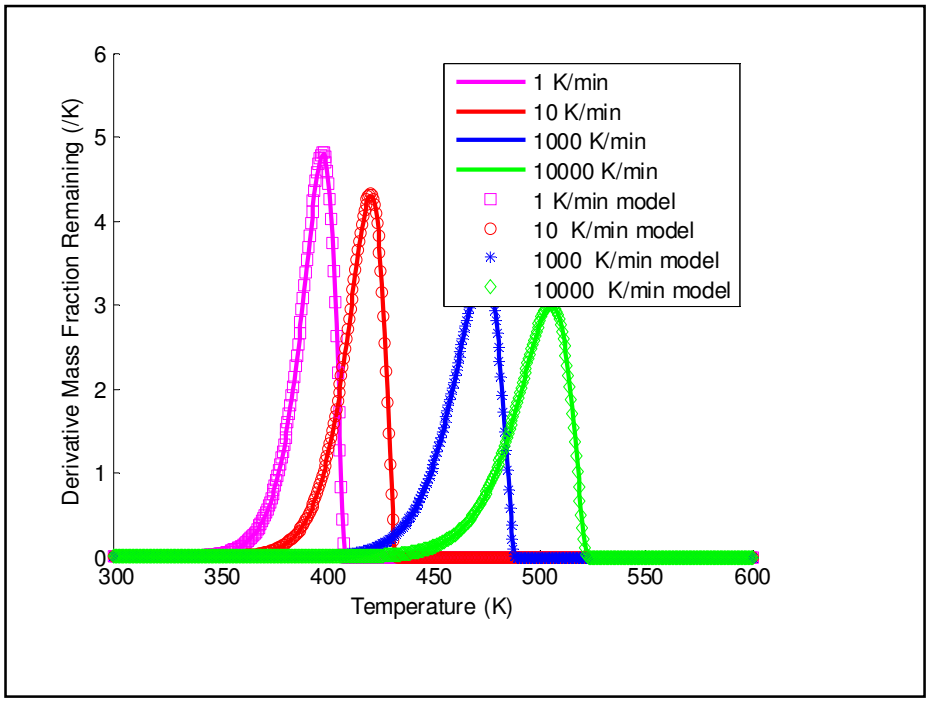


Figure 4.27: Simulated DTG curves for a shrinking core reaction at different heating rates simulated using $\Psi^{s.c}$, with model predictions for each of these heating rates

Figure 4.26 and Figure 4.27 show an excellent correlation between the simulated TGA curves and the shrinking core model. Comparing Table 4.6, Table 4.7 and Table 4.9, it can be seen that the use of o.d.e. solvers cause a slight error in model predictions. This issue has been resolved by rewriting the DAEM matrix equation for a shrinking core reaction.

4.6 Model evaluation using data reported in literature

To further test the DAEM algorithm as a model-free method for calculating E and the shrinking core algorithm to determine A, these algorithms were applied to real TGA data reported in literature (Njapha 2003). In the work of Njapha (2003), kinetics parameters were calculated using the same method described by Everson *et al.* (2006[b]).

Data points were read off the TGA curves for the combustion of a South African coal char in air. TGA curves were created by interpolation between the points which were read off the original curves. These are presented in Figure 4.28.

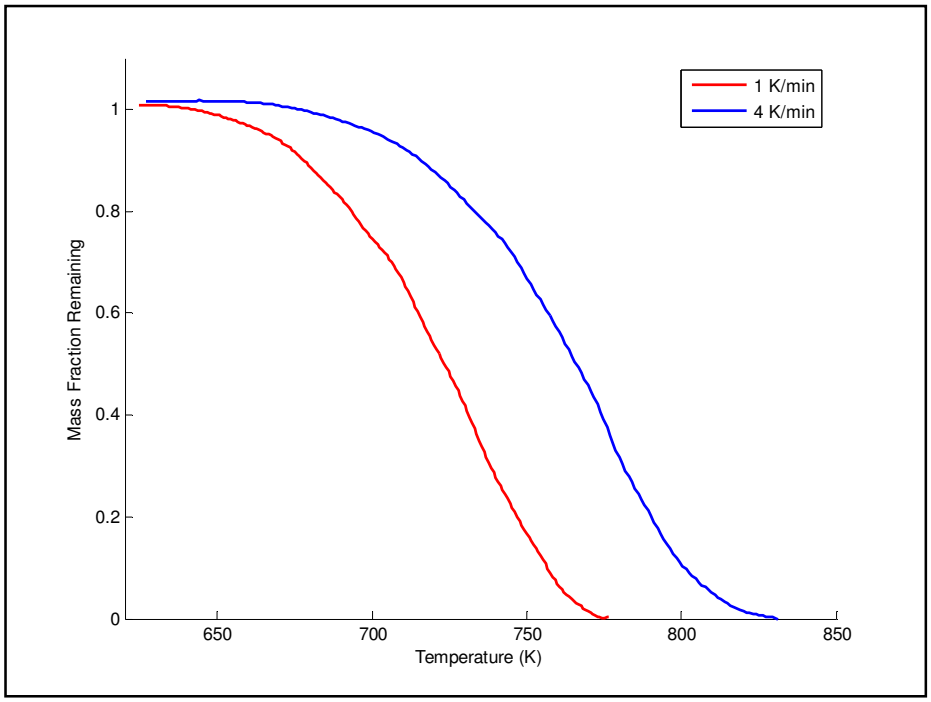


Figure 4.28: TGA curves for char combustion in air reported by Njapha (2003)

The TGA data from these curves was fed into the DAEM algorithm to calculate the E for the process. This E and the temperature at which it was calculated were used in the shrinking core algorithm to calculate the A^* for the process. These values are reported and compared to the author's values in Table 4.10. It should be noted that the value of A^* obtained is compared to the value of Z reported by Njapha (2003), where Z is a lumped value which factors in the partial pressure of oxygen.

Table 4.10: Values of kinetic parameters calculated for char combustion compared to those reported by Njapha (2003)

Kinetic Paramter	**Value calculated by DAEM algorithm**	**Value calculated by Njapha (2003)**	**% Error**
E (KJ/mol)	140.51	139 (± 10)	1.09
A^* / Z (min^{-1})	5.40×10^6	3.26×10^6	56.77

The value of E calculated by the DAEM algorithm is quite close to that calculated by Njapha (2003) and falls within the reported margin of error. The difference in the calculated value of A^* is quite large however. This could be due to the difference in the value of E used for the

calculation, the assumption that the reaction reaches a conversion of 63.21 % or errors in reading off the data points from the original curves. Using the kinetic parameters calculated, as well as those reported by Njapha (2003), curves were created with the $\Psi^{s.c.}$ matrix for 1K/min and 4 K/min. The comparison between both sets of model curves and the actual curves is given in Figure 4.29.

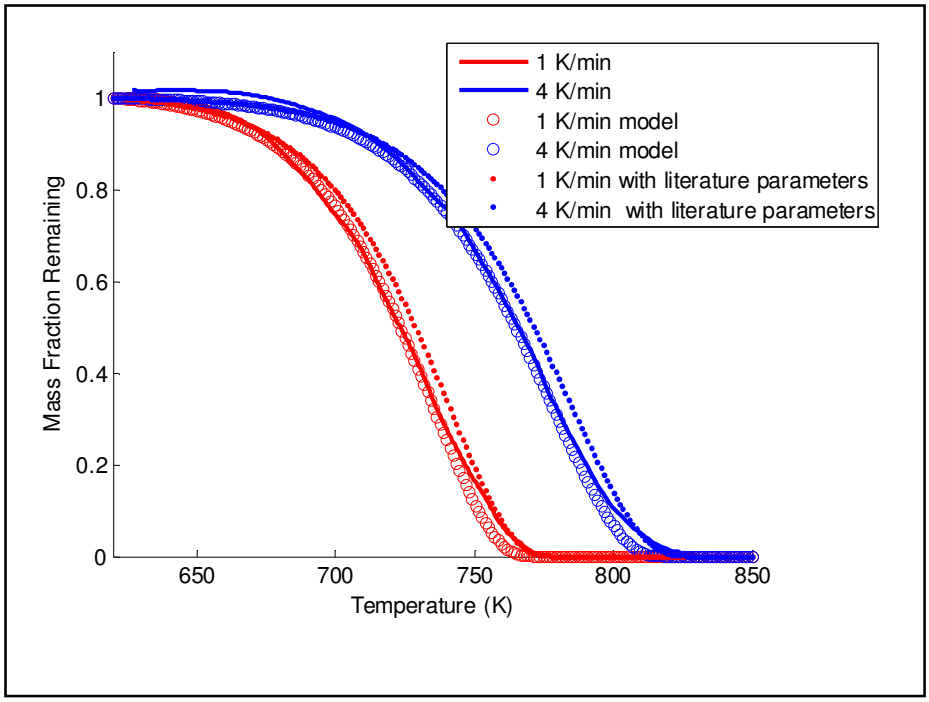


Figure 4.29: TGA curves for char combustion in air reported by Njapha (2003) with model predictions using calculated parameters and parameters reported by Njapha (2003)

Figure 4.29 shows that the kinetic parameters calculated from the DAEM and shrinking core algorithms used in this work provide better approximations to the experimental data than those calculated using the method of Everson *et al*. (2006[b]). This validates the methods used to calculate both E and A^*. However, this is not the model fit obtained in the actual work of Njapha (2003). In his work, a good fit to experimental data is obtained by taking into account the effects of oxygen partial pressure and using a partial differential equation to model the curves.

4.7 Conclusion

The simulation of TGA data provides a test of how robust the algorithm is when applied different types of reactions. The effects of multiple reactions, non-constant heating rates and

a non first-order reaction mechanism were investigated. It has been shown that the DAEM inversion algorithm is a model-free method of calculating the E of pyrolysis, combustion and in general all solid-gas model forms. Research Question 3, found in Section 1.4, is answered by this conclusion.

If the reaction mechanism is not first-order, the calculated value of E must be used in conjunction with an appropriate model to calculate the pre-exponential factor of the reaction. However, these simulations are carried in an ideal environment. The algorithm therefore needs to be applied to real TGA data, which is the subject of Chapter 5 and Chapter 6.

A key issue relating to TGA experiments has also been raised. When conducting these experiments, it is important to check the correlation between the programme heating rate and the actual heating rate that the sample is exposed to. The assumption of a constant heating rate leads to inaccuracies in the model calculations and predictions. However, the DAEM algorithm is able to use instantaneous values for the heating rate in order to correctly calculate kinetic parameters of coal conversion processes.

Chapter 5: Pyrolysis Results

In this chapter, the results of real TGA experiments on the pyrolysis of a South African coal are presented and discussed. The DAEM algorithm was applied to the data from these experiments in order to obtain kinetic parameters of the pyrolysis reactions. These were then used to model the reactions at the different heating rates used in the experiments. The modeled reactions were then compared to the real data. The accuracy of the fits and possible sources of error are discussed.

5.1 Low temperature TGA experiments

For the first set of experiments, the Perkin-Elmer STA600 TGA was used. Coal samples were pyrolized in nitrogen from 298 K to 1173 K at different heating rates. The TGA curves for these pyrolysis reactions are presented in Figure 5.1:

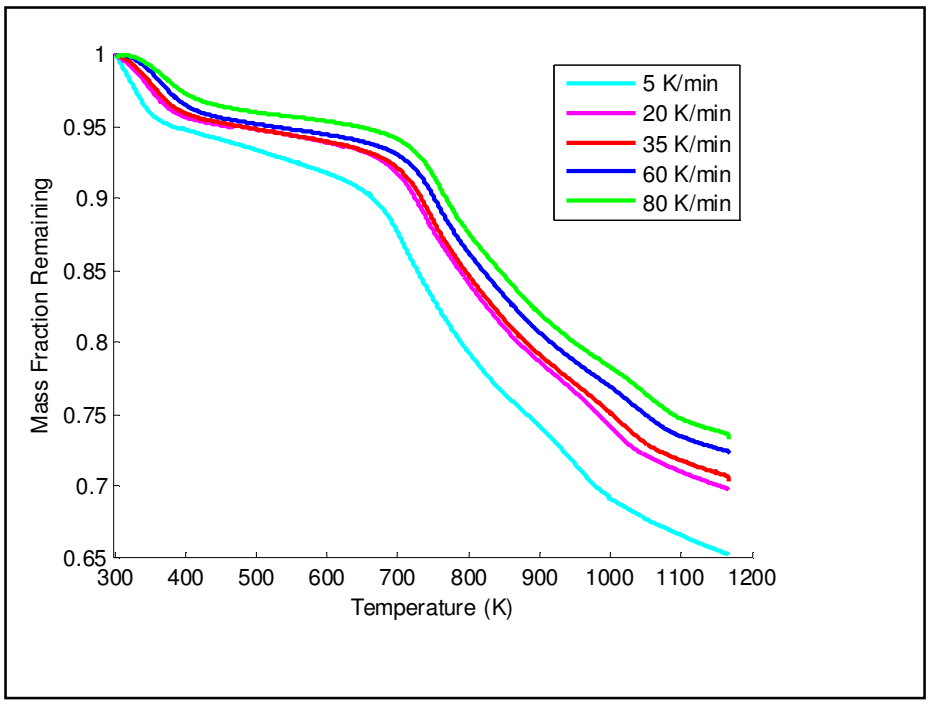


Figure 5.1: TGA curves for the pyrolysis of a South African coal at different heating rates in a Perkin-Elmer STA600 TGA

From Figure 5.1, it can be seen as the heating rate increases, the curves shift to the right, as with the simulated curves. However, all the curves do not level off at the same conversion. This indicates that pyrolysis is not complete at a temperature of 1173 K. The samples need to be heated to higher temperatures or held at 1173 K for a long period in order to drive off all

volatiles. However, holding the temperature constant at 1173 K for long periods reduces the lifespan of the furnace. This was the reason for conducting experiments in a higher temperature TGA.

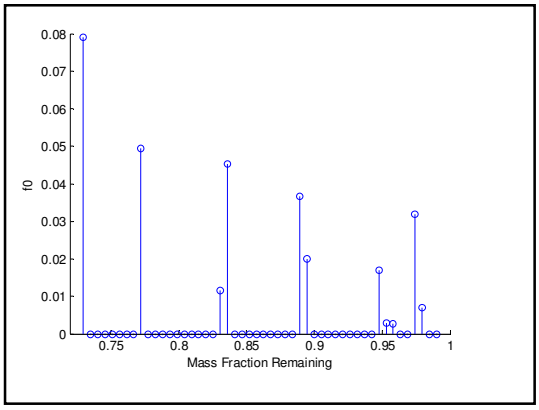
It is also noted that the 5 K/min curve does not follow the general shape of the higher heating rate curves. This provides some indication that reaction kinetics are dependent on heating conditions. For this reason, the 5 K/min curve will be ignored at present and returned to at a later stage in the discussion.

5.1.1 Higher Heating Rates

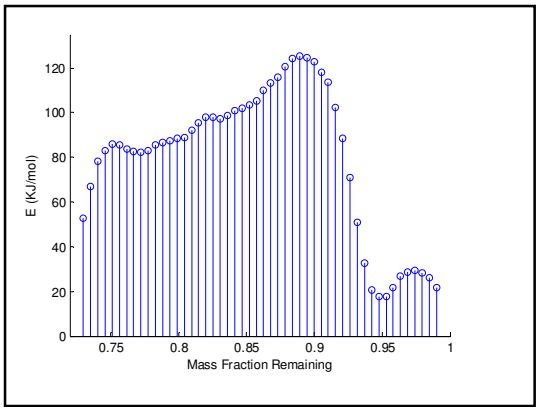
The DAEM inversion algorithm was applied to these real TGA curves in order to calculate kinetic parameters and to determine whether the DAEM is sufficient to model the pyrolysis behavior of South African coals. Data for the heating rates of 35 K/min and 60 K/min were used in the algorithm, with the assumption of a constant heating rate. This kinetics evaluation procedure is preferred over the method used by Everson *et al*. (2010) since only two TGA curves are required. This means that fewer experiments are required and less data needs to be processed overall.

The TGA data sets were reduced by linear interpolation in order to simplify the computation. From the data, 50 conversions were chosen at which to calculate the kinetic parameters. The values of these parameters for each conversion are plotted in Figure 5.2.

(a)



(b)



(c)

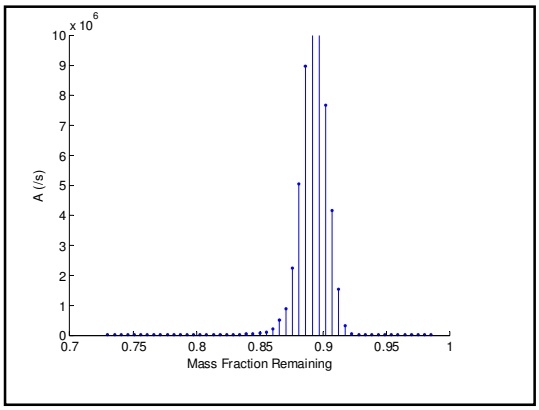


Figure 5.2: Kinetic parameters calculated for coal pyrolysis (a) Initial mass fraction of each component (b) Activation Energy of each reaction (c) Pre-exponential factor of each reaction

Upon examination of the values of f_0 and E, it was concluded that there are seven first-order reactions occurring during pyrolysis of this coal, as seen in Figure 5.2 (a). The first reaction occurring during pyrolysis is the loss of moisture from the coal, at a temperature of around 373 K. It should be noted that Figure 5.2 only takes into account the decomposition reactions, so the fixed carbon and ash content is not included in Figure 5.2 (a). The sum of f_0 values and the average values of E and A for each reaction are given in Table 5.1.

Table 5.1: Kinetic parameters of coal pyrolysis in a Perkin-Elmer STA600 calculated using the DAEM inversion algorithm

Reaction Number	f_0	E (KJ/mol)	A (s^{-1})
1	0.0389	28.92	358.90
2	0.0027	21.85	8.00
3	0.0226	17.72	0.76
4	0.0567	124.94	1.07×10^{10}
5	0.0568	195.75	2.00×10^{4}
6	0.0494	82.39	260.50
7	0.0790	52.68	1.81

Table 5.1 shows that the seven reactions occurring during coal pyrolysis in this TGA have E's ranging from 17.72 KJ/mol to 195.75 KJ/mol. Values of E below 100 KJ/mol are considered low for pyrolysis, since values reported in literature usually range from 100 KJ/mol upwards, as seen later in Table 5.3. Reaction 1, with an E of 28.92 corresponds to the loss of moisture from the coal.

Table 5.1 also indicates that the values of E do not necessarily increase as the reactions proceed or as the temperature increases. In addition, the value of A is not constant for all reactions, but instead has a large range from 0.759 s^{-1} to 1.073×10^{10} s^{-1}. No correlation is noted between the values of E and A.

The kinetic parameters obtained from the DAEM algorithm were then used to model the reactions at the two heating rates used in the calculation. Model curves are compared to actual experimental curves in Figure 5.3 and Figure 5.4.

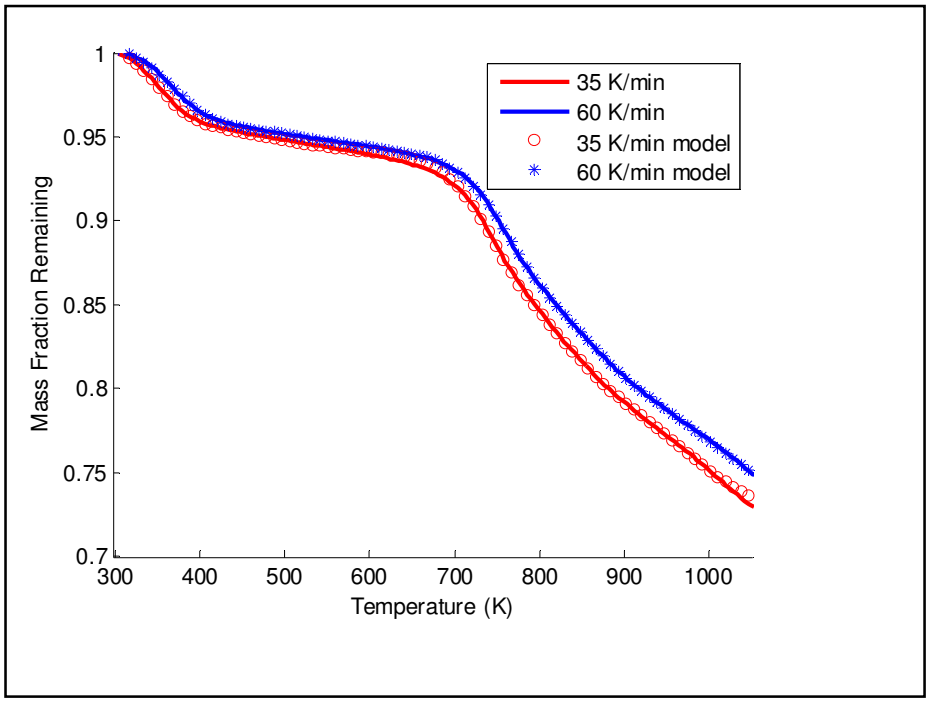


Figure 5.3: TGA curves for coal pyrolysis at heating rates of 35 K/min and 60 K/min, with DAEM predictions for each heating rate

Figure 5.3 shows that the model is a good prediction of experimental data for the two heating rates used in the algorithm. The model prediction for the DTG curves are provided in Figure 5.4.

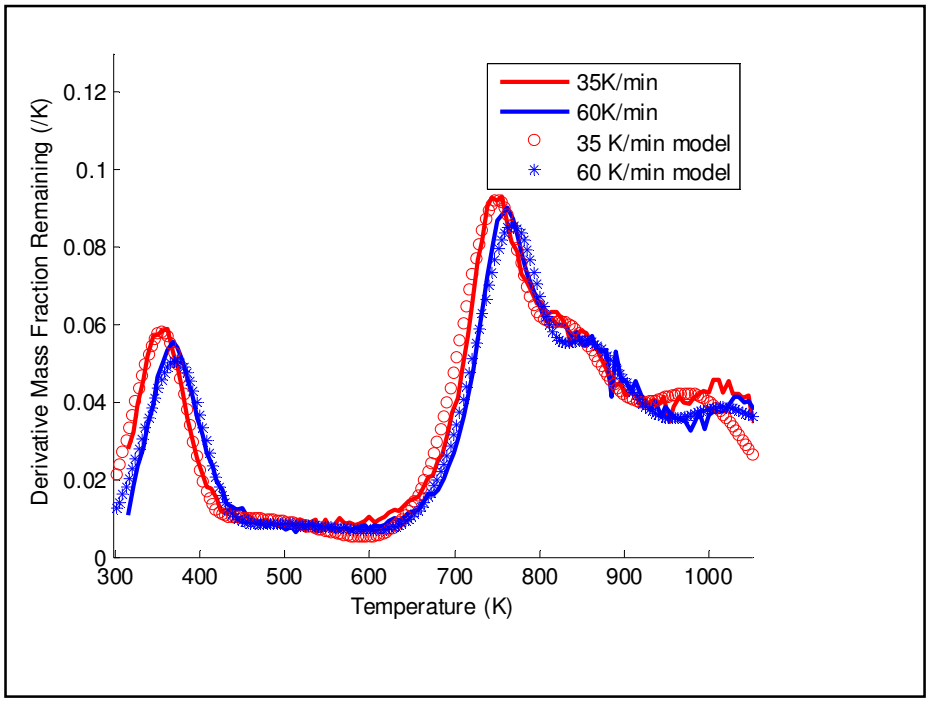


Figure 5.4: DTG curves for coal pyrolysis at heating rates of 35 K/min and 60 K/min, with DAEM predictions for each heating rate

The modeled DTG curves in Figure 5.4 are also a good fit to experimental data. The DAEM is thus able to model coal pyrolysis well for the two heating rates used to calculate kinetic parameters.

The kinetics parameters in Table 5.1 were then used to model the reactions at the two heating rates not used in the calculation, namely 20 K/min and 80 K/min. The aim of this was to test whether the model is capable of extrapolation to higher and lower heating rates for real experiments. The TGA curves are compared to model predictions in Figure 5.5.

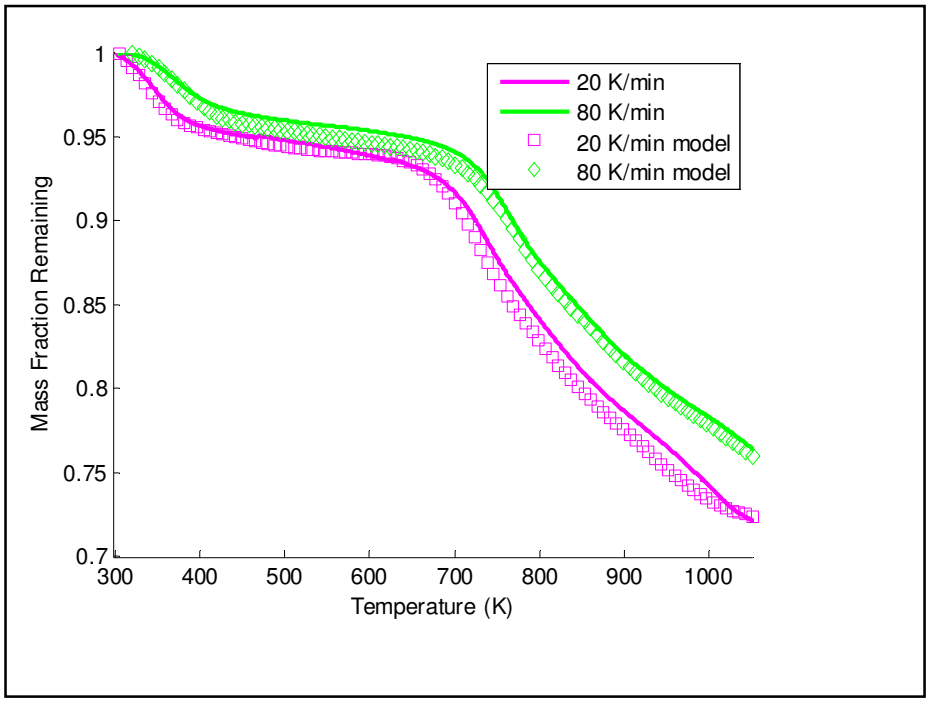


Figure 5.5: TGA curves for coal pyrolysis at heating rates of 20 K/min and 80 K/min with DAEM predictions for each heating rate

Figure 5.6 shows the DTG curves for pyrolysis at the heating rates of 20 K/min and 80 K/min with the DAEM predictions for these heating rates.

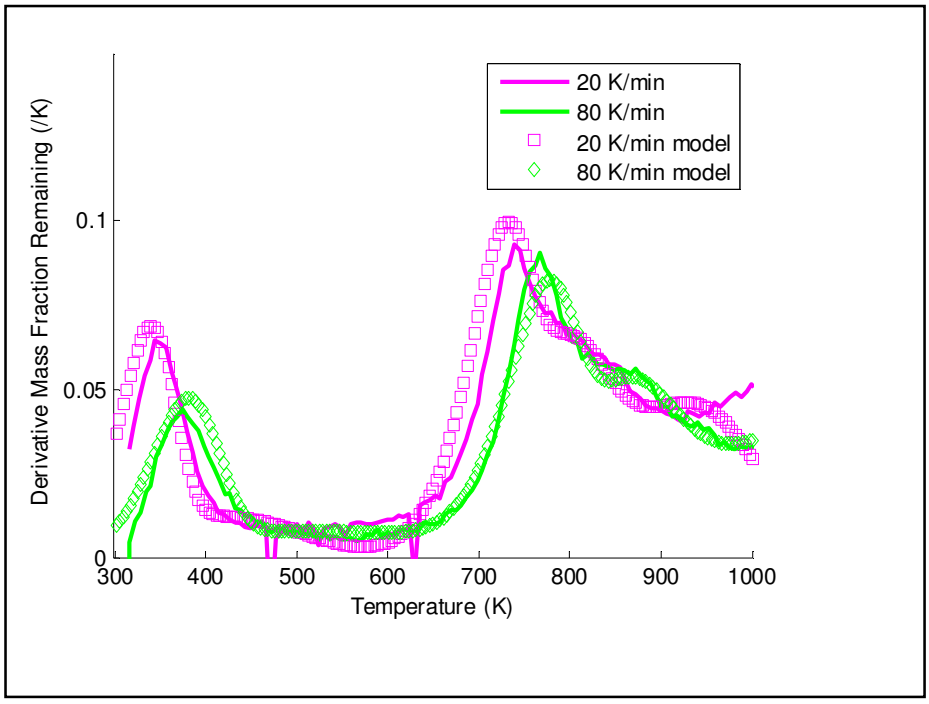


Figure 5.6: DTG curves for coal pyrolysis at heating rates of 20 K/min and 80 K/min with DAEM predictions for each heating rate

A poor prediction of model results to experimental results is observed in Figure 5.5 and Figure 5.6 for the two heating rates not used in the algorithm. This is similar to what has been reported by Navarro *et al* (2008), who applied the DAEM algorithm to TGA data at heating rates of 5 K/min and 10 K/min. These authors used the calculated kinetics to model curves for the two heating rates used in the algorithm and for a heating rate of 20 K/min. They found that the DAEM models experimental data well for the heating rates used in the algorithm, but under-predicts the experimental data for 20 K/min.

One possible reason for the ill fit, investigated in this work, is that the sample was not exposed to a constant heating rate. During the experiments, it was noted that there was some difference between the temperature of the sample and that specified by the TGA programme at each recorded time. Since the DAEM calculations use a constant value for the heating rate, it was considered important to test this assumption. Data was available for the programme and sample temperatures at each recorded point in time. The discrete derivatives of these data sets were calculated to provide the curves of heating rate vs. time, shown in Figure 5.7.

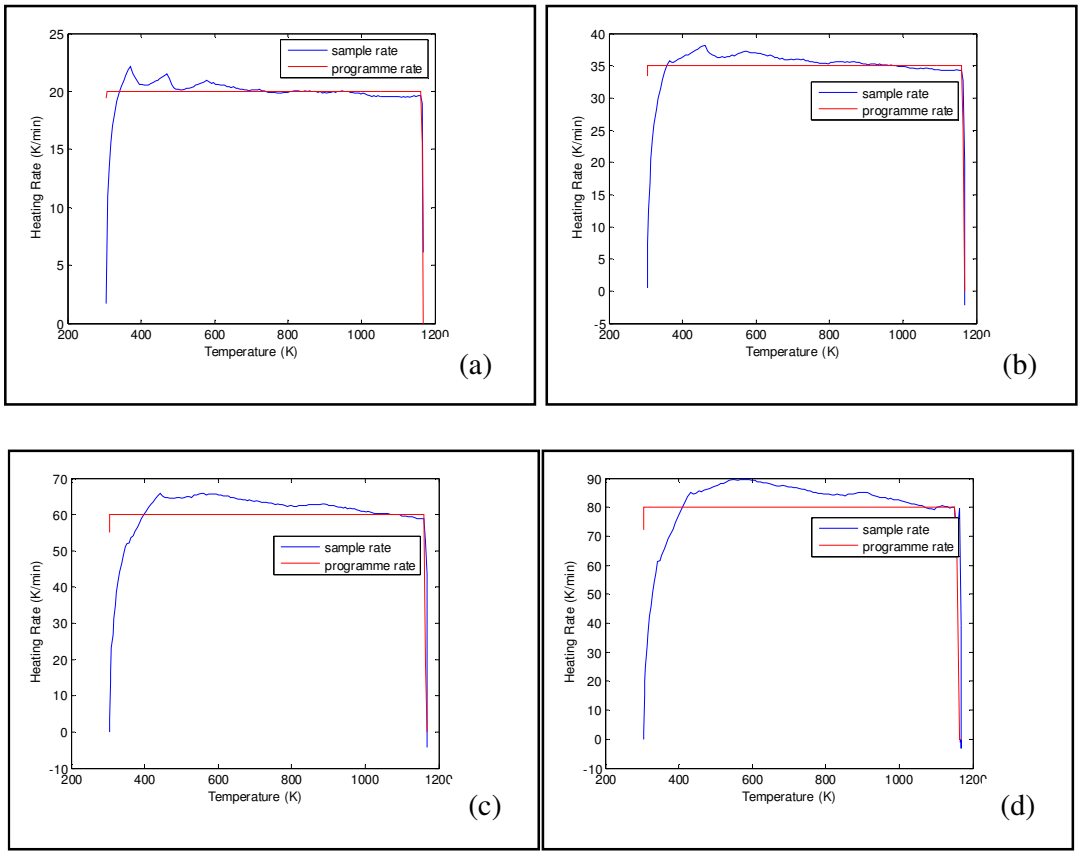


Figure 5.7: Comparison of programme heating rates and actual heating rates of the samples for coal pyrolysis in a Perkin Elmer STA600 TGA

The plots in Figure 5.7 show clearly that the heating rate is not constant at all temperatures or conversions. The assumption of a constant heating rate can therefore cause errors in model calculations and predictions. Since is possible to calculate the value of the heating rate at the temperatures used, an instantaneous value for the heating rate can be used in the calculations. The algorithm was modified to use an instantaneous heating rate and tested for any improvement in the model predictions. The kinetic parameters calculated using the instantaneous heating rate values are provided in Figure 5.8.

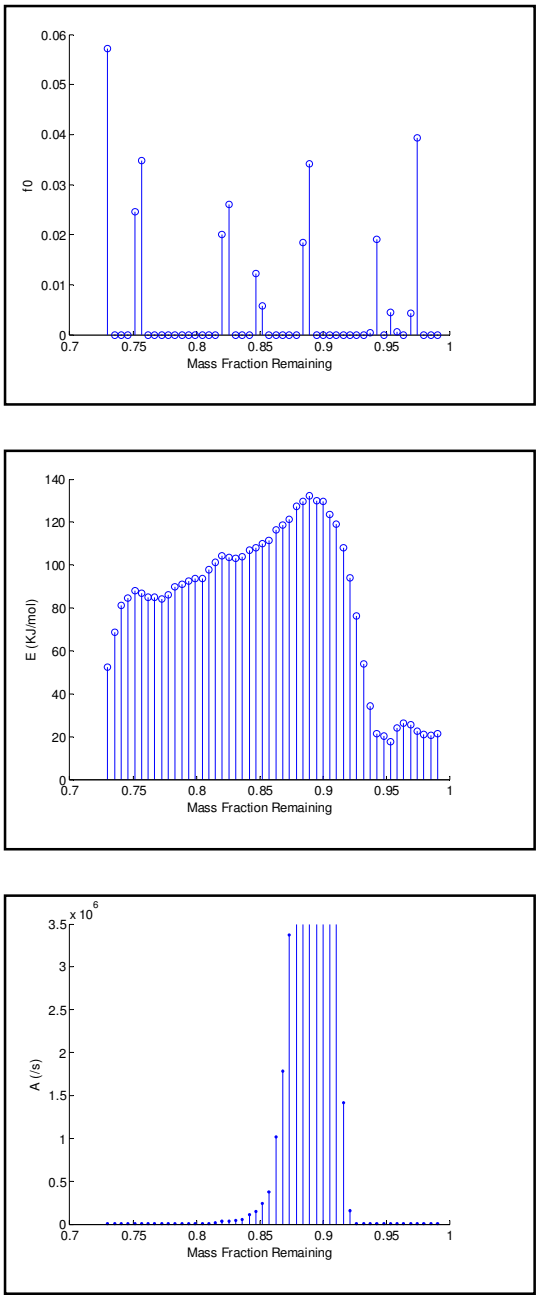


Figure 5.8: Kinetic parameters calculated for coal pyrolysis using instantaneous heating rates (a) Initial mass fraction of each component (b) Activation Energy of each reaction (c) Pre-exponential factor of each reaction

Figure 5.8 (a) shows that there are actually 8 reactions happening during this pyrolysis process. The values of the kinetic parameters obtained for each reaction are summarised in Table 5.2.

Table 5.2: Kinetic parameters of coal pyrolysis in a Perkin-Elmer STA600 TGA calculated using an instantaneous heating rate in the DAEM inversion algorithm

Reaction	f0	E (KJ/mol)	A (s^{-1})
1	0.0048	24.87	44.39
2	0.0584	21.98	31.02
3	0.0044	17.64	1.08
4	0.0526	130.93	2.64×10^{7}
5	0.0180	108.89	1.97×10^{5}
6	0.0462	103.95	3.54×10^{4}
7	0.0593	87.39	283.68
8	0.0571	52.54	1.75

The results in Figure 5.8 (a) and Table 5.2 show an additional reaction, which was missed when the constant heating rate assumption was used. These values are compared to literature values in Table 5.3. This Table also contains other results obtained in this work, which will be discussed in Section 5.1.2 and Section 5.2.

Table 5.3: Distribution of E's for pyrolysis of different coals

Coal Type	E Range	Reference
Witbank coal – low temp. TGA with high heating rates	17 – 109 KJ/mol	This work – Table 5.2
Witbank coal – low temp. TGA with low heating rates	32 – 159 KJ/mol	This work – Table 5.4
Witbank coal – high temp. TGA	14 – 88 KJ/mol	This work – Table 5.5
Japanese sub-bituminous	150 – 400 KJ/mol	Miura, 1995
Datong	100 – 500 KJ/mol	Li *et al*., 2009
Puertollano coal	100 – 200 KJ/mol	Navarro *et al*., 2008
German gas-flame coal	123 – 228 KJ/mol	Juntgen, 1984

The values of E calculated for a South African coal are low compared to those reported in literature. Reported values range from 100 KJ/mol, while the range of E's calculated in the high temperature TGA lies well below 100 KJ/mol.

Using the parameters in Table 5.2, curves were again modelled for the two intermediate heating rates of 35 K/min and 60 K/min. The experimental curves are compared to the model predictions in Figure 5.9.

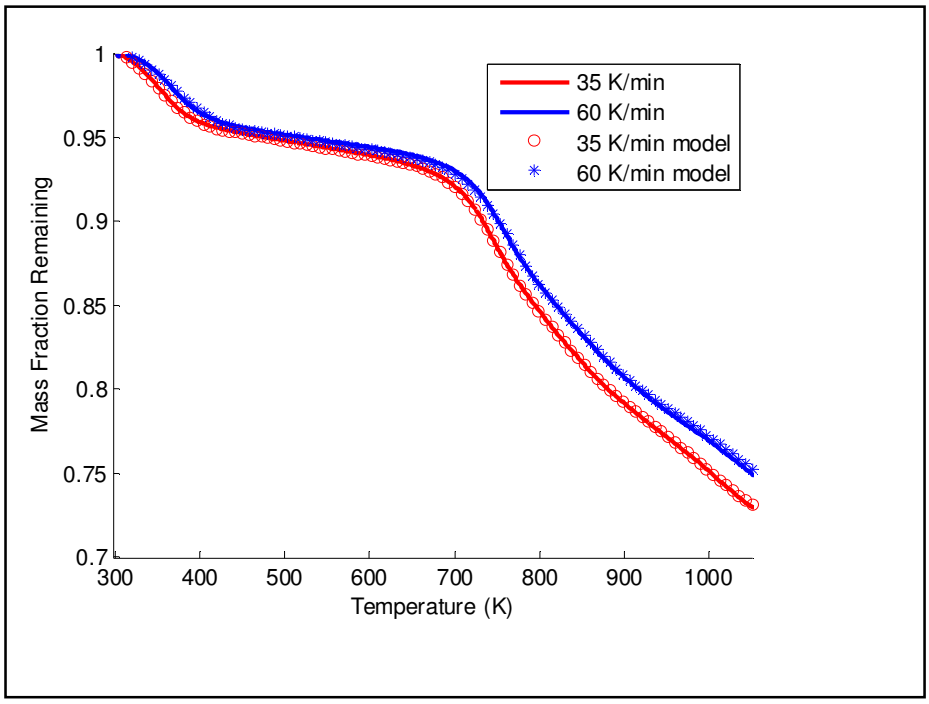


Figure 5.9: TGA curves for coal pyrolysis at heating rates of 35 K/min and 60 K/min with DAEM predictions using parameters calculated from instantaneous heating rates

In Figure 5.9, a better correlation between the model curves and experimental curves is observed. This is especially true for the portion of the 35 K/min curve between temperatures of 550 K and 700 K. Figure 5.7(b) shows a major inconsistency in the sample heating rate in this temperature range. It should be remembered that the modelled curves are for constant heating rates. Errors between the model and experimental results can be attributed to the non-constant heating rates of the samples. The parameters calculated from the instantaneous heating rate data were also used to model DTG curves for heating rates of 35 K/min and 60 K/min, as shown in Figure 5.10.

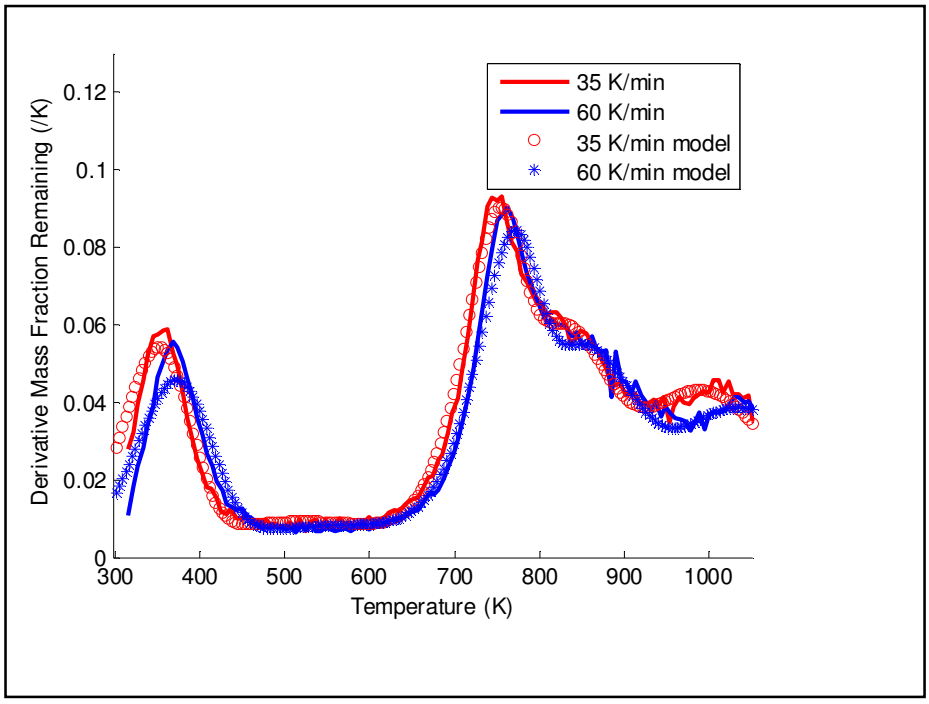


Figure 5.10: DTG curves for coal pyrolysis at heating rates of 35 K/min and 60 K/min with DAEM predictions using parameters calculated from instantaneous heating rates

Figure 5.10 also indicates an improved model fit in the region between 500 K and 700 K for the 35 K/min curve.

For heating rates of 20 K/min and 80 K/min (i.e. those not used in the algorithm), the TGA and DTG curves with model predictions are presented in Figure 5.11 and 5.12 respectively.

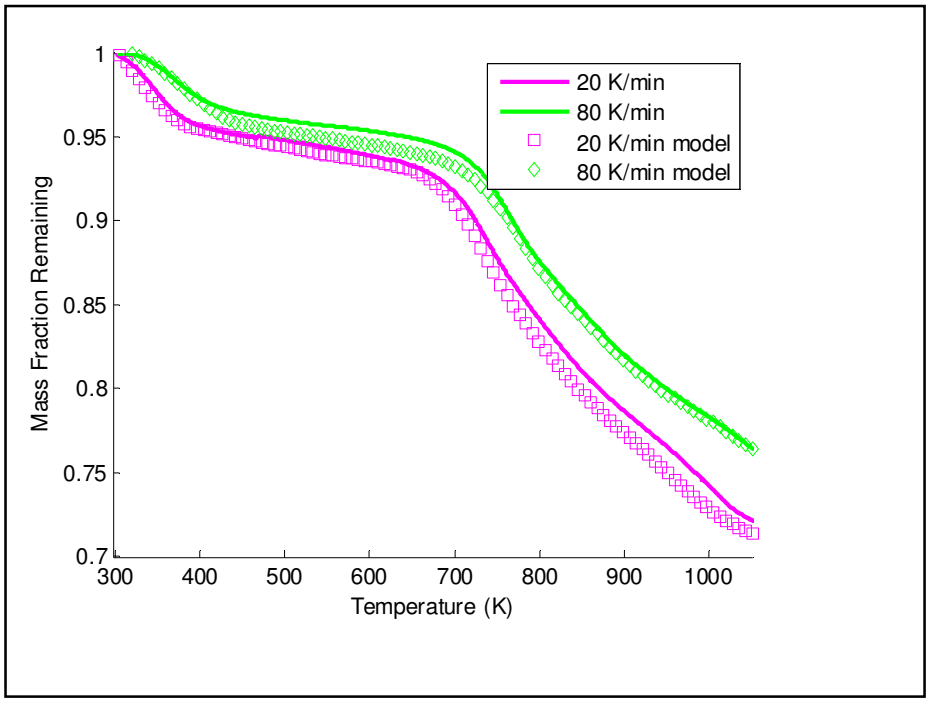


Figure 5.11: TGA curves for coal pyrolysis at heating rates of 20 K/min and 80 K/min with DAEM predictions using parameters calculated from instantaneous heating rates

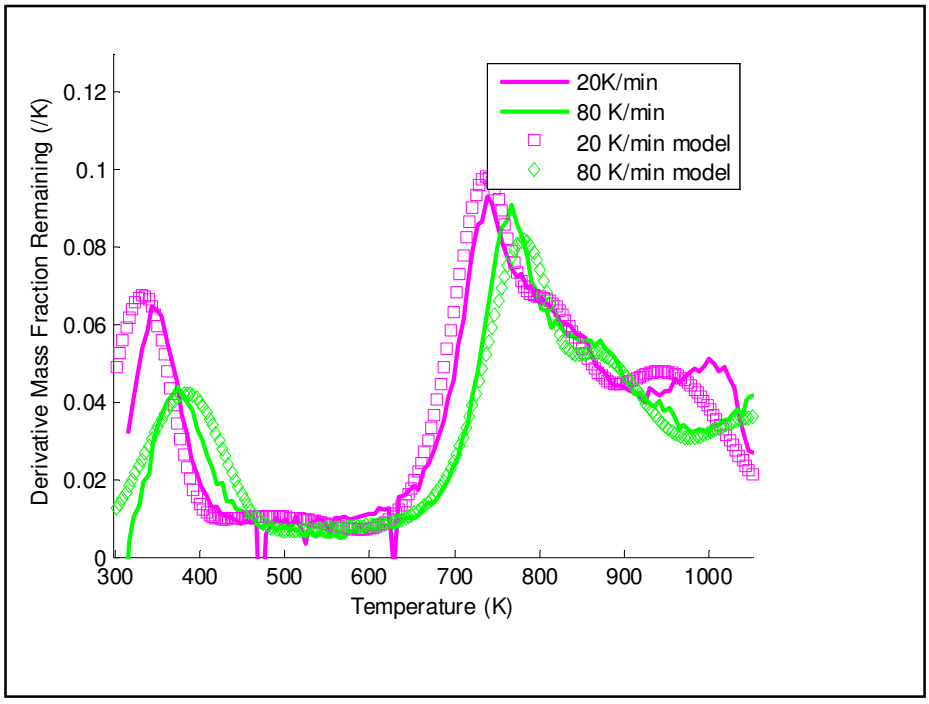


Figure 5.12: DTG curves for coal pyrolysis at heating rates of 20 K/min and 80 K/min with DAEM predictions using parameters calculated from instantaneous heating rates

A poor correlation between the model and experimental curves is still seen in Figure 5.11 and 5.12.

Using the parameters calculated in Table 5.2, curves were then simulated with constant heating rates of 25 K/min and 90 K/min. These curves were then compared to the experimental curves for 20 K/min and 80 K/min respectively. The comparison is provided in Figure 5.13 (a) and Figure 5.14 (a). The reason for this test is that the actual heating rates experienced by the samples were higher than the programme heating rates, so simulated curves with the higher heating rates should provide better approximations to the data.

In a further attempt to improve the model predictions, curves were simulated using the actual heating rate profiles of the TGA curves, which will be called B1 for the 20 K/min curve and B2 for the 80 K/min curve. The correlation between the model and the experimental data can be found in Figure 5.13 (b) and Figure 5.14 (b)

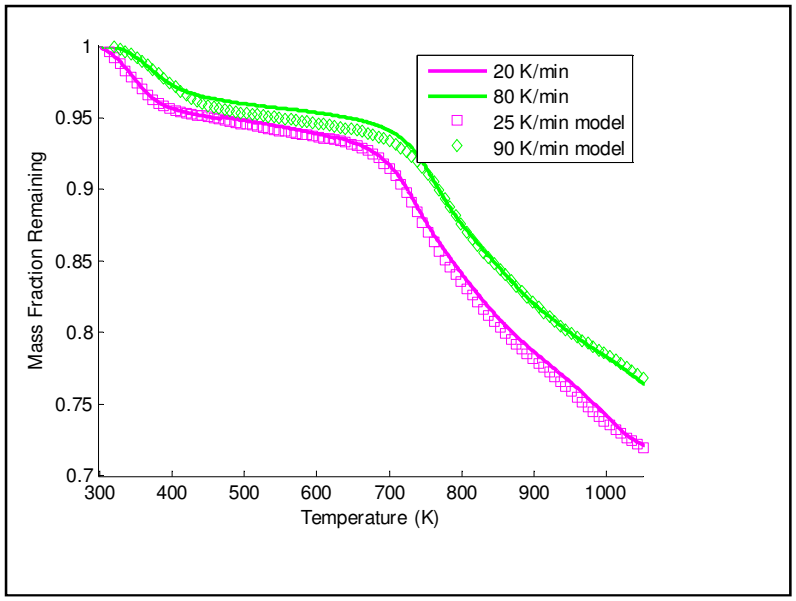


Figure 5.13 (a): TGA curves for coal pyrolysis at heating rates of 20 K/min and 80 K/min with DAEM predictions for constant heating rates of 25 K/min and 90 K/min using parameters calculated from instantaneous heating rates

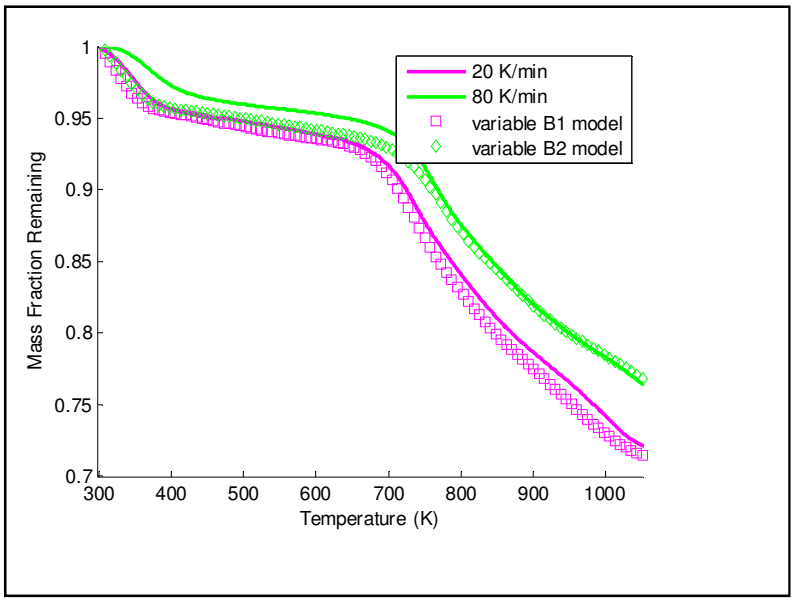


Figure 5.13 (b): TGA curves for coal pyrolysis at heating rates of 20 K/min and 80 K/min with DAEM predictions for actual heating rate profiles using parameters calculated from instantaneous heating rates

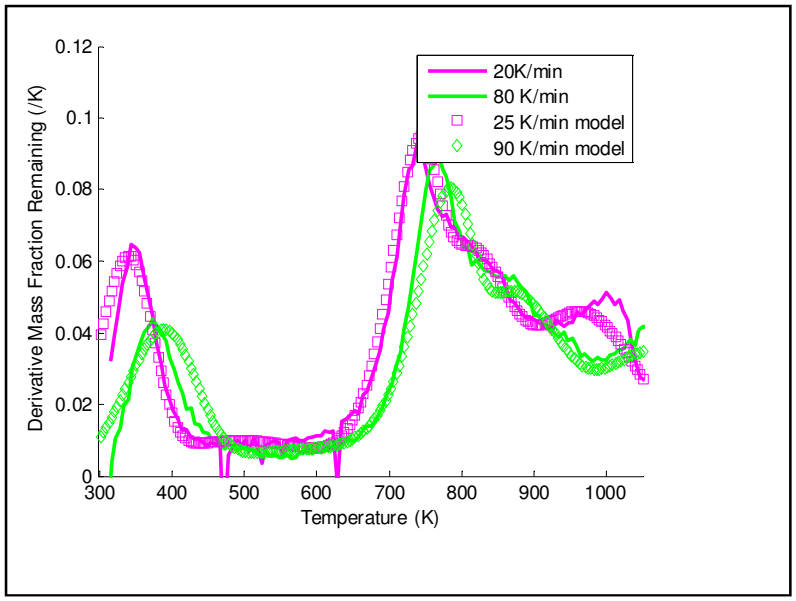


Figure 5.14 (a): DTG curves for coal pyrolysis at heating rates of 20 K/min and 80 K/min with DAEM predictions for constant heating rates of 25 K/min and 90 K/min using parameters calculated from instantaneous heating rates

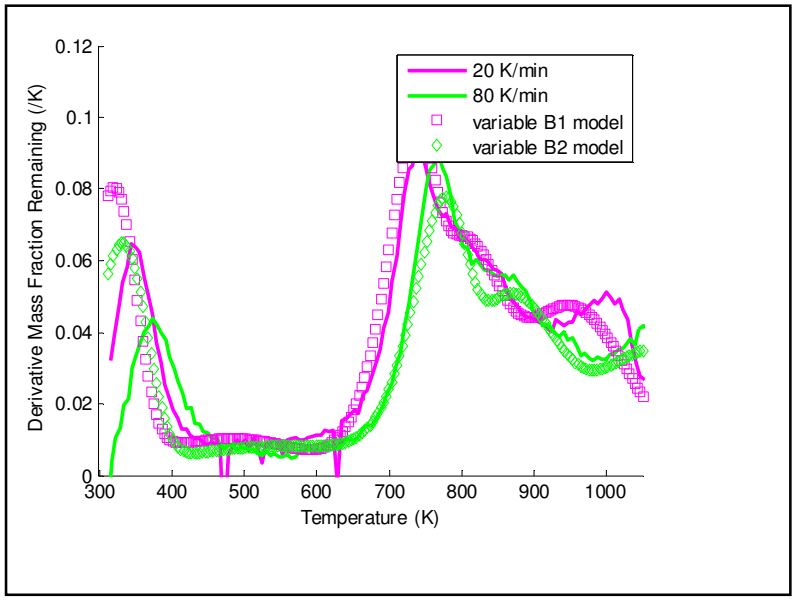


Figure 5.14 (b): DTG curves for coal pyrolysis at heating rates of 20 K/min and 80 K/min with DAEM predictions for actual heating rate profiles using parameters calculated from instantaneous heating rates

A slightly more accurate prediction of the experimental curves than previously is found in Figure 5.13 (a) and Figure 5.14 (a), when curves were simulated with higher heating rates. However, it must be noted that the actual heating rates of these experimental curves are not constant, which is the reason for the discrepancy between the model predictions and experimental curves.

Figure 5.13 (b) and Figure 5.14 (b) show that the curves modelled with instantaneous heating rate profiles are a worse fit to experimental data than the curves in Figure 5.13 (a) and Figure 5.14 (a).

5.1.2 Lower Heating Rates

As mentioned previously, the shape of the 5 K/min curve differed from the other curves. It was therefore decided to investigate the effect of lower heating rates on reaction kinetics. Pyrolysis runs for heating rates of 5 K/min and 8 K/min were also carried out in this TGA. The purpose of this was to test whether the kinetic parameters obtained from lower heating rate data correspond to those calculated with the higher heating rate curves. This would indicate whether the kinetics are dependent on the heating rate. If so, the kinetics would only apply within a range of heating conditions. Figure 5.15 shows the TGA curves for these lower heating rates.

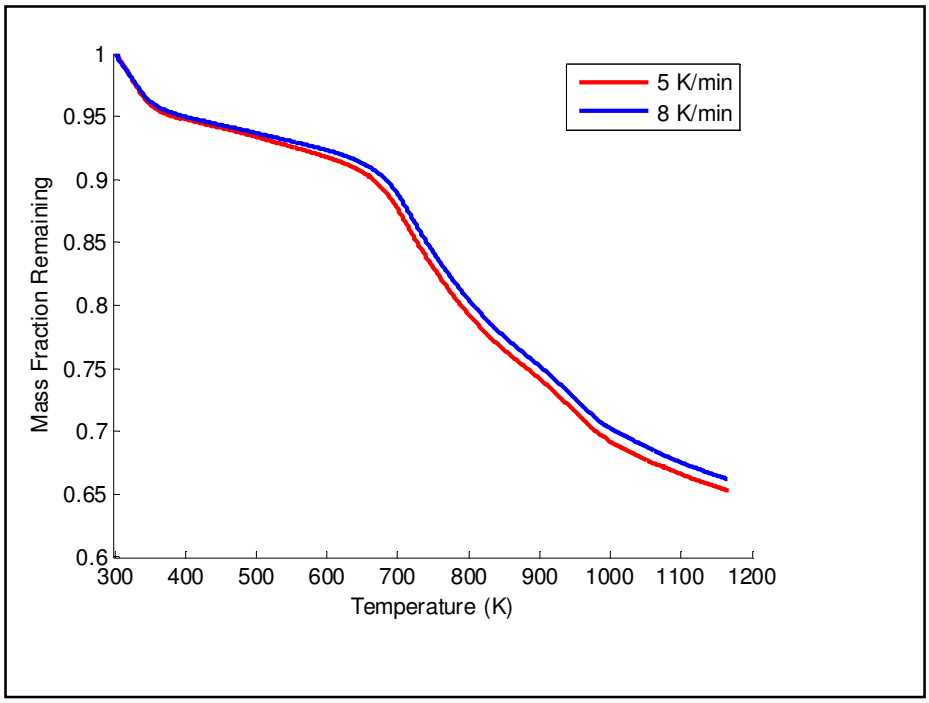


Figure 5.15: TGA curves for the pyrolysis of a South African coal at low heating rates

For heating rates of 5 K/min and 8 K/min, the DTG curves are given in Figure 5.16.

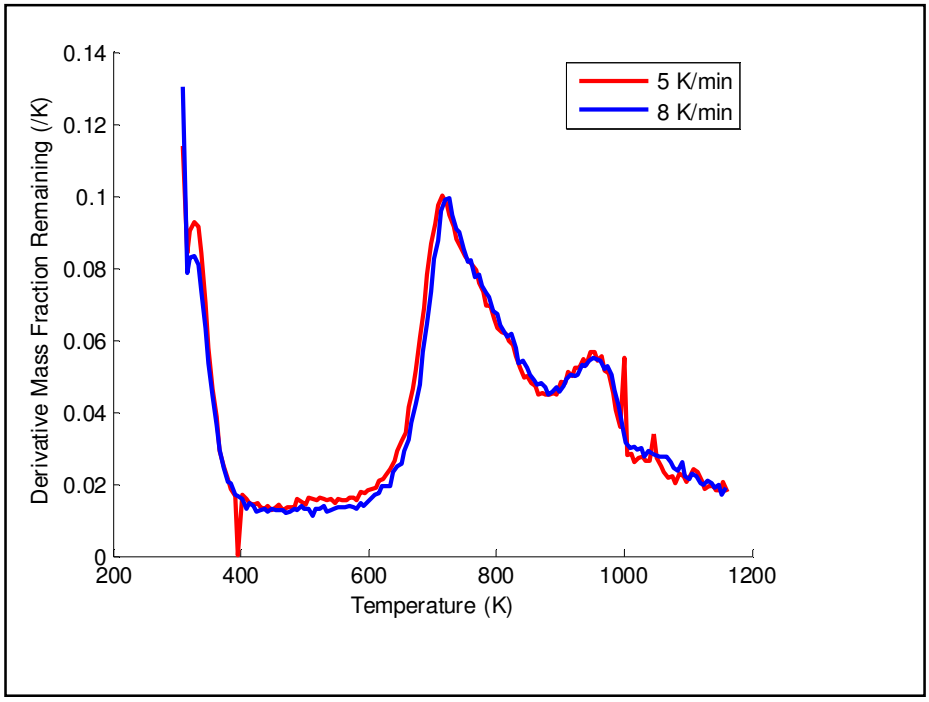
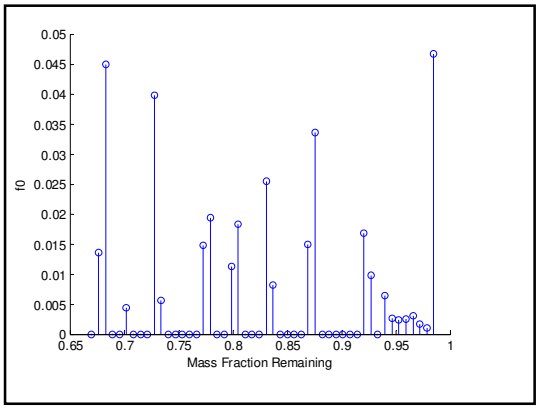


Figure 5.16: DTG curves for the pyrolysis of a South African coal at low heating rates

The kinetic parameters calculated from these curves are shown in Figure 5.17.



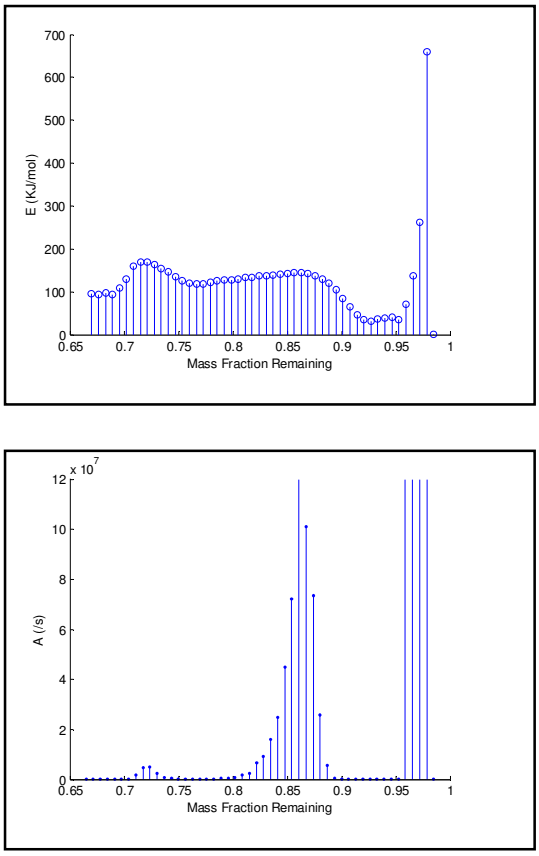


Figure 5.17: Kinetic Parameters calculated for coal pyrolysis at lower heating rates (a) Initial mass fraction of each component (b) Activation Energy of each reaction (c) Pre-exponential factor of each reaction

Nine reactions are found from the plot in Figure 5.17 (a), while the higher heating rate data shows only seven reactions. As mentioned in Chapter 4, lower heating rates provide a more high resolution image of the steps involved in pyrolysis. This is the reason that the algorithm is able to find more reactions from the lower heating rate data. The values of the kinetic parameters calculated for each reaction are provided in Table 5.4:

Table 5.4: Kinetic parameters of coal pyrolysis in a Perkin-Elmer STA 600 TGA calculated using lower heating rates in the DAEM inversion algorithm

Reaction Number	f0	E (KJ/mol)	A (/s)
1	0.01	37.35	323.25
2	0.02	32.77	1.43
3	0.05	139.93	7.61×10^{7}
4	0.03	138.77	1.49×10^{7}

5	0.03	128.68	8.52×10^{5}
6	0.03	119.73	7.29×10^{4}
7	0.05	158.71	2.18×10^{6}
8	0.44×10^{-2}	129.05	1.23×10^{4}
9	0.06	95.85	101.97

Results from higher heating rate data proved that it is important to investigate the instantaneous heating rate of the sample. The sample and programme heating rates are plotted in Figure 5.18.

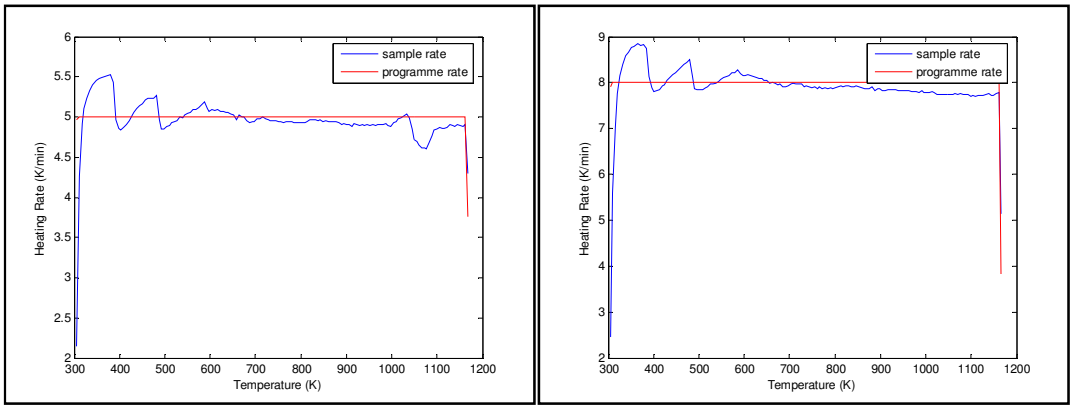


Figure 5.18: Comparison of programme heating rates and actual heating rates of the samples for coal pyrolysis at lower heating rates in a Perkin Elmer STA600 TGA

It is noted from Figure 5.18 that the sample heating rate is not constant. However, since the discrepancy between the sample and programme heating rates is small, the constant heating rate assumption is assumed valid for this calculation. The parameters in Table 5.4 are therefore considered correct. The curves modelled with these kinetic parameters are compared to experimental curves in Figure 5.19 and Figure 5.20.

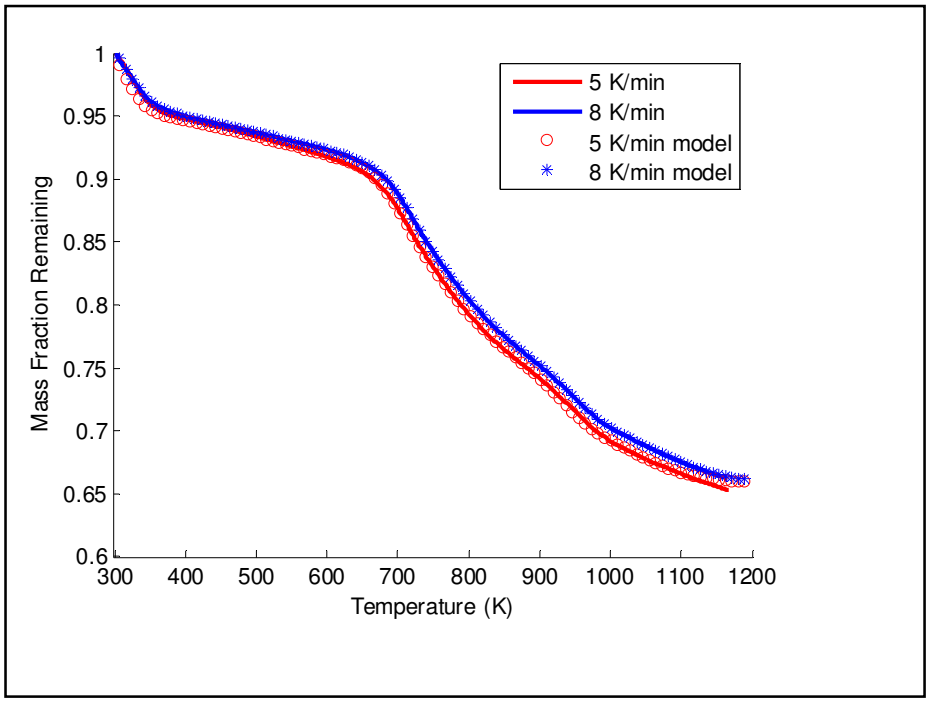


Figure 5.19: TGA curves for coal pyrolysis at heating rates of 5 K/min and 8 K/min with DAEM predictions for each heating rate

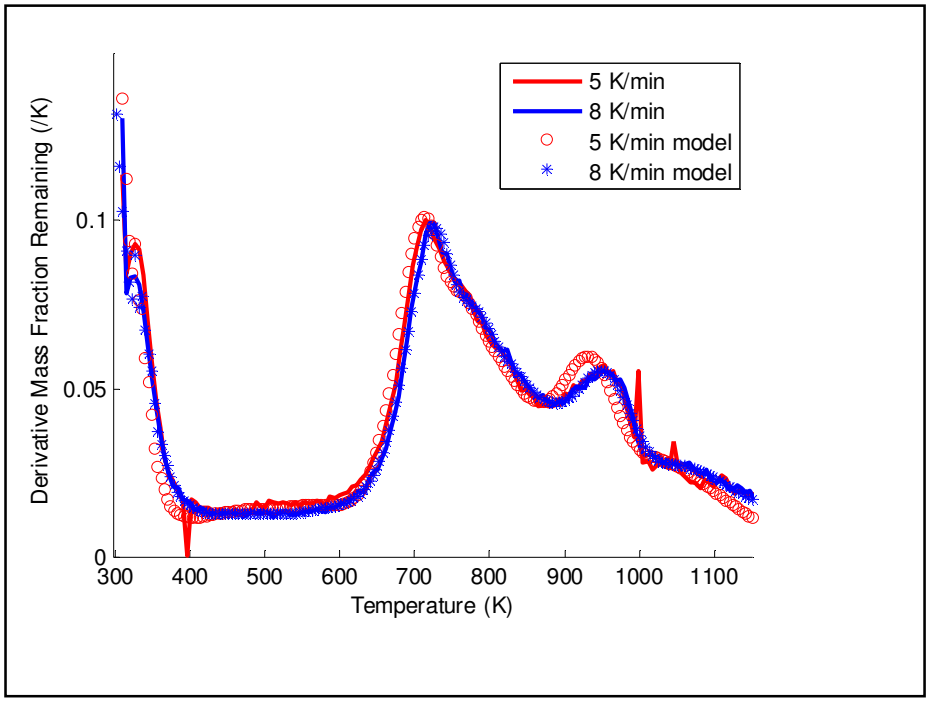


Figure 5.20: DTG curves for coal pyrolysis at heating rates of 5 K/min and 8 K/min with DAEM predictions for each heating rate

A good fit between experimental data and model predictions is observed in Figure 5.19 and Figure 5.20. The kinetic parameters differ from those calculated with higher heating rate data, indicating that reaction kinetics are dependent on heating rate. To further test this assumption, the calculated parameters from the lower heating rate data were used to model a curve for 35 K/min. This curve was compared to the experimental curve, as shown in Figure 5.21.

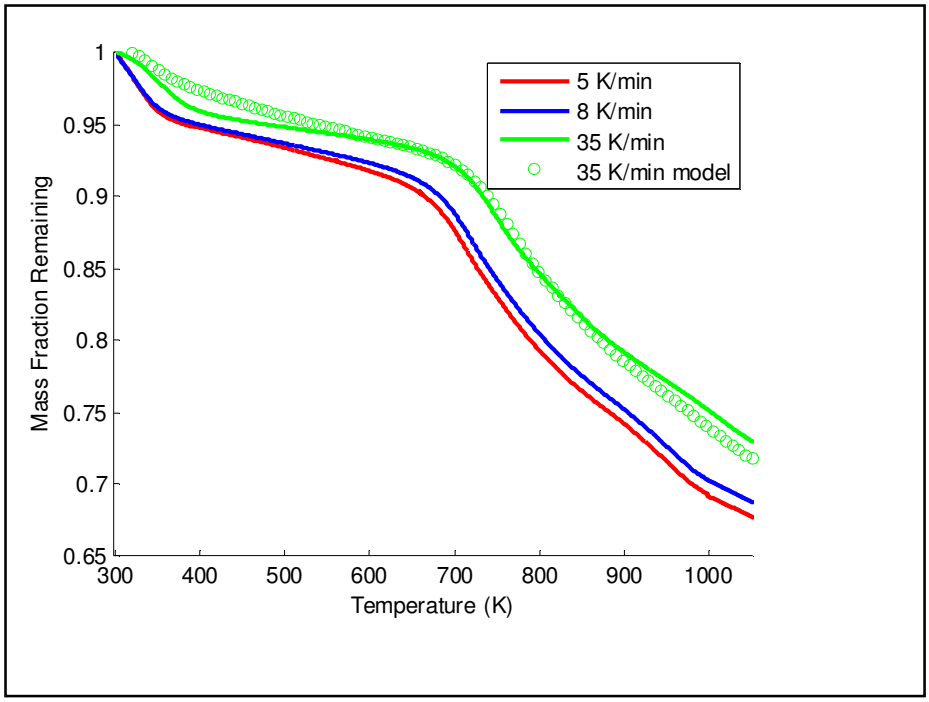


Figure 5.21: Comparison of model curve to experimental curve for 35 K/min using parameters obtained from lower heating rate data

Figure 5.21 shows that the model curve is not a good prediction of experimental data, but instead follows the general shape of the lower heating rate curves. This implies that the algorithm and the model only apply within a range of heating rates for this coal. The range can be found by examining the set of curves and finding those which are similar in shape. A further investigation into this observation is required, but is not within the scope of this work. It is left to the reader to decide which set of heating rates to use.

The results obtained from the low temperature TGA experiments show that the DAEM is able to model coal pyrolysis under certain conditions. One of these is that the difference in heating rates used must not be too large. In this TGA, it is observed that the heating rate which the sample is exposed to is not actually constant. This is an important consideration in modelling. The results also indicate that complete pyrolysis did not occur in this TGA. Heating the

samples to higher temperatures might allow for complete pyrolysis. This was the motivation for conducting experiments in the high temperature TGA.

5.2 High temperature TGA experiments

Another set of pyrolysis experiments was carried out in the higher temperature Thermal Analysis Q600 TGA, as described in Section 3.4.2 (a). With this instrument, coal samples were heated to 1573 K at different heating rates, followed by a 10 minute holding period at 1573 K. The TGA curves for these runs are presented in Figure 5.22.

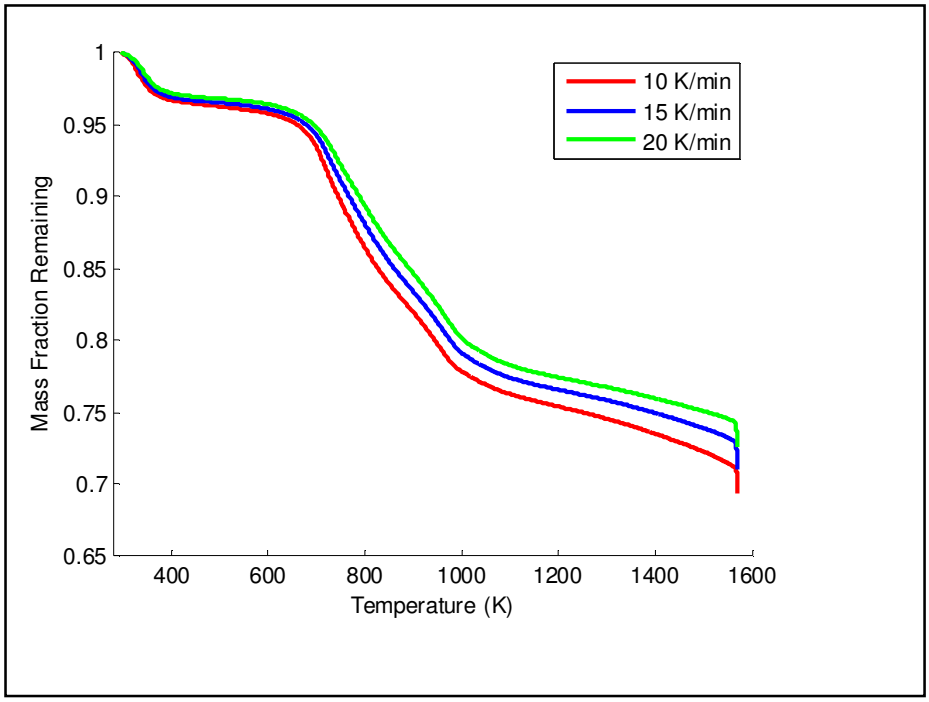


Figure 5.22: TGA curves for the pyrolysis of South African coal at different heating rates in a TA Instruments Q600 TGA

Figure 5.22 also shows that curves shift to the right as the heating rate increases. Following the temperature increase, the temperature was held constant at 1573 for 10 minutes. This isotherm is evident in the TGA curves.

The DTG profiles of the samples at the heating rates used are presented in Figure 5.23.

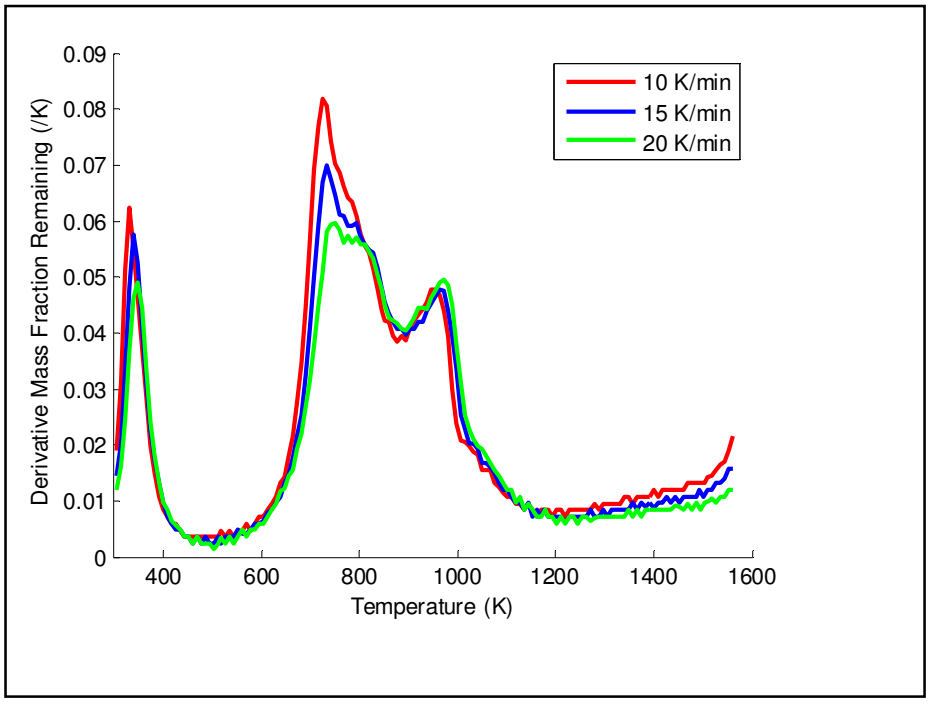
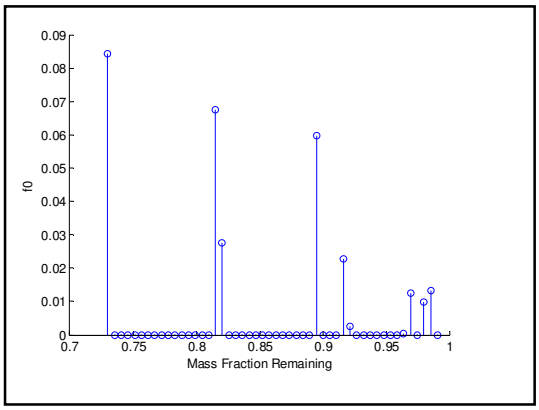


Figure 5.23: DTG curves for the pyrolysis of South African coal at different heating rates in a TA Instruments Q600 TGA

The data for heating rates of 10 K/min and 15 K/min was fed into the algorithm to calculate the kinetic parameters for the pyrolysis process. These are plotted at each conversion in Figure 5.24.



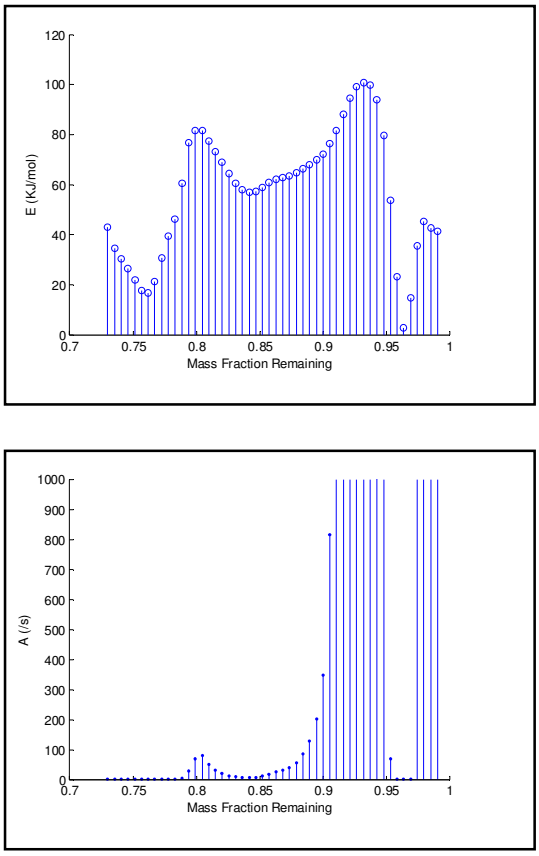


Figure 5.24: Kinetic Parameters calculated for coal pyrolysis in a high temperature TGA (a)Initial mass fraction of each component (b)Activation Energy of each reaction (c)Pre-exponential factor of each reaction

According to the results from the high temperature TGA, the pyrolysis process consists of 6 reactions. The values of f_0, E and A for each of these reactions is given in Table 5.5:

Table 5.5: Kinetic parameters of coal pyrolysis in a TA Instruments Q600 TGA calculated using the DAEM inversion algorithm

Reaction Number	**f_0**	**E (KJ/mol)**	**A (s^{-1})**
1	0.02	43.84	5.63×10^4
2	0.01	14.86	0.36
3	0.02	88.03	0.85×10^4
4	0.06	69.80	200.35
5	0.09	70.92	26.14
6	0.08	42.85	0.0215

Table 5.5 shows a range of E's from 14 to 88 KJ/mol. These values are lower than the values reported in literature for other types of coal, as shown in Table 5.3. The loss of moisture from the coal is described by Reaction 1, which has an E of 43.84 KJ/mol. This value corresponds well to the value of 43.8 KJ/mol reported by Prado & Vyazovkin (2011) for the E of water evaporation.

The values of the kinetic parameters in the Table 5.5 are significantly different to those obtained from the lower temperature TGA curves. A possible cause for this might be the constant heating rate assumption. Data for the sample temperature at each point in time was used to plot the heating rate profiles of the sample. These are presented in Figure 5.25.

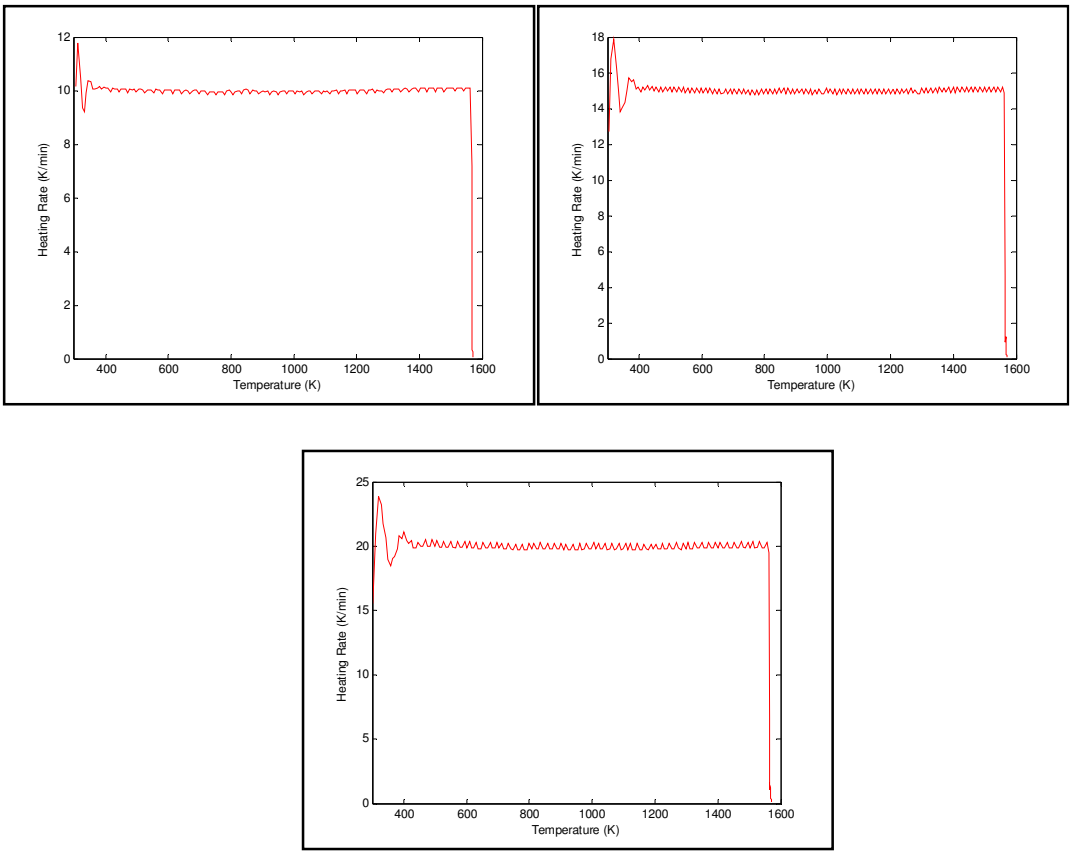


Figure 5.25: Actual heating rates of the samples for coal pyrolysis in a TA instruments Q600 TGA

The heating rate profiles in Figure 5.25 are linear, except for an initial spike, which can be attributed to the control system of the furnace trying to maintain a constant heating rate. This TGA therefore has a major advantage over the lower temperature TGA in terms of

controlling the heating rate of a sample. For these results, the constant heating rate assumption will be considered valid when using the DAEM inversion algorithm.

The kinetic parameters were once again used to model the pyrolysis reactions at the heating rates used for the experiments. These curves are compared to the original TGA curves in Figure 5.26.

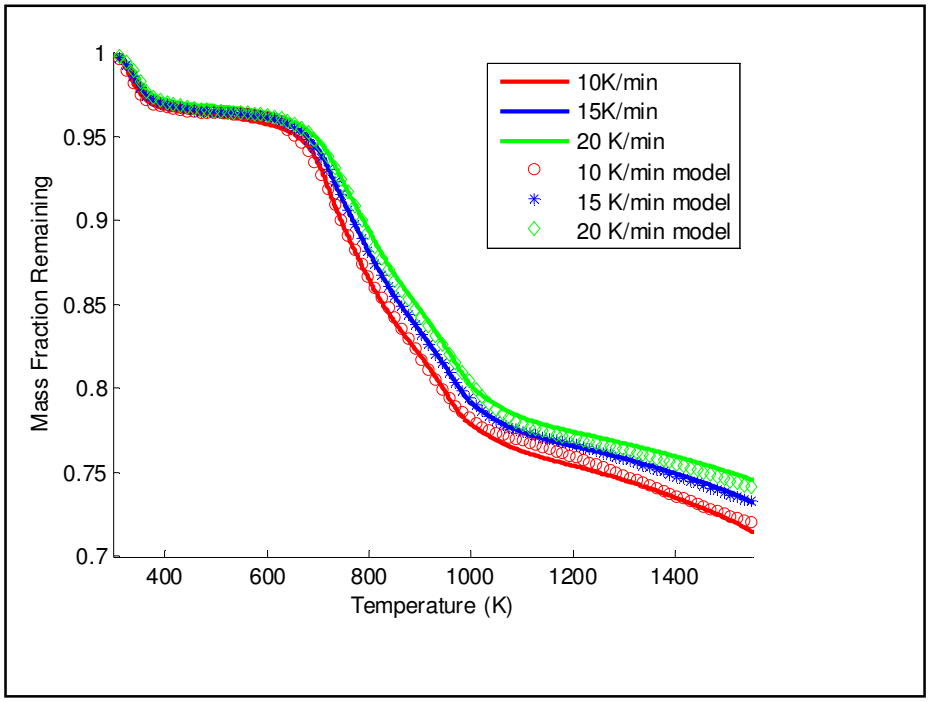


Figure 5.26: TGA curves for the pyrolysis of South African coal at different heating rates in a TA Instruments Q600 TGA, with DAEM predictions for each heating rate

Model fits to the DTG curves are shown in Figure 5.27.

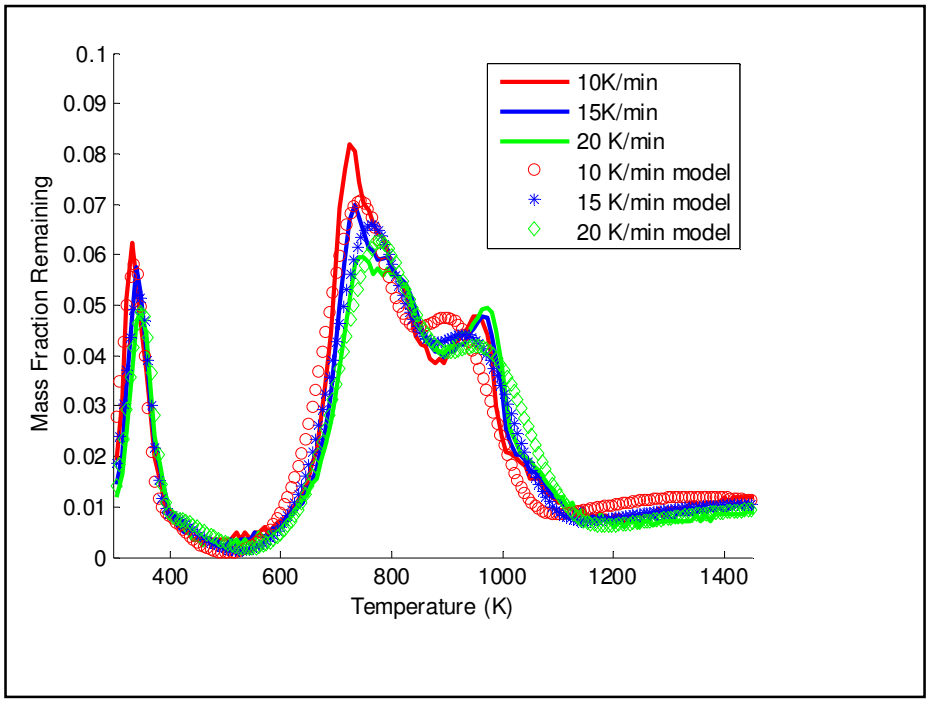


Figure 5.27: DTG curves for the pyrolysis of South African coal at different heating rates in a TA Instruments Q600 TGA, with DAEM predictions for each heating rate

Figure 5.26 and Figure 5.27 indicate a good fit between experimental data and model predictions, even though the kinetics are different to those calculated from the lower temperature TGA.

A possible reason for the difference in kinetic parameters is that the flowrate and pressure of Nitrogen is different for both TGA due to the sizes of the furnace being different. The higher temperature TGA also requires a smaller sample mass. Another reason is that the range of heating rates used is between the two ranges used in the lower temperature TGA.

The kinetic parameters reported were then used to predict a coal pyrolysis reaction at an ultra-high heating rate of 10000 K/min. It has been pointed out in Section 5.1.2 that the use of comparatively low heating rate data might not provide an accurate prediction of ultra-high heating rates. However, these predictions may provide some information about pyrolysis behaviour at heating rates which are common in industry but not attainable in laboratories. The model predictions for TGA and DTG curves at a heating rate of 10000 K/min are provided in Figure 5.28 and Figure 5.29 respectively.

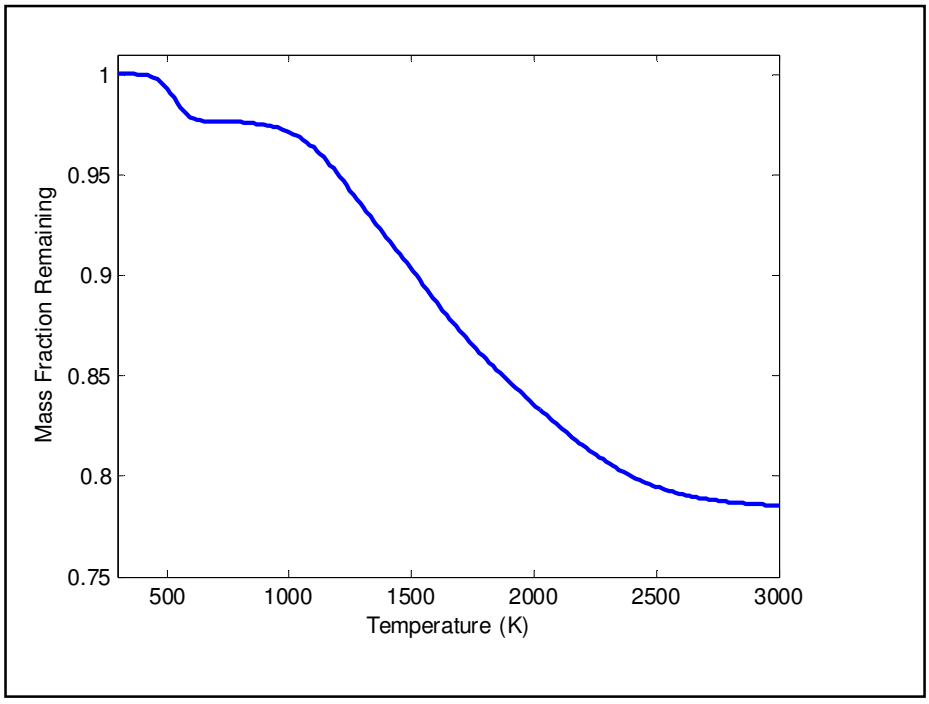


Figure 5.28: DAEM prediction of a TGA curve for a heating rate of 10 000 K/min

Figure 5.28 indicates that at a heating rate of 10000 K/min, devolatilization of this coal takes place at much higher temperatures. The loss of moisture can be seen at 500 K, while the loss of remaining volatiles appears to be a single event in this curve.

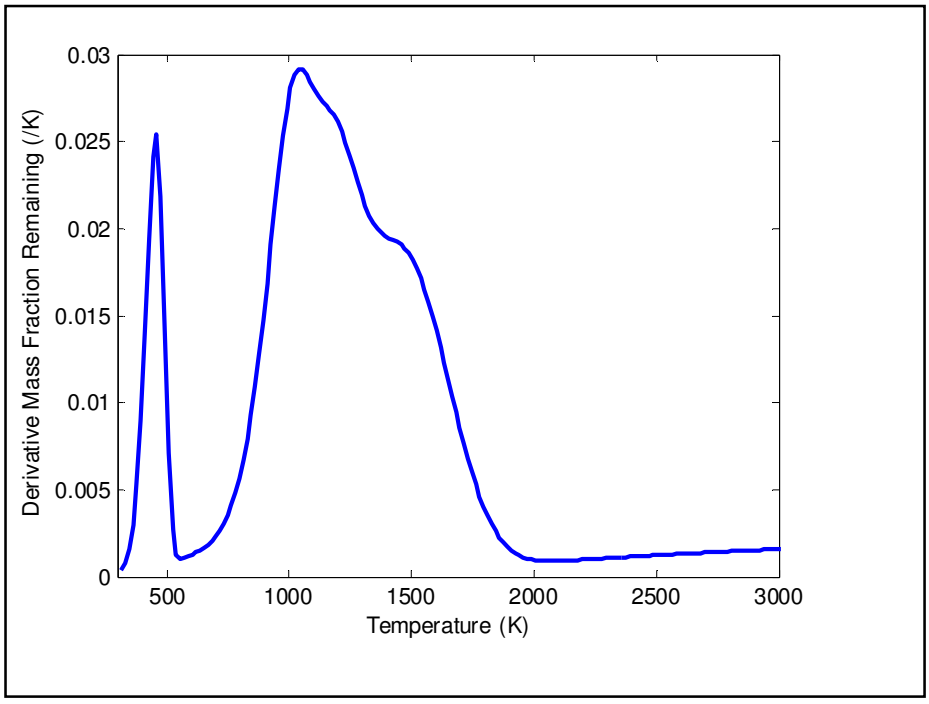


Figure 5.29: DAEM prediction of a DTG curve for a heating rate of 10 000 K/min

The DTG curve in Figure 5.29 also provides a description of the pyrolysis reaction. The moisture loss is again evident at 500 K. The major fraction of the volatiles is released between 700 K and 2000 K. The DTG peaks in this temperature region appear "merged", in contrast to lower heating rate peaks, which are more distinct.

5.3 Conclusion

Thermo-gravimetric data obtained from non-isothermal pyrolysis experiments has been analysed in this chapter for each TGA. Results show that the DAEM inversion algorithm is suitable for calculating the kinetics of pyrolysis of a South African coal from the Witbank region, as well as modelling the pyrolysis process using these kinetics. This answers Research Question 1, posed in Chapter 1, Section 1.4.

However, this algorithm is can only be used within certain heating rate ranges. It is important to check that the data used in the algorithm is not obtained from two vastly different heating rates. This can be done by examining the TGA curves to ensure that the same general shape is followed by both curves.

Another important finding from this chapter is that the constant heating rate assumption used in the algorithm is not always valid. When conducting TGA experiments, the sample

temperature data should always be examined. The instantaneous heating rate of the sample should be compared to that specified by the TGA programme to check whether the assumption can be used.

The problem of a non-constant heating rate was overcome in this case by making changes to the algorithm. The code used to calculate the kinetics was altered to take in an instantaneous heating rate value at each temperature. This value was calculated from the temperature *vs*. time data. The use of instantaneous heating rate values resulted in an improved model fit to the experimental data. This finding answers Research Question 2.

It was also found that data from the two TGA's provide different sets of reaction kinetics when used in the DAEM algorithm. This leads to the conclusion that the calculated kinetic parameters are not intrinsic values for this coal. Since each set of kinetics provides a good model fit to the experimental results, they will be assumed to be applicable to the reaction conditions in their respective TGA's only. For industrial applications, it is advised to match the conditions in the TGA to those of the large-scale reactors as closely as possible.

Chapter 6: Combustion Results

This chapter describes the results of TGA experiments on the combustion of a South African coal char. The data from these experiments was used in the DAEM algorithm in order to calculate the E of combustion. This algorithm could be used since it was established in Chapter 4 that the calculation of E is a model-free method. The calculated value of E was then used in another algorithm to calculate the value of the pre-exponential factor based on the shrinking-core model. It was assumed that the char combustion consisted of a single reaction. The kinetic parameters were then used to model the combustion reaction according to the shrinking core model. The model was compared to the experimental data in order to validate the model. Finally, combustion of raw coal was carried out and the results were compared to those of char.

6.1 Low Temperature TGA experiments

6.1.1 Char Combustion

The Perkin-Elmer STA 600 TGA was used for a set of char combustion experiments. Char was formed by heating the coal from 303 K to 1173 K in Nitrogen at 15 K/min. The char was cooled down to 303 K and then heated from 303 K to 1173 K in Oxygen at different heating rates. The results of these char combustion experiments are shown in Figure 6.1:

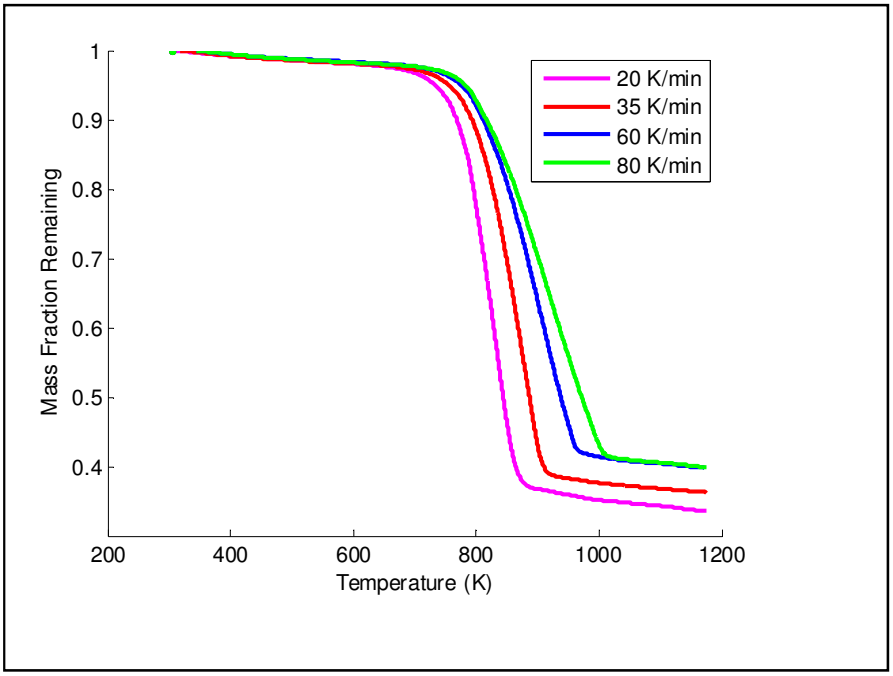


Figure 6.1: TGA curves for the combustion of a South African char at different heating rates in a Perkin-Elmer STA600 TGA

From the curves in Figure 6.1, it can be seen that as the heating rate increases, the curves shift to the right, indicating that the combustion reaction is taking place at a higher temperature. It is also evident that during the char preparation process, complete devolatilization of the char did not occur. This is indicated by the fact that all the curves do not reach the same level once the combustion reaction is complete. A larger fraction of the char reacts at lower heating rates. The derivative curves for each of these TGA curves are shown in Figure 6.2.

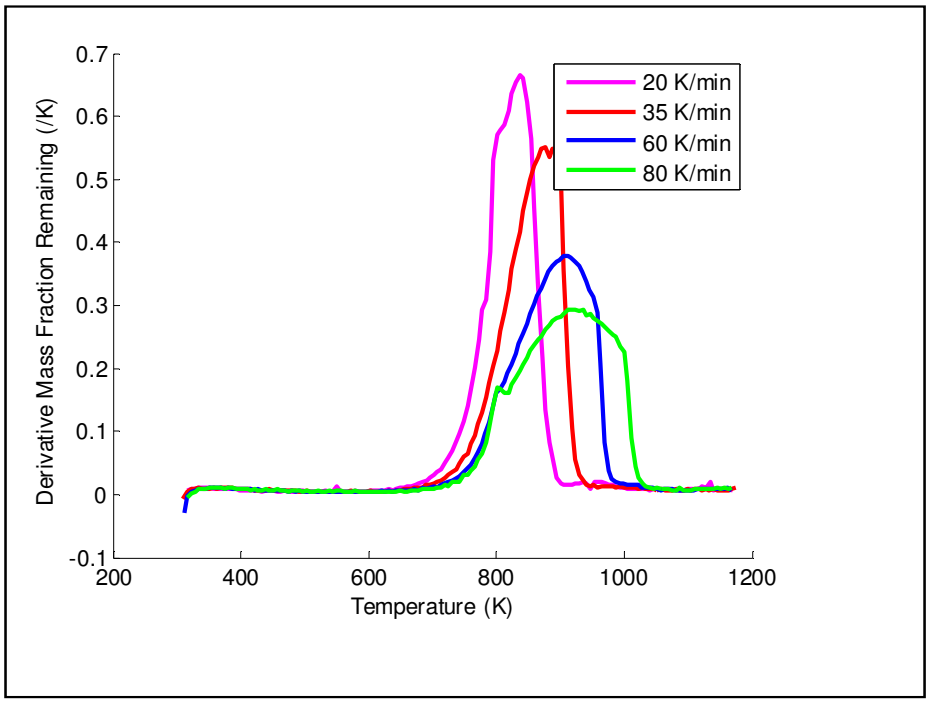
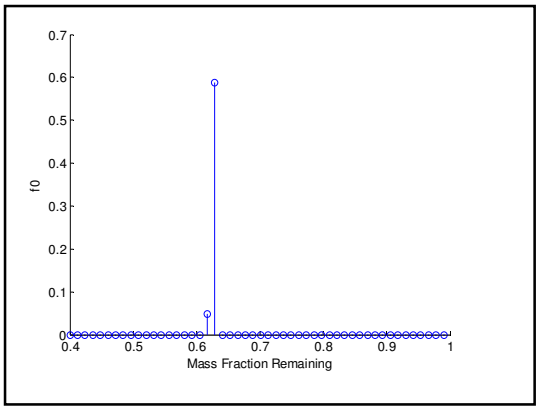


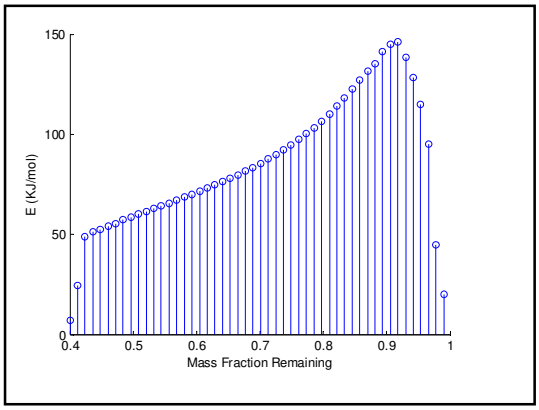
Figure 6.2: DTG curves for the combustion of a South African char at different heating rates in a Perkin-Elmer STA600 TGA

The derivative curves have two peaks, which could either indicate that two reactions are occurring, or be attributed to noise in the system. The data from these TGA curves was fed into the DAEM algorithm for constant heating rates in order to calculate the E of char combustion. TGA data for heating rates of 35 K/min and 60 K/min was used in the algorithm. The kinetic parameters obtained are shown in Figure 6.3.

(a)



(b)



(c)

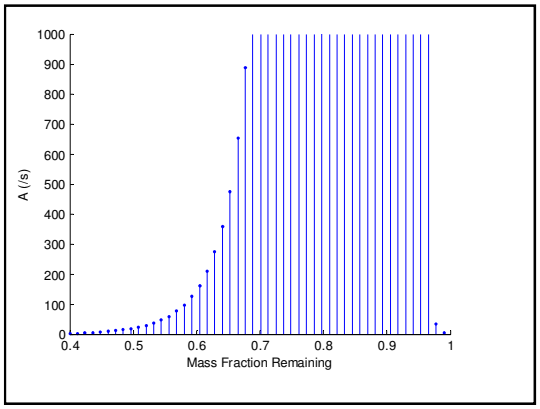


Figure 6.3: Kinetic parameters calculated for char combustion (a) Initial mass fraction of each component (b) Activation Energy of each reaction (c)Pre-exponential factor of each reaction

Figure 6.3 (a) shows that there is only a single reaction occurring during the combustion of the char. The values of f_0 are set to zero, except at one point. The corresponding values of E and A at that point are given in Table 6.1. The value of E is assumed correct since a model-free method was used to calculate it.

Table 6.1: Kinetic parameters of char combustion in a Perkin-Elmer STA600 TGA calculated using the DAEM inversion algorithm

f_0	0.63
E (KJ/mol)	73.90
A (s^{-1})	241.97

The value of f_0 shows that 63 % of the coal has reacted. This corresponds well to the proximate analysis. These parameters were then used to model a combustion reaction for heating rates of 35 K/min and 60 K/min, according to the DAEM. The reaction would therefore be modelled as a single, first-order reaction, since only a single value for f_0 has been found. The comparison of this reaction model to the experimental data can be found in Figure 6.4.

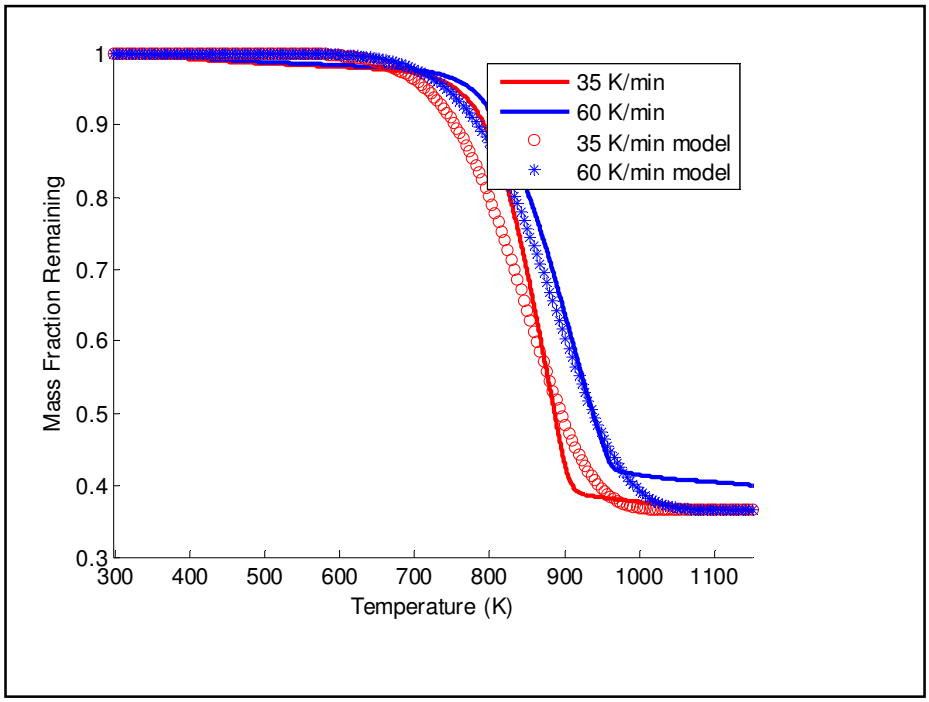


Figure 6.4: TGA curves for the combustion of a South African char at heating rates of 35 K/min and 60 K/min, with DAEM predictions for each heating rate

Figure 6.4 shows that the DAEM is not a good description of char combustion. This is expected since it is known that char combustion is not a first order reaction. The value of A in Table 6.1 is incorrect since it is based on the assumption of a first-order reaction. It should be

noted that the calculation of f_0 requires a value for A. However, since there is only a single reaction occurring, the value of f_0 calculated by the algorithm is correct, as this value is (1-ash). If there were multiple reactions happening in the combustion process, each calculated value of f_0 could not be relied upon as the correct value, since its calculation depends on the value of A.

It was then attempted to model a shrinking core reaction using the calculated value of E. This value was used with the temperature at which it was calculated in a new algorithm to calculate the value of A assuming a shrinking core reaction mechanism, as done in Section 4.4.2. The value of A for the reaction calculated by this algorithm is 203.97 s^{-1}. To test whether the shrinking core is appropriate for the combustion of this particular coal, the kinetic parameters were then used to model the reaction at the two heating rates used in the algorithm. The reaction was modelled using the $\Psi^{s.c.}$ matrix described in Section 4.5. The models are compared to experimental data in Figure 6.5:

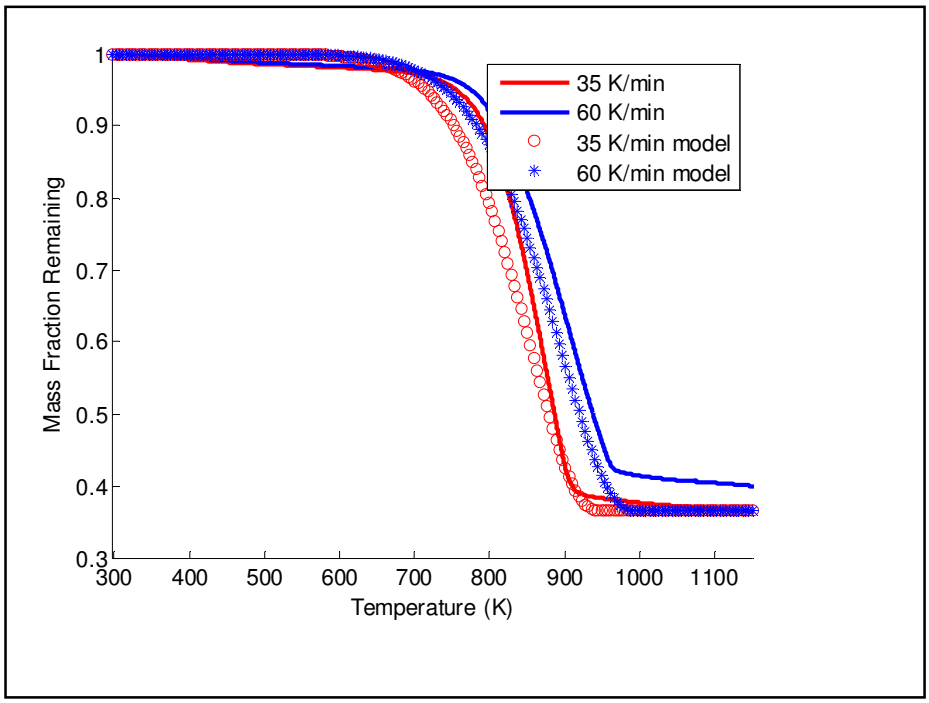


Figure 6.5: TGA curves for the combustion of a South African char at heating rates of 35 K/min and 60 K/min, with shrinking core model predictions for each heating rate

It is clear from Figure 6.5 that model does not correlate to the experimental data. For this reason, it is concluded that the shrinking core model does not describe the combustion of this South African coal char in oxygen.

Everson *et al* (2006 [a&b]) found that the shrinking core is applicable to the combustion of a South African char in air. The poor fit in Figure 6.5 could be due to differences in the coals used. Another reason is the use of oxygen as the reactant instead of air. Combustion in oxygen has a steeper slope than combustion in air, which changes the value of the kinetic parameters calculated by the algorithm. Figure 6.5 shows that the model curve is less steep than the experimental curve.

One reason for the difference between combustion in oxygen and air is that the presence of nitrogen in air affects the transport of oxygen to the char particle surface (Li *et al*., 2010). This finding is backed up by Qiao *et al*. (2010), who concluded that the thermal conductivity of the gases surrounding the particle affects the ignition temperature of the particle. This ignition temperature is a measure of the activation energy of the coal sample (Hull & Agarwal, 1988). Combustion of this char in air might therefore result in a better fit of the shrinking core model to experimental data.

Using the same method of integration as above, it may be attempted to use other combustion models with the calculated value of E to find A, and then model the reaction based on these parameters. However, it is beyond the scope of this work to find the appropriate model. In this work, it is claimed that the DAEM can be used as a model-free method to calculate the E of combustion. From this point on, only the values of E will be obtained from combustion data and these values will be examined.

In Chapter 5 it was concluded the assumption of a constant heating rate could affect the DAEM results. The heating rate data was therefore analysed in order to check whether this was the cause of the bad fit. The programme and sample heating rates for the two heating rates used in the algorithm are plotted in Figure 6.6.

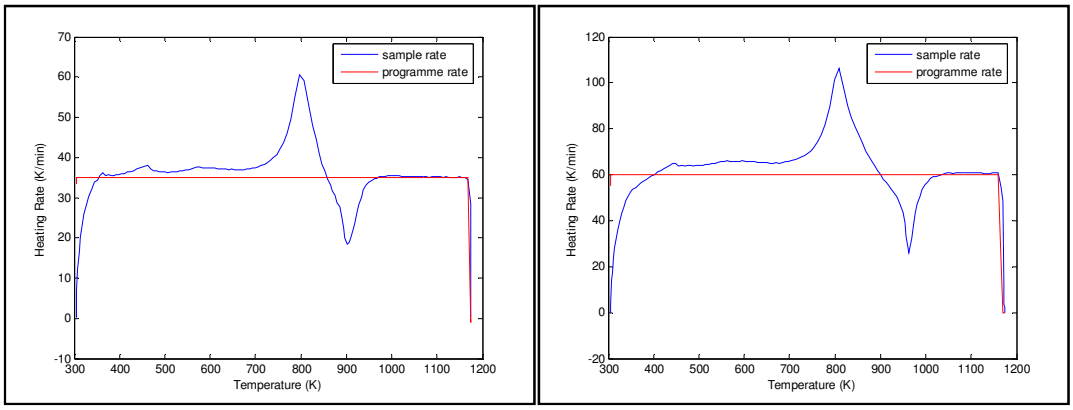
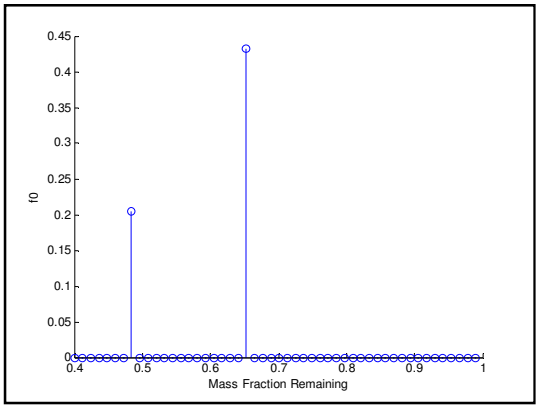


Figure 6.6: Comparison of programme heating rates and actual heating rates of the samples for char combustion in a Perkin Elmer STA600 TGA

It can be seen from Figure 6.6 that the sample heating rate is not constant, although the heating rate profile is quite different from that of the pyrolysis experiments. At a temperature above 700 K, the heating rate profile exhibits a sharp peak, indicating a highly exothermic reaction. This is characteristic of coal combustion. The peak is immediately followed by a sharp dip, which is assumed to be an effect of the furnace control system trying to maintain the furnace temperature.

An instantaneous heating rate was then used in the DAEM algorithm to calculate the activation energy for the char combustion process. The values of f_0 and E calculated at each conversion are shown in Figure 6.7.

(a)



(b)

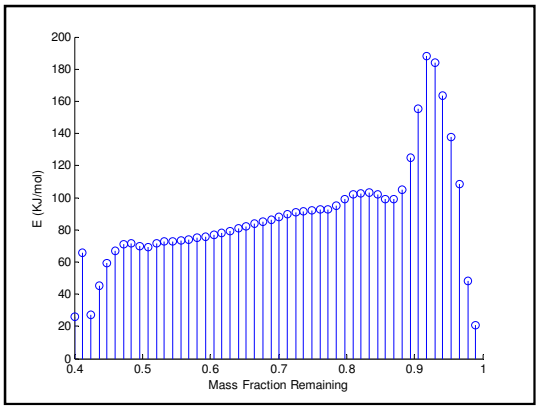


Figure 6.7: Kinetic parameters calculated for char combustion using instantaneous heating rates (a) Initial mass fraction of each component (b) Activation Energy of each reaction

According to Figure 6.7, two reactions are taking place during the combustion of this char. This finding is in agreement with the DTG profile, which shows two peaks. The values of f_0 and E for each of these reactions are given in Table 6.2.

Table 6.2: Kinetic parameters of char combustion in a Perkin-Elmer STA600 TGA calculated using an instantaneous heating rate in the DAEM inversion algorithm

Reaction Number	**E (KJ/mol)**
1	82.39
2	71.39

Table 6.2 shows two distinct values of activation energy. These values are not close enough to assume a single reaction and use an average value. It is noted that the value of E reported in Table 6.1, which is74.4 KJ/mol, lies between 71.4 KJ/mol and 82.4 KJ/mol. Figure 6.7 (a) also shows that these values were calculated at two different conversions

It is generally agreed that char combustion is a single reaction. The additional reaction found here could be a volatile combustion reaction, since it is known that the char sample has not been completely devolatilized in the pyrolysis step. It is not known which E corresponds to the combustion of fixed carbon and which corresponds to volatile combustion.

This finding reiterates the importance of investigating the sample heating rate, instead of assuming a constant heating rate. For the calculations done with a constant value, only a

single reaction is found, with the value of activation energy lying between the values in Table 6.2.

6.1.2 Raw Coal Combustion

Combustion experiments were then carried out on raw coal samples in order to compare the kinetics of coal and char combustion. The TGA curves for these coal combustion reactions are presented in Figure 6.8.

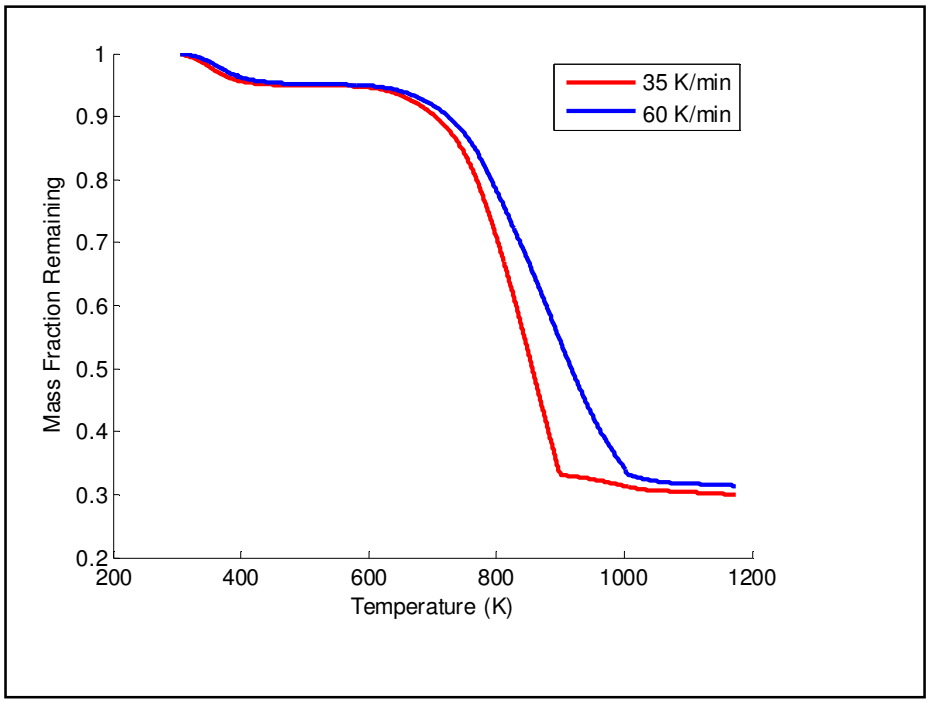


Figure 6.8: TGA curves for the combustion of a South African coal at two different heating rates in a Perkin-Elmer STA600 TGA

The derivative curves are shown in Figure 6.9.

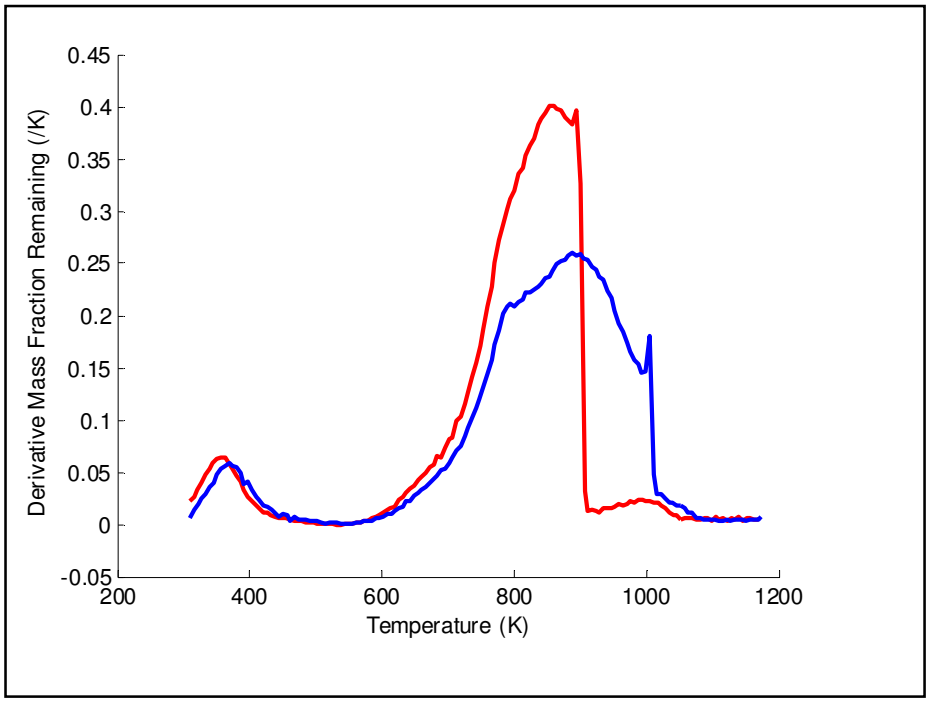
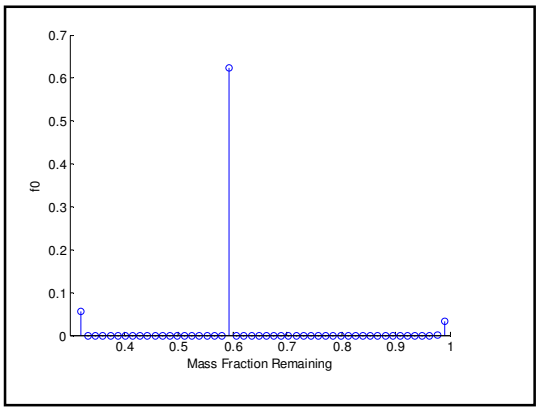


Figure 6.9: DTG curves for the combustion of a South African coal at two different heating rates in a Perkin-Elmer STA600 TGA

The combustion curves for the raw coal samples have a few significant differences compared to those of char. For raw coal combustion, the moisture loss can clearly be seen up to 400 K. Immediately following the fixed carbon combustion, there is another peak which could be a remaining volatile component. The data for raw coal combustion was used in the algorithm to calculate the value of the activation energy for each step. Initially, the assumption of a constant heating rate was used. The values of f_0 and activation energy calculated at each conversion are shown in Figure 6.10.

(a)



(b)

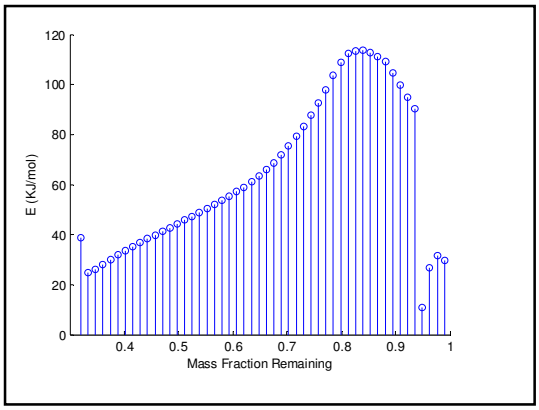


Figure 6.10: Kinetic parameters calculated for coal combustion (a) Initial mass fraction of each component (b) Activation Energy of each reaction

Figure 6.10 (a) shows that there are three points at which f_0 is greater than zero, corresponding to the three reactions seen in Figure 6.9. The values of f_0 and E at these points are given in Table 6.3. The temperatures at which they were calculated are also provided, to indicate which reaction region the values form part of. It should be remembered that these f_0 values are not completely accurate since they are based on a value for A.

Table 6.3: Kinetic parameters of coal combustion in a Perkin-Elmer STA600 TGA calculated using the DAEM inversion algorithm

Reaction Number	f_0	E (KJ/mol)	Temperature (K)
1	0.03	29.61	333.3
2	0.62	55.34	832.6
3	0.06	38.64	973.0

The first reaction in Table 6.3 is the loss of moisture from the coal. The E for this reaction is similar to the value shown in Table 5.1, for the moisture loss step in pyrolysis. The second reaction, with activation energy of 55.34 KJ/mol, corresponds to the combustion of carbon in the coal. The final reaction is probably the decomposition of a residual volatile component in the coal.

The heating rate profiles for the raw coal combustion were then examined to assess the validity of the constant heating rate assumption. These profiles are shown in Figure 6.11.

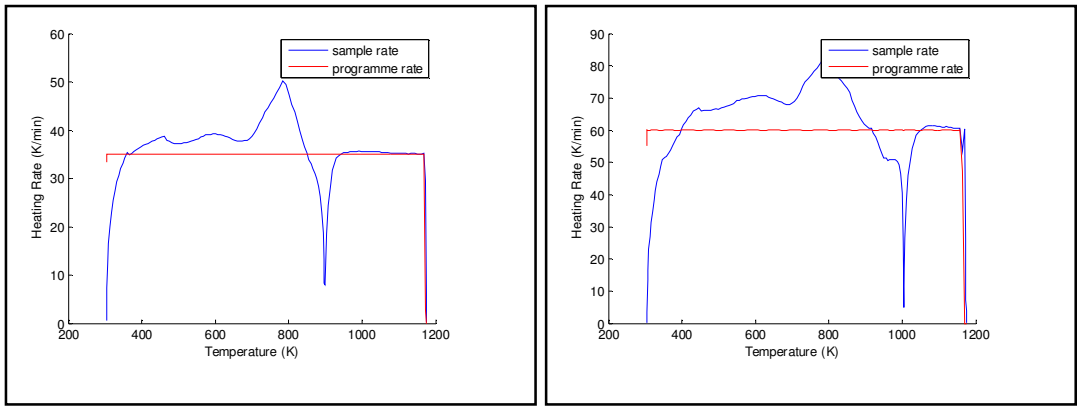


Figure 6.11: Comparison of programme heating rates and actual heating rates of the samples for coal combustion in a Perkin Elmer STA600 TGA

Figure 6.11 shows that the heating rate profiles for char combustion and coal combustion are similar in that there is a sharp peak, followed by a sharp drop in heating rate. However, there is a larger discrepancy between the sample and programme rates for raw coal. This indicates that the constant heating rate results could give quite a large error in the calculated values of activation energy for each step. An instantaneous value for the heating rate was then used in the algorithm and the values of f_0 and E obtained are given in Table 6.4:

Table 6.4: Kinetic parameters of coal combustion in a Perkin-Elmer STA600 TGA calculated using an instantaneous heating rate the DAEM inversion algorithm

Reaction Number	**f_0**	**E (KJ/mol)**
1	0.40	25.59
2	0.39	59.50
3	0.28	59.64

The values in Table 6.4 are different from those values in Table 6.3, proving that the assumption of a constant heating rate affects the calculation of kinetic parameters. For the first reaction, the E is lower than that calculated with the constant heating rate assumption. This value is close to the value calculated for pyrolysis using an instantaneous heating rate, shown in Table 5.2. The fixed carbon combustion reaction and the last reaction have higher E's than previously calculated. It is also noted that these two reactions have E values which are quite similar.

6.1.3 Comparison of char combustion and raw coal combustion

The combustion of raw coal was compared to the combustion of char in terms of their activation energies. For the raw coal, only the E value for the second reaction was considered, since this is the fixed carbon combustion reaction. For the char combustion, two values for E have been found, namely 71.4 KJ/mol and 82.4 KJ/mol, as shown in Table 6.2. As mentioned, it is not known which of these values correspond to fixed carbon combustion. However, both of these values are higher than the activation energy of raw coal combustion. The reason for the lower activation energy of raw coal combustion is the presence of volatiles. These volatile usually ignite at a lower temperature than the fixed carbon and this ignition assists the ignition of the fixed carbon.

For heating rates of 35 K/min and 60 K/min, the temperatures at the peaks of the DTG curves were compared for coal and char combustion, to provide an indication of relative reactivity. This is not a standard reactivity test, but is useful for the comparison of the reactivities of coal and char at a particular heating rate. A fuel with a higher peak temperature (T_{DTGmax}) is more reactive than a fuel with a lower peak temperature (Ciuryla *et al.*, 1979). The peak temperatures for the coal and char at the two heating rates are provided in Table 6.5.

Table 6.5: Comparison of relative reactivity of coal to char

Heating Rate	35 K/min	60 K/min
Fuel	**T_{DTGmax}**	
Char	877.5	912.8
Coal	863.0	887.9

The results in Table 6.5 show that the char samples have higher T_{DTGmax} values than their parent coals and are thus less reactive. It may be recommended that raw coal instead of char be used in utility boilers, as the peak combustion temperature is lower for raw coal.

6.2 High Temperature TGA experiments

For the second set of char combustion experiments, the Thermal Analysis Q600 TGA was used. This TGA contains a furnace which can reach a temperature of 1773 K. The char was prepared by heating samples at a rate of 15 K/min to 1573 K and holding at this temperature for 10 minutes. Once the char had cooled down in an inert atmosphere, combustion at two different heating rates to a temperature of 1173 K was carried out. Heating rates higher than 5

K/min could not be used for combustion in this TGA, as the furnace could not control the exothermicity of the reaction, and this caused a 'kink' in the TGA curve. The TGA curves for char combustion are shown in Figure 6.12.

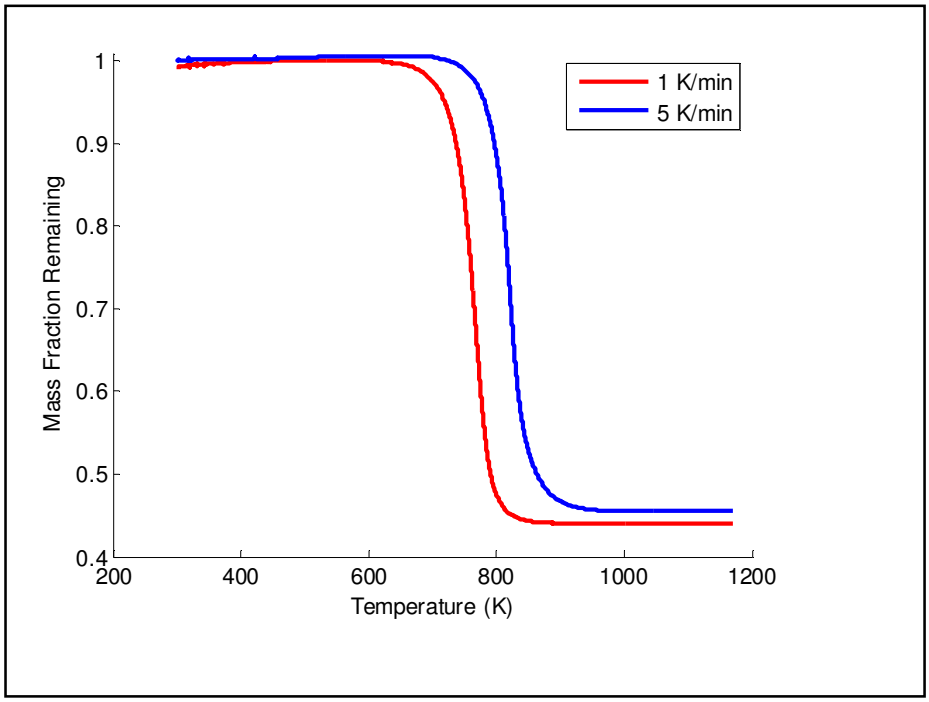


Figure 6.12: TGA curves for the combustion of a South African char at different heating rates in a TA Instruments Q600 TGA

The curves in Figure 6.12 show that the char has been completely devolatilized prior to the combustion, as there is no further mass loss after the fixed carbon combustion. The derivative curves for the char combustion are shown in Figure 6.13.

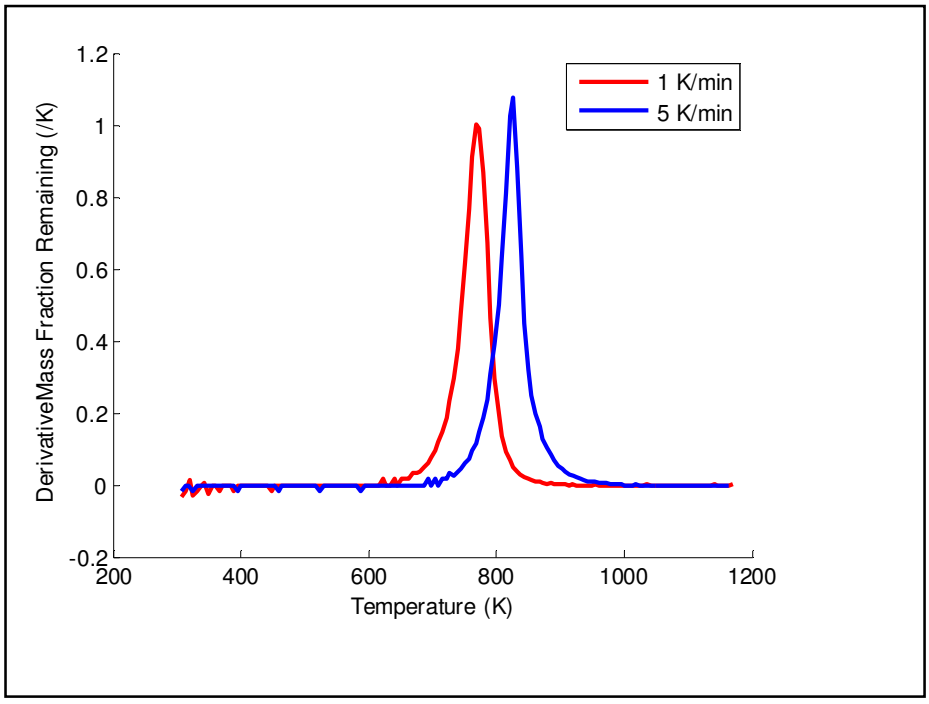
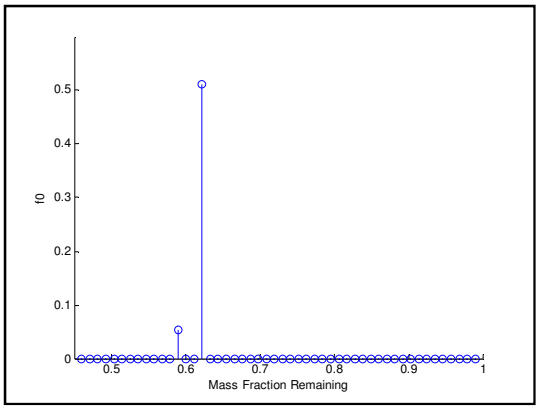


Figure 6.13: DTG curves for the combustion of a South African char at different heating rates in a TA Instruments Q600 TGA

The derivative curves have a single peak, indicating a single event, which is expected of char combustion. The single peak also shows that complete davolatilization of the char occurred during the char preparation process. This is different from what is observed in the lower temperature TGA, proving that coal needs to be heated up to temperatures of at least 1573 K in order to remove all volatile materials. The lower temperature TGA is not capable of complete devolatilization of char under non-isothermal conditions.

The TGA data was used with the DAEM algorithm in order to calculate an activation energy for char combustion. The calculate values of f_0 and E at each conversion are presented in Figure 6.14.

(a)



(b)

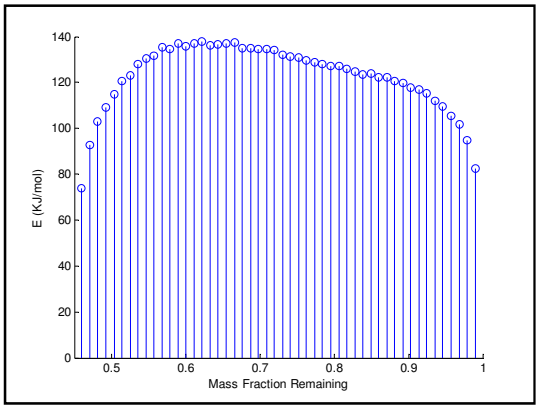


Figure 6.14: Kinetic parameters calculated for char combustion in a TA Instruments Q600 TGA (a) Initial mass fraction of each component (b) Activation Energy of each reaction

Figure 6.14 (a) shows that a single reaction is occurring during the combustion of this char, which is in agreement with the derivative curve in Figure 6.13. The values of $f_0$and E at this point are given in Table 6.6.

Table 6.6: Kinetic parameters of char combustion in a TA Instruments Q600 TGA calculated using the DAEM inversion algorithm

f_0	0.56
E (KJ/mol)	137.4

The value of E calculated from this TGA data is higher than that calculated from the low temperature TGA data. One reason for this is the range of heating rates used, as discussed in the previous chapter. A more likely reason is that the char was completely devolatilized in the

high temperature TGA. No volatiles were present to aid with the ignition of the char, thus causing a higher activation energy.

For this set of experiments, the constant heating rate assumption was also investigated. The sample heating rates are plotted in Figure 6.15.

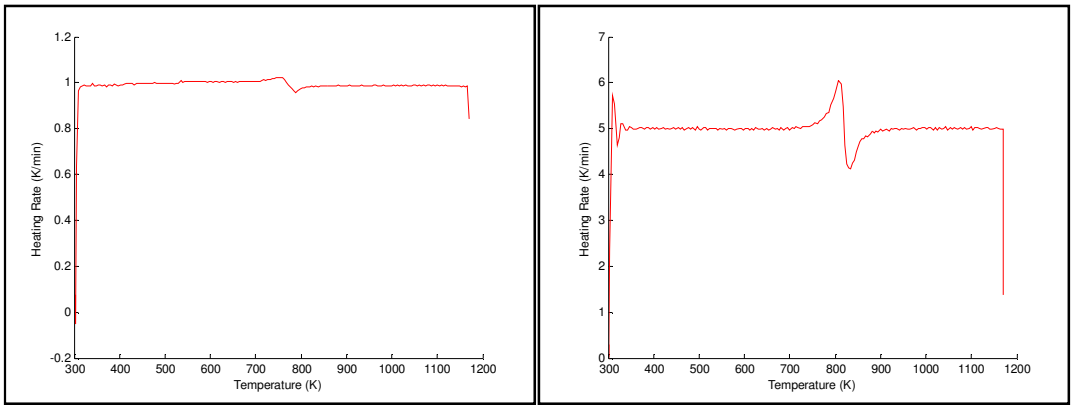


Figure 6.15: Actual heating rates of the samples for char combustion in a TA Instruments Q600 TGA

The heating rate profiles in Figure 6.15 show that the sample heating rates are relatively constant, except at one point, where there is a spike, followed immediately by a drop. The temperature at this point corresponds to the temperature at the peak of the DTG curve for each reaction. This is the point at which the exothermic combustion reaction is occurring. The heating rate profiles are similar to what is observed in the lower temperature TGA, except that the deviation from the programme heating rate is much smaller. It is assumed that these deviations have a negligible effect on the DAEM calculation of E.

6.3 Comparison of the calculated values of E to literature values

The values of E calculated for combustion in both TGA's were compared to the values of E calculated for combustion of char, coal and graphite by various authors. This is presented in Table 6.7.

Table 6.7: Activation energy of combustion for coals, chars and graphite

Sample	Reactant	E (KJ/mol)	Reference
Witbank char – low temp. TGA	Oxygen	82.4 or 71.4	This work
Witbank char – high	Oxygen	137.4	This work

temp. TGA			
Witbank coal – low temp. TGA	Oxygen	59.5	This work
South African Discard	21 % Oxygen	133	Everson *et al.*, 2010
Indonesian Coal	Air	151.7	Muthuraman *et al.*, 2010
Indian Coal	Air	119.3	Muthuraman *et al.*, 2010
Low rank Indonesian coal	Oxyfuel	82.46	Li *et al.*, 2010
Low rank Indonesian coal	Air	74.66	Li *et al.*, 2010
Brazilian Bituminous Coal	Air	104.2	Filho & Milioli, 2008
Nuclear Graphite	Dry Air	158.56	Xiaowei *et al.*, 2004
Graphite	Oxygen	237.6	Zhang *et al.*, 1997

According to Table 6.7, Witbank char ranks amongst the highest of the fuels in terms of combustion E. However, the E of combustion of the raw coal is significantly lower. Coals which have E's more than 100 KJ/mol are not suitable for use in boilers, as their ignition properties are unstable (Wagner, 2008). This is another reason that the combustion of the raw Witbank coal is preferred over the combustion of the char in industrial boilers. It is also observed that the char combustion has an E well below that of graphite.

6.4 Conclusion

In this chapter, thermo-gravimetric data from char and coal combustion experiments was used in conjunction with the DAEM algorithm in order to calculate the kinetics of these reactions. It was also attempted to use the shrinking core model to describe the combustion process. Results show that the shrinking core model is not suitable for the modelling of combustion of a South African coal in oxygen.

However, it should be noted that it is not a claim of this work that the DAEM can be used to model the combustion process. Instead, the DAEM can be used as a model-free method to

calculate the E for combustion. Once a value of E is calculated, it can be used with the appropriate model, to calculate the pre-exponential factor and model combustion. The appropriate model can be found by trial and error, but this did not form a part of this work.

In this chapter, the importance of examining the heating rate is again shown. Because combustion reactions are highly exothermic, they cause a spike in the heating rate of the sample. The control system of the furnace will then attempt to maintain the correct temperature, causing a drop in heating rate. These changes affect the values of the kinetic parameter calculated by the algorithm. An instantaneous value for the heating rate should therefore be used when calculating reaction kinetics.

It was also observed from low temperature TGA experiments that coal is not devolatilized completely at a temperature of 1173 K. The remaining volatiles then combust when the char is heated in oxygen. This may give the impression that char combustion consists of more than one reaction. For complete devolatilization, the coal needs to be heated to at least 1573 K, as indicated by high temperature TGA curves.

Another important finding is that volatile matter in coal assists in the combustion of the fixed carbon. Research Question 6 has been answered by this finding. For raw coal, the E of combustion is lower than that of char. Char combustion in the lower temperature TGA has a lower E and it is known that this char contains volatiles. In addition, the relative reactivity of the raw coal in oxygen is higher than that of the char, as indicated by the peak combustion temperature. For these reasons, it is not advisable to pyrolize coal prior to combustion in industrial boilers.

Chapter 7: Conclusions and Recommendations

7.1 Conclusions

The conversion of coal to provide energy is one of the major causes of South Africa's contribution to greenhouse gas emissions. These emissions can be reduced by correct design and efficient operation of coal conversion equipment. In order for this to be achieved, kinetics of coal conversion reactions need to be easily available. This was the motivation for the work which has been presented here.

Based on the DAEM, Scott *et al*. (2006) developed a method of calculating kinetics of coal pyrolysis from TGA data. The aim of this work was to use the method developed by Scott *et al*. (2006) as a model-free method to calculate the activation energy of coal char combustion.

7.1.1 Simulated TGA data

The first step in this work was the testing of the algorithm on simulated TGA curves. Curves were created with specific E's and A's for different types of reactions.

(a) Simulated Pyrolysis

For pyrolysis, TGA curves were generated at different heating rates for a single first-order reaction, seven first-order reactions and a single reaction with variable heating rates. The DAEM algorithm was applied to these TGA curves for to calculate the kinetic parameters of the reactions. The findings are as follows:

- The DAEM is able to regenerate the original kinetic parameters accurately and correctly for single and multiple first-order reactions.
- These parameters can be used to model the TGA curves at the two heating rates used in the calculation, as well as extrapolate these predictions to higher and lower heating rates.
- The assumption of a constant heating rate may lead to inaccuracies and errors in the DAEM algorithm calculations and model predictions. This issue can be overcome by using an instantaneous heating rate value in the DAEM algorithm.

(b) Simulated Combustion

To simulate TGA curves for coal combustion, a shrinking core mechanism was used. The DAEM algorithm was then tested on these combustion curves. The conclusions from these tests are:

- The DAEM is able to correctly calculate the E for a shrinking-core model reaction.
- A formal proof was given that the method of calculating E in the DAEM algorithm does not rely on a reaction model.
- The hypothesis that the DAEM is a model-free method of calculating the E of coal and char combustion has been proved.
- This algorithm is unable to calculate the A of a non-first order reaction.
- In order to calculate the A, a new algorithm was written based on the shrinking core model and the calculated value of E.
- The E calculated and the corrected A could be used to accurately model a shrinking core reaction at the two heating rates used in the calculation, as well as extrapolate these predictions to higher and lower heating rates.

7.1.2 Pyrolysis Results

Following the theoretical development of the model, pyrolysis experiments were conducted in a TGA using a Witbank coal sample. Two TGA's were available for this work. The DAEM algorithm was then applied to the real TGA data for pyrolysis. The findings are summarised below:

- The DAEM is suitable for the modelling of coal pyrolysis.
- The algorithm can be used within narrow heating rate ranges. These ranges used should be those which yield similarly shaped curves.
- The actual heating rate of a sample in a TGA is not always constant. Sample heating rate data should be examined. If the heating rate is not constant, an instantaneous value should be used in the algorithm.
- Data from the two different heating rate ranges in the low temperature TGA yielded different sets of kinetics. The higher temperature TGA data also provided different kinetics. Thus the kinetic parameters calculated are not intrinsic values, but are a function of reaction conditions.

7.1.3 Combustion Results

Experiments were then carried out on the combustion of char formed from the coal. The DAEM was used to calculate the E for combustion. This E was used in the shrinking core algorithm to calculate the A for the reaction, and the parameters were used to model a shrinking core reaction at the heating rates used. Combustion experiments on raw coal were

also carried out. The combustion of raw coal and char was compared in terms of the E value and peak combustion temperature. The following conclusions were drawn from this section:

- The shrinking core model is not suitable for modelling the combustion of this South African coal in oxygen.
- The correct model for calculating A and modelling the combustion reaction can be found by trial and error but is not within the scope of this work.
- The importance of examining the sample heating rate data is again emphasised.
- The combustion of raw coal has a lower E than the combustion of char, due to the volatile content of raw coal. These volatiles assist in coal combustion.
- The peak temperature of combustion is lower for raw coal than for char. Raw coal is therefore recommended for industrial use.

7.2 Recommendations

Following the conclusions drawn from this work, recommendations for the next steps to be taken and for future work in this project are presented.

7.2.1 Application of the DAEM

The DAEM algorithm has been used for coal pyrolysis and combustion. This model should be tested on other coal conversion reactions, including CO_2 gasification. A model-free method for calculating the activation energy of these reactions would simplify the design of equipment used for these reactions.

Since the shrinking core model has been found unsuitable for modelling of char combustion in oxygen, it is recommended that other combustion models be used to calculate the A of combustion and model the reactions. In particular, the random pore model should be tested. A good fit between model predictions and experimental results indicates an accurate model.

Experiments on char combustion in air should also be carried out, so as to determine whether any of the models are more applicable to combustion in air as opposed to combustion in oxygen.

The conditions used in the TGA should be matched as closely as possible to those of industrial equipment. This is because kinetic parameters obtained are related to the reaction conditions.

7.2.2 Mathematical / Statistical improvements to the model

The algorithm requires data from only two heating rates. Often, data will be available for more than two heating rates. It is recommended that a statistical method be developed to use all heating rates and find the most accurate values for the calculated parameters.

Model fits to simulated and real TGA curves were assessed visually. A statistical method would allow a better assessment of model fits.

7.2.3 Information to be gained from kinetic parameters

Only one type of coal has been used in this work. The values of E of combustion should be calculated for coals which are used in industrial boilers and for coals which have been rejected from use. These values should be compared in order to find a cut-off value, which can then be used to evaluate different coals.

The effect of blending of biomass, different types of coals, or other fuels, including biomass, on the combustion E should be investigated. Lowering the E by blending would be advantageous, as long as the blend behaves as a single fuel.

The kinetic parameters calculated can be used to simulate combustion under isothermal conditions, such as those found in fluidised eds. This will provide information which can be used to optimise fluidised bed design for different coals.

8. References

Abdel-Hafez, A.H., 1988. *Rate expression for shrinking-core bituminous char combustion*, Chemical Engineering Science, **43**(4), p. 839-845

Anthony, D.B., Howard, J.B., Hottel, H.C. & Meissner, H.P., 1975. *Rapid devolitilization of pulverised coal.*, 15th Symposium on Combustion, Tokyo, Japan, **vol. 1**. Pittsburgh: The Combustion Institute; p. 1303-1317.

Arenillas, A., Rubeira, F., Pevida, C & Pis, J.J., 2001. *A comparison of different methods for predicting coal devolatilisation kinetics*, J. Anal. Appl. Pyrolysis, **58–59**, p. 685-701

Baranco, R., Rojas, A., Barraza, J. & Lester, E., 2009. *A new char combustion model 1. Formulaiton*, Fuel, **88**, p. 2335-2339

Bjorkman, A., 2001. *Projects on coal characterization*, Fuel, **80**, p. 155-166

Cai, H.Y., Guell, A.J., Chatzakis, I.N., Lim, J.Y., Dugwell, D.R. & Kandiyoti, R., 1996. *Combustion reactivity and morphological change in coal chars: effect of pyrolysis temperature, heating rate and pressure*, Fuel, **75**(1), p. 15-24

Chen, J.C., 1996. *Distributed Activation Enrgy of Heterogeneous Coal Ignition*, Combustion and Flame, **107**, p. 291-298

Ciuryla, V.T., Weimer, R.F., Bivans, D.A. & Motika, S.A., 1979. *Ambient-pressure thermogravimetric characterization of four different coals and their chars*, Fuel, **58**, p. 748-754

Cumming, J.W., 1989. *A DTG combustion study on Anthracitic and other coal chars*, Thermochimica Acta, **155**, p. 151-161

DeSai, P.R. & Wen, C.Y., 1978. *Computer Modelling of the MERC Fixed Bed Reactor*, United States Department of Energy, Morgantown Energy Research Centre, Morgantown, W.V.

Dhar, P.S., 1986. *A comparative study of different methods for the analysis of TGA curves*, Computers & Chemistry, **10**(4), p. 293-297

Donskoi, E. & McElwain, D.L.S., 2000. *Optimisation of coal pyrolysis modelling*, Combustion and Flame, **122**, p. 359-367

Doyle, C.D., 1962. *Estimating isothermal life from thermogravimetric data*, Journal of Applied Polymer Science, **6**(24), p. 639-642

Ebrahimi-Kahrizsangi, R. & Abbasi, M.H., 2008. *Evaluation of reliability of Coats-Redfern method for kinetic analysis of non-isothermal TGA*, Trans. Nonferrous Met. Soc. China, **18**, p. 217-221

Everson, R., Neomagus, & Kaitano, R., 2005. *The modeling of the combustion of high-ash coal–char particles suitable for pressurised fluidized bed combustion: shrinking reacted core model*, Fuel, **84**, p. 1136-1143

Everson, R.C., Neomagus, H.W.J.P., Kasaini, H. & Njapha D, 2006[a]. *Reaction kinetics of pulverized coal chars derived from inertinite-rich coal discards: Characterisation and combustion*, Fuel, **85**, p. 1067-1075

Everson, R.C., Neomagus, H.W.J.P & Njapha D, 2006[b]. *Kinetics of non-isothermal thermogravimnetric analyser results using a new method for the evaluation of the temperature integral and multi-heating rates*, Fuel, **85**, p. 418-422

Everson, R.C., Neomagus, H.W.J.P, Kaitano, R., Falcon, R. & du Cann, V.M., 2008. *Properties of high ash coal-char particles derived from inertinite-rich coal: II. Gasification Kinetics with Carbon Dioxide*, Fuel, **87**, p. 3403-3408

Filho, C.G.d.S. & Milioli, F.E., 2008. *A thermogravimetric analysis of the combustion of a Brazilian mineral coal*, Quim. Nova, **31**(1), p. 98-103

Flynn, J.H. & Wall, L.A., 1966. *A quick, direct method for the determination of activation energy from thermogravimetric data*, Journal of Polymer Science Part B: Polymer Letters, **4**(5), p. 323-328

Haenel, M.W., 1992. *Recent progress in coal structure research*, Fuel, **71**, p. 1211-1223

Hull, A.S. & Agarwal, P.K., 1988. *Estimation of kinetic rate parameters for coal combustion from measurements of the ignition temperature*, Fuel, **77**(9/10), p. 1051-1058

Hurt, R.H. & Haynes, B.S., 2005. *On the origin of power-law kinetics in carbon oxidation*, Proceedings of the Combustion Institute, **30**, p. 2161-2168

Ishida, M. & Wen, C.Y., 1968. *Comparison of kinetic and diffusional models for solid-gas reactions*, AIChE Journal, **14**(2), p. 311-317

Juntgen, H., 1984. *Review of the kinetics of pyrolysis and hydropyrolysis in relation to the chemical constitution of coal*, Fuel, **63**, p. 731-737

Keuleers, R.R., Janssens, J.F. & Desseyn, H.O., 2002. *Comparison of some methods for activation energy determination of thermal decomposition reactions by themogravimetry*, Thermochimica Acta, **385**, p. 127-142

Kobayashi, H., Howard, J.B. & Sarofim, A.F., 1977. *Coal devolatilization at high temperatures*, 16th Symposium on Combustion, Cambridge, USA, **vol. 1**. Pittsburgh: The Combustion Institute; p. 411-425

Kok, M.V. & Pamir, M.R., 1995. *Pyrolysis and combustion studies of fossil fuels by thermal analysis methods*, Journal of Analytical and Applied Pyrolysis, **35**, p. 145-156

Ladner, W.R., 1988. *The Products of Coal Pyrolysis: Properties, Conversion and Reactivity*, Fuel Processing Technology, **20**, p. 207-222

Li., C.-R. & Tang, T.B., 1999. *A new method for analysing non-isothermal thermoanalytical data from solid-state reactions*, Thermochimica Acta, **325**, p.43-46

Li. X., Rathnam, R.K., Yu, J., Wang, Q., Wall, T. & Meesri, C., 2010. *Pyrolysis and Combustion Characteristics of an Indonesian Low-Rank Coal under O_2/N_2 and O_2/CO_2 Conditions*, Energy & Fuels, **24**, p. 160-164

Li, Z., Liu, C., Chen, Z., Qian, J., Zhao, W. & Zhu, Q., 2009. *Analysis of coals and biomass pyrolysis usingthe distributed activation energy model*, Bioresource Technology, **100**, p. 948–952

Linares-Solano, A., Mahajan, O.P. & Walker Jr., P.L., 1979. *Reactivity of heat treated coals in steam*, Fuel, **58**, p. 327-332

Migliavacca, G., Parodi, E., Bonfanti, L., Faravelli, T., Pierucci, S. & Ranzi, E., 2005. *A general mathematical model of solid fuels pyrolysis*, Energy, **30**, p. 1453-1468

Mitchell, R.E., Ma, L. & Kim, B., 2007. *On the burning behavior of pulverized coal chars*, Combustion and Flame, **151**, p. 426-436

Miura, K., 1995. *A New and Simple Method to Estimate f(E) and k_0(E) in the Distributed Activation Energy Model from Three Sets of Experimental Data*, Energy & Fuels, **9**, p. 302 - 307

Morgan, P.A., Robertson, S.D. & Unsworth, J.F., 1986. *Combustion studies by thermogravimetric analysis. 1. Coal oxidation*, Fuel, **65**, p. 1546-1551

Muthuraman, M., Namioka, T. & Yoshikawa., K., 2010. *A comparative study on co-combustion performance of municipal solid waste and Indonesian coal with high ash Indian coal: A thermogravimetric analysis*, Fuel Processing Technology doi:10.1016/j.fuproc.2009.12.018

Navarro, M.V., Aranda, A., Garcia, T., Murillo, R. & Mastral, A.M., 2008. *Application of the distributed activation energy model to blends devolatilisation*, Chemical Engineering Journal, **142**, p. 87-94

Njapha, D., 2003. *Determination of the kinetic models and associated parameters for the low temperature combustion and gasification of high-ash coal chars*, PhD thesis, Potchefstroomse Universiteit vir Christelike Höer Onderwys

Pitt, G.J., 1962. *The kinetics of the evolution of volatile products from coal*, Fuel, **41**, p. 267-274

Please, C.P., McGuinness, M.J. & McElwain, D.L.S., 2003. *Approximations to the distributed activation energy model for the pyrolysis of coal*, Combustion and Flame, **133**, p. 107-117

Prado, J.R. & Vyazovkin, S., 2011. *Activation energies of water vaporization from the bulk and from laponite, montmorillonite, and chitosan powders*, Thermochimica Acta, doi:10.1016/j.tca.2011.06.005

Qiao, Y., Zhang, L., Binner, E., Xu, M. & Li, C.-Z., 2010. *An investigation of the causes of the difference in coal particle ignition temperature between combustion in air and in O2/CO2*, Fuel, **89**, p. 3381-3387

Russel, N.V., Beeley, T.J., Man, C.-K., Gibbins, J.R. & Williamson, J., 1998. *Development of TG measurements of intrinsic char combustion reactivity for industrial and research purposes*, Fuel Processing Technology, **57**, p. 113-130

Sadhukhan, A.K., Gupta, P. & Saha, R.K., 2009. *Characterization of porous structure of coal char from a single devolatilized coal particle: Coal combustion in a fluidized bed*, Fuel Processing Technology, **90**, p. 692-700

Sadhukhan, A.K., Gupta, P. & Saha, R.K., 2010. *Modelling of combustion characteristics of high ash coal char particles at high pressure: Shrinking reactive core model*, Fuel, **89**, p. 162-169

Scott, S.A., Dennis, J.S., Davidson, J.F. & Hayhurst A.N., 2006. *An algorithm for determining the kinetics of devolatilisation of complex solid fuels from thermogravimetric experiments*, Chemical Engineering Science, **61**, p. 2339-2348

Smith, S.E., Neavel, R.C., Hippo, E.J. & Miller, R.N., 1981. *DTGA combustion of coals in the Exxon coal library*, Fuel, **60**, p. 458-462

SouthAfrica.info, 2008. *South Africa's Energy Supply*, accessed 24/08/2010. Link: http://www.southafrica.info/business/economy/infrastructure/energy.htm

Starinck, M.J., 2003. *The determination of activation energy from linear heating rate experiments: a comparison of the accuracy of isoconversion methods*, Thermochimica Acta, **404**, p. 163-176

Suuberg, E.M., Wojtowicz, M. & Calo, J.M., 1988. *Reaction order for low temperature oxidation of carbons*, 22nd Symposium on Combustion, The Combustion Institute, p. 79-87

U.N.-E.C.E., 1998. *International Classification on In-seam coals*, Economic Commission for Europe, Committee on Sustainable Development, Geneva, **41**, pp. (Document)

Van Niekerk, D. Mathews, J.P., 2010. *Molecular representations of Permian-age, vitrinite-rich and inertinite-rich South African coals*, Fuel, **89**, p. 73-82

Wagner, N.J., 2008. *The characterization of weathered discard coals and their behaviour during combustion*, Fuel, **87**, p. 1687-1697

Wang, F.U. & Bhatia, S.K., 2001. *A generalised dynamic model for char particle gasification with structure evolution and peripheral fragmentation*, Chemical Engineering Science, **56**, p. 3683-3697

Xiang, Y.H., Guo, R.X., Li, H.B. & Wang, Y., 2008. *Combustion Characteristics and Kinetics of Partial Gasified Coal Char*, Energy Sources Part A, **30**, p. 110-118

Xiaowei, L., Jean-Charles, R. & Suyuan, Y., 2004. *Effect of temperature on graphite oxidation behaviour*, Nuclear Engineering and Design, **227**, p. 273-280

Zhang, L.-M., Tan, Z.-C., Wang,S.-D. & Wu, D.-Y., 1997. *Combustion calorimetric and thermogravimetric studies of graphite and coal doped with a coal-burning additive*, Thermochimica Acta, **299**, p. 13-17

Appendix A: Experimental Details

A1: TGA Specifications

The two thermo-gravimetric analysers were used for this work were a Perkin-Elmer STA 600 series TGA and a Thermal Analysis Q600 TGA, both house in the school of chemical and metallurgical engineering at Wits University. Each of these was linked to a personal computer loaded with Pyris and Thermal Analysis software respectively. The equipment specifications are given in Table A1 and Table A2:

Table A1: Equipment Specifications of Perkin-Elmer STA 600 TGA

Sensor	Pure platinum pan holder and reference ring		Corrosion-resistant, making the instrument suitable for a wide variety of samples and applications
Furnace design	Vertical		Optimized for performance, user exchangeable SaTurnA sensor. Ensures even purge gas flow.
Balance design	Top loading, single beam		Easy loading and unloading in manual and automated mode
Balance resolution	0.1 ug		
Balance measurement range	Up to 1500 mg		
Temperature range	15 °C to 1000 °C		Start experiments below room temperature to capture complete moisture and solvent evaporation
Heating rate	Ambient to 1000 °C	0.1 to 100 °C/min	
Cooling rates	From 1000 °C to 30 °C	Under 10 minutes	Forced air and chiller to achieve fastest cool down for higher productivity
Temperature calibration	Metal standards such as Indium and Silver		
Temperature accuracy	< ±0.5 °C		
Temperature reproducibility	< ±0.5 °C		
Calorimetric data	Accuracy/precision	±2% based on metal standards	
Thermocouples	PT-PT/Rh (Type R)		
Sample pans	Alumina 180 µl		
Dimensions	(HxWxD) 17 / 38 / 41 cm 6.7 / 15 / 16.5 in		Small footprint allows for the best use of your laboratory space
Weight	12-16 kg		
Instrument control	Pyris software		Benchmark software in Thermal Analysis
Accessories	Mass flow control and switch	Included	Integrated mass flow gas control and switching for accurate environmental control and high precision analysis
	Autosampler	Optional, 45-position	For unattended operation 24/7
	Transparent cover	Included in autosampler configurations Optional for standard configurations	Best protection for your samples
Hyphenated techniques	Combine with MS or IR analyzers		MS or IR connectivity capabilities allow the analysis of evolved gases
Certificates/Compliance/ Quality Assurance	Developed under ISO 9001. Designed and tested to be in compliance with the legal requirements for laboratory analytical instruments		

Table A2: Equipment Specifications of TA Instruments Q600 TGA

TECHNICAL SPECIFICATIONS

System Design	Horizontal Balance & Furnace
Balance Design	Dual Beam (growth compensated)
Sample Capacity	200 mg (350 mg including sample holder)
Balance Sensitivity	0.1 µg
Furnace Type	Bifilar Wound
Temperature Range	Ambient to 1500 °C
Heating Rate – Ambient to 1000 °C	0.1 to 100 °C/min
Heating Rate – Ambient to 1500 °C	0.1 to 25 °C/min
Furnace Cooling	Forced Air (1500 to 50 °C in < 30 min, 1000 °C in 50 °C in < 20 min)
Thermocouples	Platinum/Platinum-Rhodium (Type R)
Temperature Calibration	Curie Point or Metal Standards (1 to 5 Points)
DTA Sensitivity	0.001 °C
Calorimetric Accuracy/Precision	± 2% (based on metal standards)
Mass Flow Controller with Automatic Gas Switching	Included
Vacuum	to 7 Pa (0.05 torr)
Reactive Gas Capability	Included – separate gas tube
Dual Sample TGA	Included
Auto-Stepwise TGA	Included
Sample Pans	Platinum: 40 µL, 110 µl
	Alumina: 40 µL, 90 µL

A2: Proximate Analysis Procedure

Proximate Analysis is a tool used to determine the moisture, volatile content, fixed carbon and ash is a sample. For this sample, the analysis was carried out in the Perkin-Elmer STA600 TGA. The same pre-run procedure as above needed to be observed. The analysis was carried out as follows:

1. Heat the sample at 50° c/min from 30° c to 110° c in Nitrogen at 40ml/min
2. Hold at 110° c for 3 minutes
3. Heat the sample at 30° c/min from 110° c to 700° c in Nitrogen at 40ml/min
4. Switch the gas to Oxygen at 40ml/min when the temperature is 700° c
5. Heat the sample at 30° c/min from 700° c to 900° c in Oxygen at 40ml/min
6. Hold at 900° c for 1 minute

7. Stop the run

Petrographic Analysis Procedure

Prior to conducting the actual petrographic analysis, blocks were prepared from the coal samples so that they were suitable for viewing under the microscope. For these blocks, approximately 100-200g of sample with a particle size of 1 mm was required. This was obtained through primary and secondary crushing. The preparation procedure is outlined below:

Block formation

Ensure sample cups are clean

Line cups with a thin layer of Vaseline

Fill cups halfway with coal

In a mixing cup, add hardener to epoxy resin in the ratio 1:7.

Mix well with a wooden spatula

Pour some of this mixture on top of the coal sample and mix until a thick paste is formed

Ensure that this paste is level in the cup

Write down the sample ID and place this on top of the coal

Fill the cup with the remaining resin

Allow to set for 12 hours and then remove

Polishing

Once the blocks were formed, they were polished. This was done in a Struers Tegraforce polisher. An appropriate plate was fitted into the polisher and the sample was polished using grit and polishing plates for one to two minutes. The final step was to polish using alumina powder.

Analysis

Petrographic analysis was carried out by Professor N. Wagner at the University of the Witwatersrand, Johannesburg. The equipment used for the analysis of the sample was a LEICA DM 4500P reflected light microscope. With this microscope, light travels through an objective lens and is reflected off the surface of the microscope. It contains a polarizer and analyser which change the orientation of the light. For this analysis, unpolarised light was used. The analysis was carried out as follows:

The sample was placed on a slide and flattened for an even view

A drop of immersion oil with a specific refractive index was placed on the surface of the block

The objective lens was placed in the oil

The slide was moved automatically to different positions

At each position, a particular maceral component or mineral was identified

In this way, a relative distribution of macerals and minerals was obtained. Maceral group analysis was conducted according to the ISO 7404 part 4 standard.

For measuring the reflectance of vitrinite, a fiber optic cable was used to transfer the captured reflectance values to the computer. Reflectance analysis analysis was conducted according to the ISO 7404 part 5 standard.

A hundred values were obtained for vitrinite reflectance and these were averaged to obtain a mean value.

Appendix B: Matlab codes used for simulations and algorithm calculations

In this section, copies of all Matlab codes used in this work are presented, along with descriptions and explanations of each code. Any comments preceded by '%' indicate a description and are not part of the actual code. The parameters used as inputs for these codes are also given.

The DAEM inversion algorithm works by reading real or simulated TGA data of Mass Fraction Remaining (X) *vs.* Temperature (T) for two different heating rates. These data sets are then reduced by linear interpolation in order to simplify the computation. A number of reactions or conversions is then chosen. The algorithm specifies these reactions by choosing this number of equally spaced X values. The temperatures corresponding to these X values are found for each heating rate by interpolation. Each X value and the two corresponding two temperature values and heating rates are used to calculate an E for each reaction. The value of E is then used with temperature data for one of the heating rates to calculate a value of A. The set of E and A values at each temperature is used to form the matrix Ψ. Using the reduced TGA data set, the matrix equation is then solved by inversion to calculate the values of f_0. The set of codes used for these calculations are presented here.

1. funcscotteg2

This code uses the actual DAEM inversion algorithm to calculate the values of activation energy (E), pre-exponential factor (PE), and initial mass fraction reacting (f0) for the number of reactions specified. This code is not used on its own but forms part of other codes used for calculation of kinetics with real or simulated data.

```
function c = funscotteg2(T1,T2,B,Tr,xx,B1,B2,T0);
% T1 and T2 are the temperature data sets corresponding to the values of X for the
specified number of reactions.
% B1 and B2 are the heating rates are the heating rates corresponding to T1 and T2
% Tr is the reduced set of temperature data selected for the calculation of PE.
% B is the heaitng rate corresponding to Tr
% xx is the set of X values chosen by specifying the number of reactions


warning off
options2=optimset('TolX',1e-6,'LevenbergMarquardt','off');
% This defined the error tolerance of the calculations


n=length(T1); % This specifies how many calculations there will be for E and PE
```

```
    for i=1:n

    E(i)=FMINBND('AEerror2',0,800,options2,T1(i),T2(i),T0,B1,B2);

% This applies the built-in solver 'FMINBND' to the programme 'AEerror2' with the
specified parameters. The minimum and maximum values of E that can be found by iteraton
are 0 and 800 respectively. Options2 defines the tolerance of the iteration.

    PE(i)=Ai2(E(i),T1(i),T2(i),T0,B1,B2);

% This uses the code Ai2 with the specified parameters to calculate the value of PE
using the calcualted value of E

    PE(1)=0.0000001; % The first value of PE

    chi_check20(i)=chi(E(i),PE(i),T1(i),T0,B,B2);

    chi_check100(i)=chi(E(i),PE(i),T2(i),T0,B,B2);

% the above two commands provide a check of the matrix Ψ. For one of the heating rates,
all the values of Ψ should be equal to 0.3679

end

check=[chi_check20' chi_check100']

a=isfinite(PE'); % This find all the finite vlaues of PE

PE=PE(a);

E=E(a);


q=length(Tr); %reduces no of data points in Tga set

npoints=q;

nn=length(E);

Tr1i=Tr;

for i=1:npoints

    for j=1:nn

        term1(j)=quad(@term,T0,Tr1i(i),[],[],E(j));

        chi1(i,j)=exp((-PE(j)/B)*(term1(j)));

        chi1(i,nn+1)=1;

        chi_1(i,j)=chi(E(j),PE(j),Tr1i(i),T0,B,B2); %Uses the code 'chi' to create Ψ

        chi_1(i,nn+1)=1;

    end

end

% The above loop creates the Ψ matrix usign the E and PE. The function 'term'
represents the temperature integral.

options3=optimset('TolX',10);

f0=lsqnonneg(chi_1,xx) %This uses matrix inversion to calculate the values of f0.


m=100;

T=linspace(T0,1000,m);

for i=1:m

    for j=1:nn

        term1(j)=quad(@term,T0,T(i),[],[],E(j));
```

```
        chi2(i,j)=exp((-PE(j)/B1)*(term1(j)));
        chi2(i,nn+1)=1;
        chi_2(i,j)=chi(E(j),PE(j),T(i),T0,B,B2); % Uses the code 'chi' to create Ψ
        chi_2(i,nn+1)=1;
    end
end
% This loop creates the Ψ matric for the other heating rate.

[length(f0) length(E') length(PE')]

E(n+1)=0;PE(n+1)=0; % This defined the last E and PE values as 0 since they represetnt
ash.
E'
c=[f0 E' PE']; % The final output of this code. These are the values of f0, E and PE
for each reaction.
```

The above code makes use of different codes within it. These are now presented.

2. AEerror2

This code defines the right hand and left hand side of Equation 2.17 so that a solver can be applied to solve the equation.

```
function error = AEerror2(E,T1,T2,T0,B1,B2);
% This uses the EXPINT function to find the integral from X to inf of exp(-t)/t dt
 R=8.314; % Universal gas constant in j/molK

% Each term in the temperature integral is defined here.
first=T0*exp(-E*1000/(R*T0));
aa=E*1000/(R*T0);bb=exp(-aa)/aa;
second=(E*1000/R)*EXPINT(aa);
third=T1*exp(-E*1000/(R*T1));
cc=E*1000/(R*T1);dd=exp(-cc)/cc;
fourth=(E*1000/R)*EXPINT(cc);
fifth=first;
sixth=second;
seventh=T2*exp(-E*1000/(R*T2));
ee=E*1000/(R*T2);ff=exp(-ee)/ee;
eighth=(E*1000/R)*EXPINT(ee);

ls=(1/B1)*(first-second-third+fourth); %LHS of EQ 2.17
```

```
rs=(1/B2)*(fifth-sixth-seventh+eighth); %RHS of EQ 2.17


error = sqrt((1-rs/ls)^2);
```

3. Ai2

The value of PE is calculated using the above code and Equation 2.22. The value of E calculated for each reaction is an input to this code.

```
function y = Ai2(E,T1,T2,T0,B1,B2);
R=8.314; % Universal gas constant in j/molK


%terms in EQ 2.22
first=T0*exp(-E*1000/(R*T0))
aa=E*1000/(R*T0);bb=exp(-aa)/aa;
second=(E*1000/R)*EXPINT(aa);
third=T1*exp(-E*1000/(R*T1));
cc=E*1000/(R*T1);dd=exp(-cc)/cc;
fourth=(E*1000/R)*EXPINT(cc);


Ai=-B1/(first-second-third+fourth);
y=Ai;
```

4. Chi

This code uses the calcualtes values of E and PE at each temperature and heating rate to calculate the matrix Ψ.

```
function error = chi(E,PE,T1,T0,B1,B2);
%This uses the approximation for integral from X to inf of exp(-t)/t dt to create the
matrix Ψ.
A=PE;
R=8.314; % Universal gas constant in j/molK
%terms in equation 13
first=T0*exp(-E*1000/(R*T0));
aa=E*1000/(R*T0);bb=exp(-aa)/aa;
second=(E*1000/R)*EXPINT(aa);
third=T1*exp(-E*1000/(R*T1));
cc=E*1000/(R*T1);dd=exp(-cc)/cc;
fourth=(E*1000/R)*EXPINT(cc);
```

```
%RHS of EQ6
rhs=(A/B1)*(first-second-third+fourth);
error = exp(rhs);
```

5. term

This code simple defines the exponential term ‘exp(-E/RT)

```
function y=term(T,E)
y=exp(-E*1000./(8.314*T)); % The exponential term
```

In order to test the DAEM algorithm, simulated TGA data was used in the algorithm before real data was used. This TGA data was simulated according to a number of different reaction conditions. TGA curves also needed to be created using the kinetics calculated from real data so that the model could be compared to experimental results. The codes used for the simulation will now be discussed.

6. Orates

TGA curves for single or multiple first order reactions are created using this code. The parameters f_0, E and PE as well as the heating rate need to be defined as inputs to this programme. The matrix Ψ is created and multiplied by the f_0 matrix to obtain data for mass fraction remaining.

```
function c=orates(f0,T0,E,PE,b,Tup,m);
% b is the heating rate in K/min
% Tup is the maximum temperature that the curve should reach
% m is the number of points on the curve

B=b/60;%K/sec
s=size(E');
nn=s(:,1);
T=linspace(T0,Tup,m); % This selects a number of evenly spaced temperature points

for i=1:m
    for j=1:nn
        term1(j)=quad(@term,T0,T(i),[],[],E(j));
```

```
        chi2(i,j)=exp((-PE(j)/B)*(term1(j)));
        chi2(i,nn+1)=1;
    end
end
% This loop creates the matrix Ψ using kinetic and temperature data
M=chi2*f0;
c=[T' M];
hold on
plot(T,M,'b.'); % This plots the TGA curve
x=c(:,1);y=100.*c(:,2);
deriv=-diff(y)./diff(x); % This calculates the discreet derivatives of the data sets
x=x(2:length(x));
plot(x,deriv,'b') % This plots the derivative curve on the same axes
```

7. Scotteg1

This programme was used to simulate a single, first-order reaction with a given E and PE and apply the algorithm to the simulated data to calculate the original parameters. The code used to simulate 7 first-order reactions is the same, excepts that f_0, E and PE have seven values.

```
function c = scotteg1(nrxns,rnTGA,nTGA,b1,b2,T0);
% nrxns is the number of points  at which to calculate the kinetics, or the number of
reactions
% rnTGA is the number of points that the TGA data should be reduced to
% nTGA is the number of points that orates.m uses to create the data
% b1 and b2 are the heating rates used in K/min

B1=b1/60;
B2=b2/60;
R=8.314; % Universal gas constant in j/molK
f0=[1 0]';E=80*1.69;PE=(exp(19.0269))*60; %parameters used by programme

data1=orates(f0,T0,E,PE,B1*60,900,nTGA); % Generates TGA data at heating rate B1
TT1=data1(:,1); x1=data1(:,2); % Defines temeprature and weight percent data sets
data2=orates(f0,T0,E,PE,B2*60,1000,nTGA); % Generates TGA data at heating rate B2
TT2=data2(:,1); x2=data2(:,2); % Defines temeprature and weight percent data sets
```

```
Tr1=linspace(TT1(1),TT1(length(TT1)),rnTGA)';

Tr2=linspace(TT2(1),TT2(length(TT2)),rnTGA)';

% This reduces temperature data by choosing a number of equally space temperature
points


Xr1=interp1q(TT1,x1,Tr1);

Xr2=interp1q(TT2,x2,Tr2);

Xr1(length(Xr1))=Xr1(length(Xr1)-1);

% This finds the weight percent values corresponding to the reduced number of
temperatures by interpolation


X=linspace(0.9999,0.0001,nrxns)'; % Chooses the conversions at which to calculate
kinetic parameters by selecting a number of equally spaced values


T1=interp1q(flipud(x1),flipud(TT1),X);

T2=interp1q(flipud(x2),flipud(TT2),X);

% This finds the temperatures corresponding to the above conversions by interpolation.

hold on

plot(Tr1,Xr1,'g') % Reduced TGA data for heating rate 1

plot(Tr2,Xr2,'r') % Reduced TGA data for heating rate 2

plot(T1,X,'go') % TGA data for number of reactions chosen

plot(T2,X,'ro') % TGA data for number of reactions chosen


XLABEL('Temperature K')

YLABEL('Mass Fraction Remaining')

legend('10K/min','1000K/min')

axis([T0 1500 0 1])


Xtga=Xr1;


data3=funcscotteg2(T1,T2,B1,Tr1,Xtga,B1,B2,T0); % Uses simulated data in TGA algorithm

f0=data3(:,1);E=data3(:,2);PE=data3(:,3); % Defines the output of funcscotteg2.m

c=[f0 E PE]
```

8. Firstordervariable

This code is used to simulate a first-order reaction with variable heating rates. The code used to calculate the kinetics has been modified to use an instantaneous heating rate.

```
function c = firstordervariable(nrxns,rnTGA,nTGA,b1,b2,T0,tf);

R=8.314; %j/molK

f0=[1 0]';E=80*1.69;PE=(exp(19.0269))*60;


data1=oratesv1(f0,T0,E,PE,b1,tf,nTGA); % Generates TGA data with variable heating rate
b1 which is programmed into oratesv1.m

TT1=data1(:,1);

x1=data1(:,2);

data2=oratesv2(f0,T0,E,PE,b2,tf,nTGA); % Generates TGA data with variable heating rate
b2 which is programmed into oratesv2.m

TT2=data2(:,1);

x2=data2(:,2);


Tr1=linspace(TT1(1),TT1(length(TT1)),rnTGA)';

Tr2=linspace(TT2(1),TT2(length(TT2)),rnTGA)';

Xr1=interp1q(TT1,x1,Tr1);

Xr2=interp1q(TT2,x2,Tr2);

TT1=Tr1;

TT2=Tr2;

x1=Xr1;

x2=Xr2;

x1(length(x1))=x1(length(x1)-1);


X=linspace(0.9999,0.0001,nrxns)';

T1=interp1q(flipud(x1),flipud(TT1),X);

T2=interp1q(flipud(x2),flipud(TT2),X);

plot(Tr1,x1,'g')

plot(Tr2,x2,'r')

plot(T1,X,'go')

plot(T2,X,'ro')

Xtga=x1;

Tr1=TT1;

Tr2=TT2;
```

```
hold on
axis([T0 1500 0 1])



data3=variablebnew(T1,T2,Tr1,Xtga,T0); % Uses DAEM algorithm with variable B's
f0=data3(:,1);E=data3(:,2);PE=data3(:,3);
c=[f0 E PE];
```

9. Variablebnew

This code is equivalent to funcscotteg2.m, except that it uses a value of B corresponding to each temperature.

```
function c = variablebnew(T1,T2,Tr,xx,T0);
warning off
options2=optimset('TolX',1e-6,'LevenbergMarquardt','off');
n=length(T1);
    Ts1=1.0e+003*[0.3023
    0.3196
    0.3439
    0.3647
    0.3802
    0.4131
    0.4426
    0.4720
    0.5032
    0.5309
    0.5620
    0.6001
    0.6313
    0.6746
    0.7074
    0.7629
    0.8148
    0.8650
    0.8927
    0.9100
    0.9377
```

```
    0.9689
    0.9948
    1.0243
    1.0253
    1.0485
    1.0814
    1.1126
    1.1437
    1.1991]; % Temperature Data
Bs1=[0.1825
    3.9538
    9.3066
   13.6861
   17.8224
   23.2968
   28.6496
   33.3942
   37.2871
   40.0852
   43.0049
   44.2214
   44.3431
   42.6399
   39.9635
   32.9075
   29.8662
   27.0681
   26.0949
   25.0000
   25.0000
   25.0000
   25.0000
   25.0000
   25.0000
   25.0000
   25.0000
```

```
   25.0000
   25.0000
   25.0000]; % Instantaneous heating rate data
    Ts2=1.0e+003*[0.3041
    0.3231
    0.3421
    0.3612
    0.3837
    0.4062
    0.4166
    0.4426
    0.4668
    0.4876
    0.5066
    0.5187
    0.5430
    0.5741
    0.6278
    0.6676
    0.6936
    0.7230
    0.7594
    0.7923
    0.8148
    0.8460
    0.9100
    0.9550
    0.9966
    1.0381
    1.0693
    1.1143
    1.1593
    1.1974];
Bs2=[0.6813
    8.0779
   14.5012
```

```
   20.7299
   27.9319
   33.3820
   37.2749
   41.9465
   45.2555
   49.9270
   53.6253
   59.0754
   62.3844
   64.9148
   66.2774
   65.4988
   63.5523
   60.2433
   56.7397
   54.4039
   52.4574
   49.9270
   49.9270
   49.9270
   49.9270
   49.9270
   49.9270
   49.9270
   49.9270
   49.9270];

for i=1:n
B1(i)=interp1q(Ts1,Bs1,T1(i))./60; % Finds heating rates corresponding to T1
B2(i)=interp1q(Ts2,Bs2,T2(i))./60; % Finds heating rates corresponding to T2
B(i)=B1(i);
  E(i)=FMINBND('AEerror2',1,800,options2,T1(i),T2(i),T0,B1(i),B2(i));
  PE(i)=Ai2(E(i),T1(i),T2(i),T0,B1(i),B2(i));
    chi_checkB1(i)=chi(E(i),PE(i),T1(i),T0,B(i),B2(i));
    chi_checkB2(i)=chi(E(i),PE(i),T2(i),T0,B(i),B2(i));
```

```
end
% This loop calculates E and PE at the given T's and instantaneous B's
check=[chi_checkB1' chi_checkB2']
a=isfinite(PE');
PE=PE(a);
E=E(a);
q=length(Tr);
npoints=q;
nn=length(E);
Tr1i=Tr;

for i=1:npoints
    for j=1:nn

B1(j)=interp1q(Ts1,Bs1,T1(j))./60;;
B2(j)=interp1q(Ts2,Bs2,T2(j))./60;
B(j)=B1(j);
        term1(j)=quad(@term,T0,Tr1i(i),[],[],E(j));
        chi1(i,j)=exp((-PE(j)/B(j))*(term1(j)));
        chi1(i,nn+1)=1;
        chi_1(i,j)=chi(E(j),PE(j),Tr1i(i),T0,B(j),B2(j));
        chi_1(i,nn+1)=1;
    end
end % Creates the matrix Ψ
options3=optimset('TolX',10);
f0=lsqnonneg(chi_1,xx)
E(n+1)=0;PE(n+1)=0;
c=[f0 E' PE'];
```

10. Oratesv1 & Oratesv2

This simulates TGA data with variable heating rates. The codes are the same as orates but the T's and B's are defined by the matrices in variablebnew.m. The codes will therfore not be displayed.

11. Model

TGA curves for reactions with a shrinking core mechanism can be simulated using this code. An ode solver is used to create the curves

```
function c = model(tf,nTGA,B,T0);

% tf is the final temperature of the TGA plot


M0 = 1; & Inital mass fraction

temp=linspace(T0,tf,nTGA)';

options=odeset('RelTol',1e-2);

[t,state1] = ode45('model13',temp,M0,options,B); % Applies an ode solver to the rate
equation on model13.m to create the data

M1 = state1(:,1);

c=[t M1];

hold on

plot(t,M1,'b')

axis([280 tf 0 1])

xlabel('Temperature (K)');

ylabel('Mass Fraction Remaining');


x=c(:,1);y=100.*c(:,2);

deriv=-diff(y)./diff(x); % Calculates the discrete derivative of the data set

x=x(2:length(x));

plot(x,deriv,'b')
```

12. Model13

This contains the rate equation which the ode solver is applied to.

```
function rate = model13(t,s,dummy,B);

% t is the temperature data set

% s is the initial condition that M0 is zero

% dummy is the error tolerance

M = s(1);

B;

T=t;

R=8.314; %j/molK
```

```
A1=(exp(19.0269))*60;
E1=80*1.69;%kj/mol
k1=1*(A1/B)*exp(-E1*1000/(R*T)); Arrhenius term
rhs=-1*(k1*1*(M)^(2/3))-0*(k2*1*(M)^(2/3)); % shrinking core reaction
if (rhs>=0)
    rhs=0; % Does not allow mass to become negative
else
rhs = rhs;
end
rate=rhs;
```

13. Shrinking core

This code is the equivalent of scotteg1.m and scotteg2.m except that a shrinking core reaction is simulated as opposed to a first-order reaction.

```
function c = shrinkingcore(nrxns,rnTGA,nTGA,b1,b2,T0,tf);

B1=b1/60;%1st heating rate K/sec
B2=b2/60;%2nd heating rate K/sec
R=8.314; %j/molK

data1=model(tf,nTGA,B1,T0); % Creates TGA data for shrinking core reaction at B1
TT1=data1(:,1);
x1=data1(:,2);
data2=model(tf,nTGA,B2,T0); % Creates TGA data for shrinking core reaction at B2
TT2=data2(:,1);
x2=data2(:,2);

Tr1=linspace(TT1(1),TT1(length(TT1)),nTGA)';
Tr2=linspace(TT2(1),TT2(length(TT2)),nTGA)';
Xr1=interp1q(TT1,x1,Tr1);
Xr2=interp1q(TT2,x2,Tr2);
TT1=Tr1;
TT2=Tr2;
x1=Xr1;
x2=Xr2;
```

```
x1(length(x1))=x1(length(x1)-1);


X=linspace(0.9999,0.00001,nrxns)';

T1=interp1q(flipud(x1),flipud(TT1),X);

T2=interp1q(flipud(x2),flipud(TT2),X);

hold on

plot(Tr1,x1,'g')

plot(Tr2,x2,'r')

plot(T1,X,'go')

plot(T2,X,'ro')

 Xtga=x1;

 Tr1=TT1;

XLABEL('Temperature K')

YLABEL('Mass Fraction Remaining')

legend('50K/min','25K/min')

axis([T0 1500 0 1])

hold off

data3=funcscotteg2(T1,T2,B1,Tr1,Xtga,B1,B2,T0);

f0=data3(:,1);E=data3(:,2);PE=data3(:,3)

l=length(f0)-1;

f0=f0(1:l); E=E(1:l); PE=PE(1:l); % makes all vectors the same length

c=[f0 E PE T1 T2 X] % Displays temperature and conversion data so that they can be used
for further calculaions.
```

14. Anew

This algorithm was developed to calculate the value of A using the calculated value of E at the temperature at which it was calculated with the shrinking core model.

```
function c = Anew(f0,E,T1,B1,a,b);

% fo and E are the values calculted by shrinkingcore.m

T1 is the temperature data for heating rate B1 corresponding to the number of
conversions

T0=298.15;

R=8.314; %j/molK

b1=B1/60;

f=find(f0>0) % Finds the non-zero vaues of f0

f0=f0(f);

E=E(f) % finds the E's at which f0 is not zero
```

```
T1=T1(f) & Finds the T's at which the E's were calculated
f0=sum(f0); Total mass fraction reacted
E=sum(E)/length(E) % Calculates the average E
Tf=sum(T1)/length(T1) % Calculates the average T1

uo=(E*1000)/(R*T0); % Transformed variable
uf=(E*1000)/(R*Tf); % Transformed variable

% Terms in the expanded integral expression
first=T0*exp(-uo);
third=Tf*exp(-uf);
fourth=(E*1000/R)*expint(uf);

I =-3*(1-b)^(1/3)+3*(1-a)^(1/3); Integral form of the shrinking core function

A=(-b1*I)/(first-second-third+fourth); % Calculates A
c=[f0 E A]
```

15. Modelsc

This is used to model a shrinking core reaction by re-writing the Ψ matrix instead of using an ode solver.

```
function c=modelsc(f0,T0,E,PE,b,Tup,m);

f=f0(1,:); % initial fraction reacting
w=f0(2,:); % ash content
B=b/60;%K/sec
s=size(E');
nn=s(:,1);
T=linspace(T0,Tup,m);

for i=1:m
    for j=1:nn
        term1(j)=quad(@term,T0,T(i),[],[],E(j));
        chi2(i,j)=exp((-PE(j)/B)*(term1(j))); % Defines the martix Ψ
        chi2(i,nn+1)=1;
```

```
        chinew(i,j)=(1+(log(chi2(i,j))/(3*(f^(1/3))))).^3; % Rewrites the rate
experssion
        chinew(i,nn+1)=1;
    end
end

M=chinew*f0;
I=find(M<=(f0(end)));
M(I)=f0(end);
c=[T' M];
hold on
plot(T,M,'b.');
axis([T0 1200 0 1])
x=c(:,1);y=100.*c(:,2);
deriv=-diff(y)./diff(x);
x=x(2:length(x));
plot(x,deriv,'b')
```

16. Scnewchi

This is the same code as shrinkingcore.m, but the data used is from modelsc.m. The code will therefore not be displayed.

17. Pyrolysis

This code applies the DAEM algorithm to actual TGA data. The data is stored in separate files so that this code may be changed to data from different sources.

```
function c = pyrolysis(nrxns,nTGA,b1,b2,T0);

B1=b1/60;%1st heating rate K/sec
B2=b2/60;%2nd heating rate K/sec
R=8.314; %j/molK

data1=pyro35n(T0); % Real TGA data for lower heating rate
TT1=data1(:,1);
x1=data1(:,2);
data2=pyro60n(T0); % Real TGA data for higher heating rate
```

```
TT2=data2(:,1);
x2=data2(:,2);

Tr1=linspace(TT1(1),TT1(length(TT1)),nTGA)'; % reducing TGA points
Tr2=linspace(TT2(1),TT2(length(TT2)),nTGA)'; % reducing TGA points
Xr1=interp1q(TT1,x1,Tr1);
Xr1(1)=0.9999;
Xr2=interp1q(TT2,x2,Tr2);
Xr2(1)=0.9999;
Xr2(end)=0.724;
% Initial and end values may need to be defined to allow calculations

TT1=Tr1;
TT2=Tr2;
x1=Xr1;
x2=Xr2;
x1(length(x1))=x1(length(x1)-1);

X=linspace(0.985,0.73,nrxns)'; % Choosing conversions
T1=interp1q(flipud(x1),flipud(TT1),X);
T2=interp1q(flipud(x2),flipud(TT2),X);

plot(T1,X,'go')
hold on
plot(T2,X,'ro')
plot(TT1,x1,'g')
plot(TT2,x2,'r')

deriv1=-100*diff(x1)./diff(TT1); Calculating Derivatives
Tt1=TT1(2:length(TT1))';
deriv2=-100*diff(x2)./diff(TT2);
Tt2=TT2(2:length(TT2))';

plot(Tt1,deriv1,'b')
plot(Tt2,deriv2,'y')
```

```
Xtga=x2; % Data for either heating rate may be used to calculate A
data3=funcscotteg2(T1,T2,B2,Tr2,Xtga,B1,B2,T0); % Applying DAEM algorithm to data
f0=data3(:,1);E=data3(:,2);PE=data3(:,3);

c=[f0 E PE]

% Plotting kinetic parameters as a function of conversion
f0=f0(1:50);
figure(2);
stem(X,f0)
XLABEL('Mass Fraction Remaining');
YLABEL('f0');
E=E(1:50); X=X(1:50);
figure(3);
stem(X,E)
XLABEL('Mass Fraction Remaining');
YLABEL('E (KJ/mol)');
PE=PE(1:50);
figure(4);hold on
stem(X,PE,'.b')
XLABEL('Mass Fraction Remaining');
YLABEL('A (/min)');
```

18. Pyrolysis1

This code is uses the instantaneous heating rate algorithm with real TGA data.

```
function c = pyrolysis1(nrxns,rnTGA,nTGA,T0);

R=8.314; %j/molK

data1=pyro35n(T0); % Real TGA data for lower heating rate
TT1=data1(:,1);
x1=data1(:,2);
tt1=data1(:,4); % Time data
data2=pyro60n(T0); % Real TGA data for higher heating rate
TT2=data2(:,1);
```

```
x2=data2(:,2);
tt2=data2(:,4); % Time data

Tr1=linspace(TT1(1),TT1(length(TT1)),nTGA)';
Tr2=linspace(TT2(1),TT2(length(TT2)),nTGA)';
Xr1=interp1q(TT1,x1,Tr1);
Xr2=interp1q(TT2,x2,Tr2);
Xr1(1)=0.9999;
Xr2(1)=0.9999;
Xr2(end)=0.724;
tr1=interp1q(TT1,tt1,Tr1);
tr2=interp1q(TT2,tt2,Tr2);
TT1=Tr1;
TT2=Tr2;
x1=Xr1;
x2=Xr2;
x1(length(x1))=x1(length(x1)-1);
b1=diff(TT1)./diff(tr1); % calculating instantaneous heating rate
Tnew1=TT1(2:length(TT1));
b2=diff(TT2)./diff(tr2);
Tnew2=TT2(2:length(TT2)); % calculating instantaneous heating rate

X=linspace(0.99,0.73,nrxns)';
T1=interp1q(flipud(x1),flipud(TT1),X);
T2=interp1q(flipud(x2),flipud(TT2),X);
B1=(interp1q(Tnew1,b1,T1))./60;
B2=(interp1q(Tnew2,b2,T2))./60;

plot(T1,X,'go')
hold on
plot(T2,X,'ro')
plot(TT1,x1,'g')
plot(TT2,x2,'r')

Xtga=x1;
data3=variablebnew(T1,T2,Tr1,B1,B2,Xtga,T0);
```

```
f0=data3(:,1);E=data3(:,2);PE=data3(:,3);
c=[f0 E PE]
```

19. Combustion and Comcustion1

These codes are the same as pyrolysis.m and pyrolysis1.m, but read combustion data instead of pyrolysis data. They will therfore not be diaplayed.